University of Tennessee, Knoxville
Trace: Tennessee Research and Creative Exchange

Doctoral Dissertations   Graduate School

8-2010

AdS/CFT Correspondence and Hydrodynamics of Relativistic Heavy Ion Collisions

James Ethan Alsup
University of Tennessee - Knoxville, jalsup1@utk.edu

To the Graduate Council:

I am submitting herewith a dissertation written by James Ethan Alsup entitled "AdS/CFT Correspondence and Hydrodynamics of Relativistic Heavy Ion Collisions." I have examined the final electronic copy of this dissertation for form and content and recommend that it be accepted in partial fulfillment of the requirements for the degree of Doctor of Philosophy, with a major in Physics.

George Siopsis, Major Professor

We have read this dissertation and recommend its acceptance:

Yuri Kamyshkov, Soren Sorensen, Carl Sundberg

Accepted for the Council:
Dixie L. Thompson

Vice Provost and Dean of the Graduate School

(Original signatures are on file with official student records.)

To the Graduate Council:

I am submitting herewith a dissertation written by James Ethan Alsup entitled "AdS/CFT Correspondence and Hydrodynamics of Relativistic Heavy Ion Collisions." I have examined the final electronic copy of this dissertation for form and content and recommend that it be accepted in partial fulfillment of the requirements for the degree of Doctor of Philosophy, with a major in Physics.

George Siopsis, Major Professor

We have read this dissertation
and recommend its acceptance:

Yuri Kamyshkov

Soren Sorensen

Carl Sundberg

Accepted for the Council:

Carolyn R. Hodges

Vice Provost and Dean of the Graduate School

(Original signatures are on file with official student records.)

AdS/CFT Correspondence and Hydrodynamics of Relativistic Heavy Ion Collisions

A Dissertation

Presented for the

Doctor of Philosophy

Degree

The University of Tennessee, Knoxville

James Ethan Alsup

August 2010

Acknowledgements

There are innumerable people that I should thank for helping me get to this point of my career. This is but a list and in no way returns the kindness I have received.

The first person I would like to thank is my wife, Kathleen. We met our last year in high school and have been together ever since. She helped guide me toward Physics after I read popular literature on the subject and became fascinated. Kathleen has been compassionate and a much loved constant for the past ten years. Foremost, I would like to thank her for providing me with an heir, little Ethan.

During my path in Physics I have had three major influences. When I first started studying Physics I found an announcement that Dr. Yuri Kamyshkov was looking for an undergraduate student to perform Monte-Carlo calculations for neutron disappearance. I immediately responded and consequently benefitted from a year and a half of direct study under Dr. Kamyshkov. I learned much about Physics and also how to ask the right questions. Also from the high energy experiment group, is my good friend Brandon White, with whom I have spent many, many nights studying for many, many years.

By the beginning of my final year as an undergraduate I convinced Dr. George Siopsis to allow me to study quasinormal modes under him. George has been the dominant force in my development ever since. He taught me how to approach theoretical problems so that I can solve them, or sometimes, simply define them. Under his guidance and support I have benefitted from travel throughout the country and world. Moreover, in the comfort of the Nielsen Physics Building, I have had

numerous influential fellow Siopsis students – Scott Ness, Chad Middleton, Suphot Musiri, Usama al-Binni, Savan Kharel, and Jason Therrien. These experiences have helped me develop an understanding of the direction and the culture of the field.

The past two years I have been a teaching assistant under Dr. Soren Sorensen. Every lecture of his I sat in demonstrated and reinforced the ideas that I hope to use in my career, including how to encourage students to be creative, independent, and enthusiastic about Physics.

I would also like to thank Dr. Carl Sundberg for being a part of my committee and having an interest in my work as a graduate student.

Lastly, I want to thank my family – parents, Bob and Lota, and siblings, Joel and Emily. They have supplied me with immeasurable love and support. To attempt an illumination would be foolish.

Abstract

The experiments performed at the Relativistic Heavy Ion Collider (RHIC) at Brookhaven National Lab have discovered a state of matter called the strongly coupled quark-gluon plasma (sQGP). The strong coupling has limited the ability of the standard theory to describe such matter, namely Quantum Chromodynamics (QCD). However, string theory's anti-de Sitter/conformal field theory (AdS/CFT) correspondence has provided a new way to study the situation and in an analytical manner. So far, hydrodynamic properties of RHIC's plasma, such as elliptic flow and longitudinal expansion, have been seen to follow from classical supergravity calculations. In this dissertation I discuss some of the field's development as well as the research done by the author and collaborators.

Contents

List of Figures

Nomenclature

x^μ	Static space-time coordinates
$\tilde{x}^\mu$	Boosted space-time coordinates
t	Time coordinate
x^1	Longitudinal coordinate
τ	Proper-time coordinate
y	Rapidity coordinate
$T^{\mu\nu}$	Stress-Energy tensor
J^α	Current
ε	Energy density
T	Temperature
p	Pressure
s	Entropy Density
ρ	Charge Density
μ	Chemical Potential
η	Shear viscosity
κ	Thermal conductivity
v_2	Elliptic flow
ϵ	Eccentricity
σ	Graviton cross-section (Sec. 2.2.2), τ power parameter elsewhere
ω, Ω	Quasinormal frequency
k_S, k_V, k_T	Scalar, Vector, Tensor harmonic eigenvalue

N	Number of colors
G	Gravitational constant
$g_{\mu\nu}$	Metric
$R_{\mu\nu}$	Ricci tensor
R	Ricci Scalar
$\mathcal{R}^2$	Kretschmann Scalar
$R_{\mu\nu\alpha\beta}$	Riemann tensor
$\mathcal{R}_{abcd}$	Projected Riemann tensor

Chapter 1

Introduction

1.1 Relativistic heavy ion collisions

The quest to understand matter has been a progression of scientific and philosophical minds for much of the past three millennia. Yet quantitative theory and experiment of "fundamental particles" have only been achieved over the past century. The beginning was labeled the "Golden Age of Physics" when Quantum Mechanics and Relativity were conceived. The field continued to progress to the advent of quantum field theory and the incorporation to gauge theories. The work then culminated in the Standard Model.

The Standard Model provides a coherent picture of particles that make up three of the four fundamental interactions – electromagnetic, strong, and weak with gravity remaining apart. Due to the capacity and complexities, discussed in this text, the strong force remains an interesting field of theoretical and experimental study.

The theory of the strong interaction is Quantum Chromodynamics (QCD) – an SU(3) gauge theory with three colors. The theory provides the explanation of the interior of protons and neutrons in terms of quarks and gluons. The quarks carry the color charge determining the strength of the interaction, similar to the electrical

charge in electromagnetism. Gluons act as the mediator of the force and also carry color charges allowing for gluon-gluon interactions.

Two of the most curious features of the theory are confinement and asymptotic freedom [1]. For large distance scales, quarks are very strongly coupled. At a certain point of separation, it becomes energetically favorable to create quarks out of the vacuum that pair with the two separated. Therefore, they can only be found in bound states of two (mesons) or three (baryons) with perhaps more exotic states existing. However, at small distance scales, the strong interaction becomes weak enough that quarks move freely. Alternatively, one may characterize the small distance scale as a large energy scale. If an experiment could reach the correct energy density, the quarks and gluons would be deconfined from the bound states.

The concept of a sea of free quarks and gluons presented a new form of matter, the quark-gluon plasma (QGP), to be studied. A crossover from hadronic matter to free quarks and gluons would allow for color charge to roam free within the confines of the system. This phase has not been seen in the universe since the early stages of the Big Bang, and the freedom could be exploited to answer fundamental questions about elementary particles and their interactions.

Necessary techniques were developed to achieve the state in the laboratory. The method explored was that of high energy collisions between nuclei. The first experiment to develop was the SPS (Super Proton Synchrotron) at CERN followed by the AGS (Alternating Gradient Source) at Brookhaven. Subsequently, RHIC (Relativistic Heavy Ion Collider) at Brookhaven, was built on the AGS. Now detectors at CERN – ALICE (A Large Ion Collider Experiment), CMS (Compact Muon Detector), and ATLAS (A Toroidal LHC ApparatuS) are just beginning to produce results.

This work is concerned with a theoretical description of the findings at RHIC [2]. The basic principle of RHIC is to accelerate heavy ions, such as gold nuclei, to speeds approaching that of light. Once at the top speed, the ions' paths are intersected and the passing collisions are studied. The diagram in figure 1.1 depicts the nuclei as
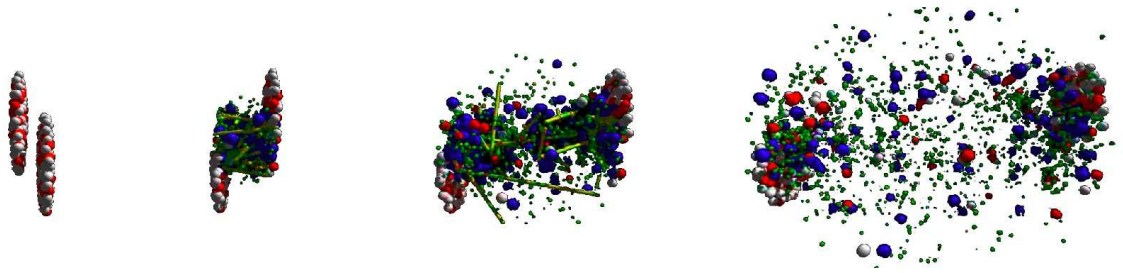
Figure 1.1: Depiction of RHIC collision.
Animation by Jeffery Mitchell, BNL [3].

Lorentz contracted pancakes that pass through one another. The outer edge contains the spectators that feel no influence from the collision, while the overlapping region contains participants that do interact. Collisions with more overlap are considered central collisions.

As the particles are traveling at virtually the speed of light, a useful tool for analyzing the fireball can be presented in lightcone coordinates. Figure 1.2 diagrams the stages of the collision, assuming the QGP is formed. The first stage consists of the nuclei traveling at $\sim c$. After the collision, roughly 5,000 particles are created and interact in complicated kinematics. The plasma then thermalizes on the order of 1 fm/c and reaches the QGP phase. As the system cools the particles start to freeze out into a hadron gas around 8 fm/c. Eventually this is followed by completely free hadrons that no longer interact at ~ 16 fm/c.

1.2   RHIC

The Relativistic Heavy Ion Collider has the ability to accelerate a heavy ion, Au or Cu, to energies of 200 GeV/nucleon. It also utilizes proton and deuterium collisions and asymmetric collisions with permutations of the species. For Au beams, this is achieved in a six step process. (1) Negative Au ions are extracted from a pulsed ion sputter source and sent down the Tandem Van de Graff where electrons are stripped off. (2a) The second stage consists of magnetic fields accelerating the positive ions toward the
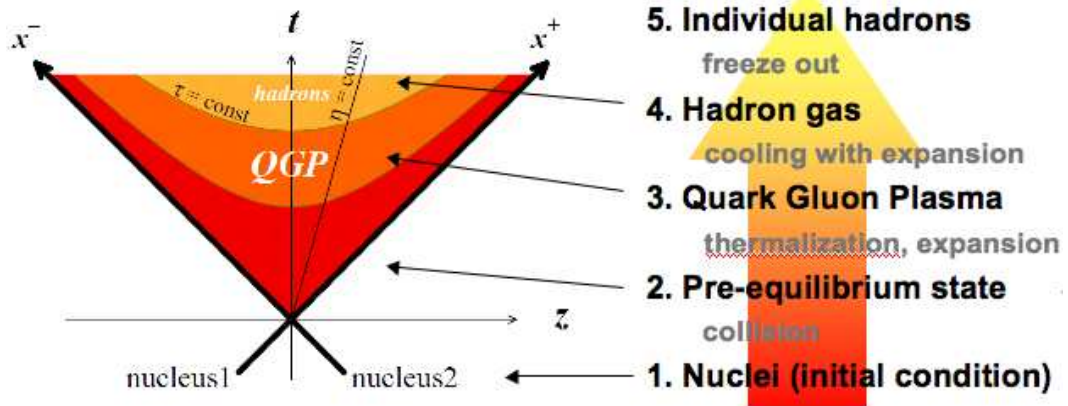
Figure 1.2: Phases of the fireball at RHIC.
Diagram by K. Itakura [4].

booster synchrotron. (2b) For proton beams, the protons are analogously sent through a linear accelerator at this stage. (3) Once in the booster synchrotron, more electrons are stripped and the positive ions are further accelerated with electromagnetic waves. (4) The next step is the Alternating Gradient Source. The remaining electrons are removed and the ions are accelerated to their top speed, $.997c$. (5) The ions are then injected into the AGS-to-RHIC transfer line where bunches ($\sim 10^9$ ions) are sent in opposite directions around RHIC. (6) Finally, the beams are guided into intersection points where the detectors are located, with luminosities reaching up to $\sim 10^{32}$ cm^{-2} s^{-1}. A diagram of the collider is seen in figure 1.3.

RHIC consists of four detectors along two semi-circular loops, each having a 3.8 kilometer circumference. Two of the detectors, STAR (Solenoidal Tracker at RHIC) and PHENIX (Pioneering High Energy Nuclear Interations eXperiment), remain active. The other two, PHOBOS and BRAHMS (Broad RAnge Hadron Magnetic Spectrometer), completed data collecting in 2005 and 2006, respectively. Each detector had its own specific purpose outlined in the next four sections.

4
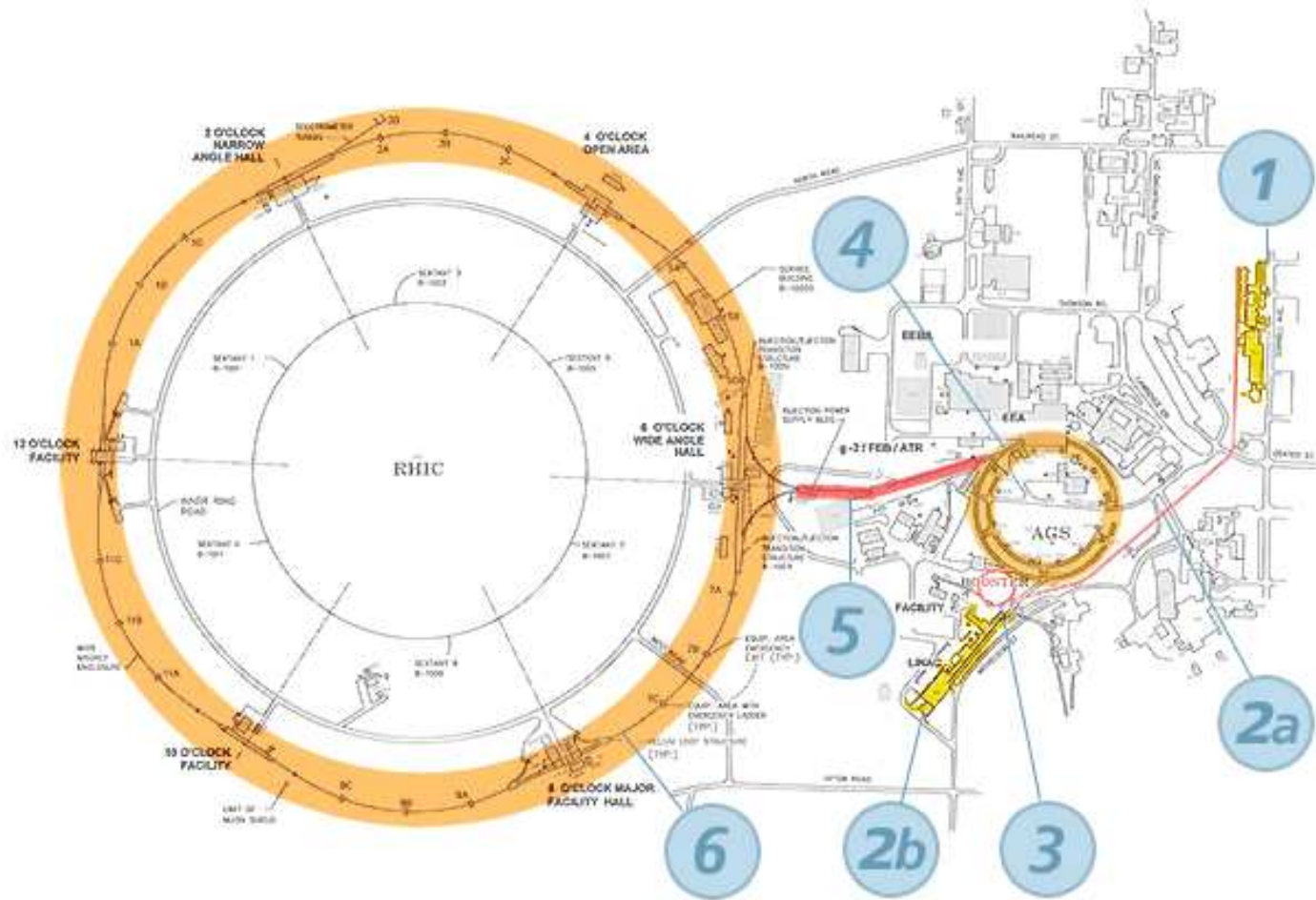
Figure 1.3: Diagram of RHIC.
The numbers are in accordance with the steps listed in the text [5].

1.2.1 STAR detector

STAR was designed to study hadron production as a whole to illuminate the QGP via its constituents. It is composed of a time-projection chamber, large solenoid magnet, silicon detectors, electromagnetic calorimeters, and time of flight detectors (figure 1.4)

The bulk of the tracking is done with the time-projection chamber that covers the entire solid angle around the beam. The magnetic field parallels the beam inside the detector which helps with particle identification.

1.2.2 PHENIX detector

PHENIX (figure 1.5) examines the electromagnetic particles which can escape the early stages of the collision without interference due to their inability to interact through the strong force. The detector is broken up into several subsections. The central arm detectors (drift chamber and fellow components) is focused on charged particle position and momentum measurements. The muon arm detectors, expectedly, are specialized for muons. The event characterization detectors allow for insight into the initial geometry of the collision. Finally, the heavy metal portion contains a large magnet that bends the charged particles' trajectories thereby allowing for the charge and momentum measurements.

1.2.3 PHOBOS dectector

PHOBOS focused on providing a global picture of the experiment, such as the temperature, size, and density in addition to relative particle production of the fireball. The detector provides overall coverage via a silicon multiplicity array. A silicon spectrometer also allows for $\sim 1\%$ particle identification and momentum measurements. There are two time of flight walls and plastic scintillators used for triggering and centrality determination. The design was originally optimized for small
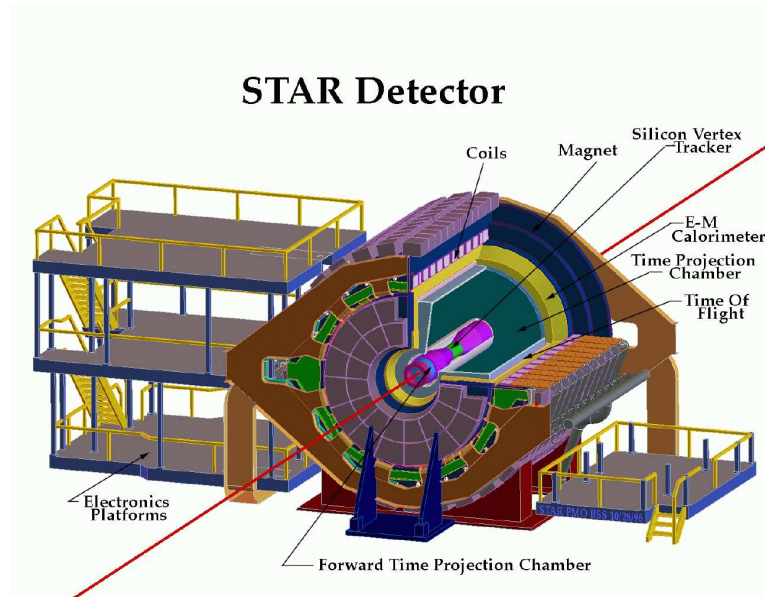
Figure 1.4: Diagram of the STAR detector.
[6].
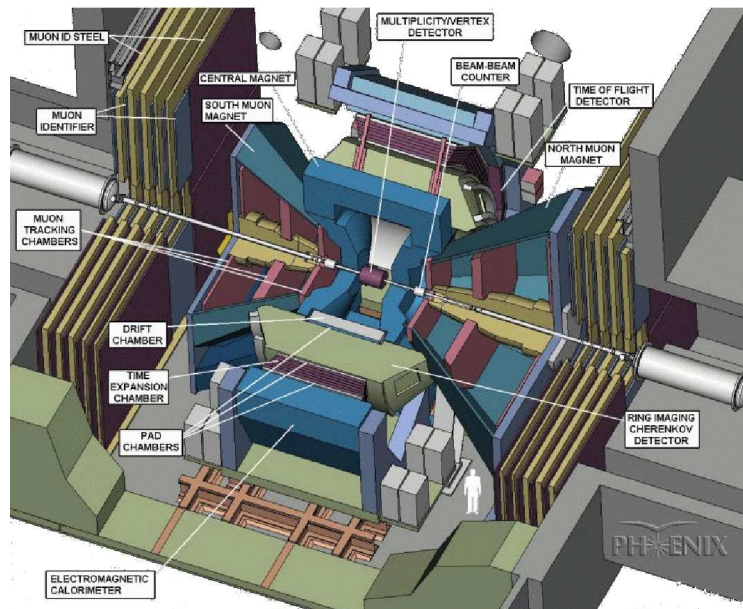
Figure 1.5: Diagram of the PHENIX detector.

p_T but has since been capable of studying high regimes as well. A view of PHOBOS is shown in figure 1.6.

1.2.4   BRAHMS dectector

BRAHMS concentrated on momentum spectroscopy, notably the rapidity distribution – explained in Chapter 2. This was achieved with the standard triggering detectors that measure the initial collision set up but was also capable of measuring the largest rapidity range with particle identification. The two spectrometer arms, seen in figure 1.7, were able to move along the beam's polar angle. One could measure the forward region with the other concentrated on the midrapidity region.

1.3   Experimental observations

There is no single observation that confirms RHIC creates the QGP. It must be inferred from several different measurements. Some of the indications of the QGP
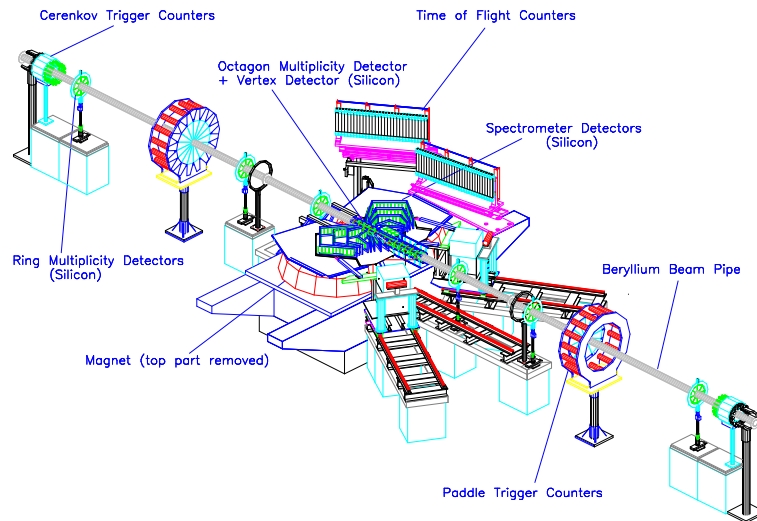
Figure 1.6: Diagram of the PHOBOS detector.
[7].
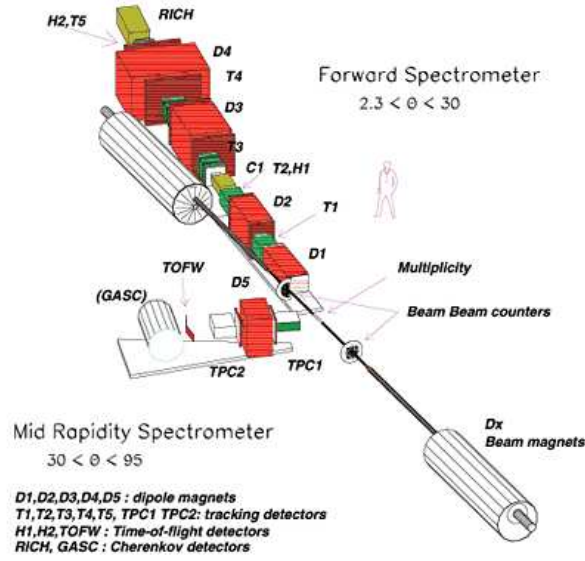
Figure 1.7: Diagram of the BRAHMS detector.
[8].

take the form of jet quenching, thermal equilibrium for hadron production and hydrodynamic flow.

For a parton traveling through a colored medium, the strong interactions will slow or stop it from traversing. This can be understood with the nuclear modification factor, R_{AA}, which is a scaling of transverse particle production from proton-proton collisions to gold-gold. If the colored medium did not interact strongly at high transverse momentum, it is expected that R_{AA} would be consistent with unity. However, strong interactions would suppress the production of high p_T hadrons. Figure 1.8 shows the measurements at PHENIX, where it was found that hadrons were suppressed by a factor of 5. However, direct photons, which interact only electromagnetically, were not suppressed.

Colored medium effects also manifest in jet quenching by creating a preferential direction of back-to-back jets. If two partons are created near the edge of the QGP, one will be able to leave the system and hadronize freely, but the other will be quenched of its energy leading to a correlation suppression. This behavior was observed at STAR

9
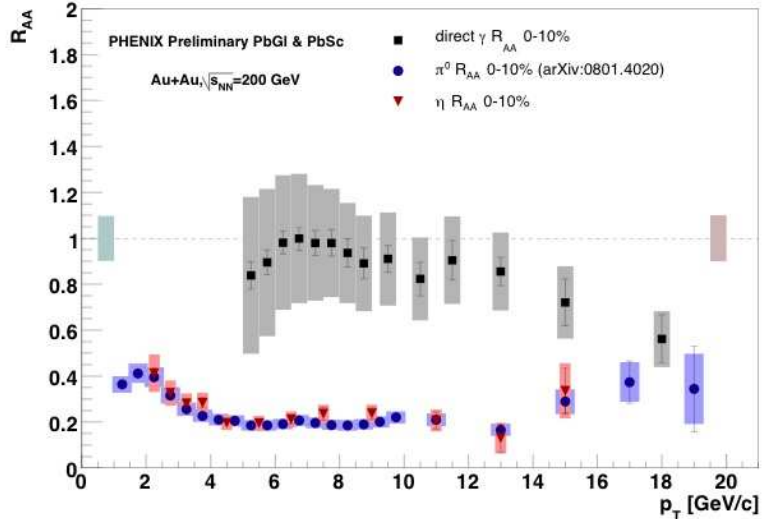
Figure 1.8: Nuclear Modification Factor for π^0, η, and direct photons.
Hadron production is suppressed but direct photons are not. For $p_T \gtrsim 10$ GeV/c, it is suggested
that the photon suppression is due to a change in cross sections between pp and pn [9].

(figure 1.9). For Au-Au collisions, it appears all of the energy of the jet that traverses
through the medium ($\Delta\phi = \pi$) is lost so that the event appears to be a single jet.
This is contradictory to what is observed in p-p or d-Au collisions, where the QGP
is not thought to be as predominant. Therefore, both the high p_T suppression and
quenching phenomenon are consistent with a strongly interacting medium for the
fireball.

Particle ratios may be used to check for equilibration of the fireball. These
are found by using the grand canonical ensemble with conserved baryon number,
strangeness and charge chemical potentials (μ_i). The partition function is given by

$$\ln Z = \sum \frac{g_i V}{(2\pi)^3} \int d^3p \ln \left[1 \pm e^{-\beta(E_i - \mu_i)} \right]^{\pm 1}, \tag{1.1}$$

where g_i is the degeneracy, V the volume, p momentum, m_i the mass, β the inverse
temperature, and $E_i = \sqrt{p^2 + m_i^2}$ is the energy with $\pm$ corresponding to fermions or
bosons, respectively [11]. From the partition function, we find the number of particles
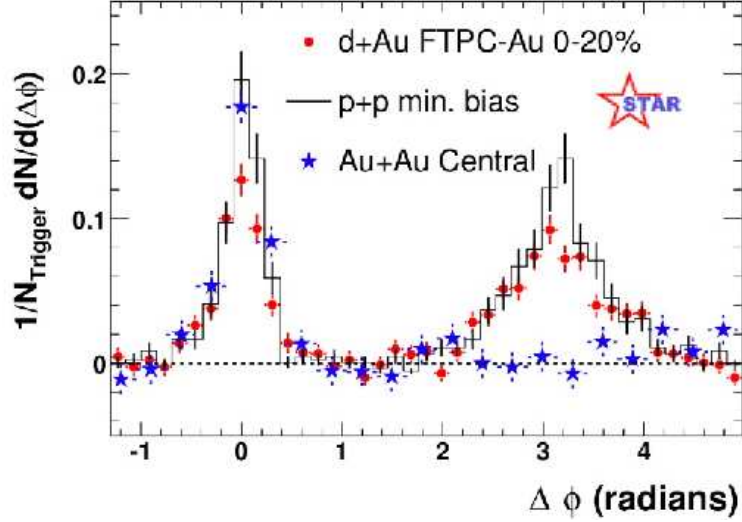
Figure 1.9: Jet quenching measured at STAR.
Back-to-back jets are emitted in the collision. One jet travels a short distance through the medium ($\Delta\phi = 0$) and is detected. However, the one that travels further is suppressed [10].

for each species as

$$N_i = T\frac{\partial \ln Z}{\partial \mu_i} = \frac{g_i V}{(2\pi)^2} \sum_{k=1}^{\infty} \frac{m_i^2 T}{k} K_2\left(\frac{km_i}{T}\right) e^{\beta k \mu_i}, \tag{1.2}$$

where the function K_2 is the modified Bessel function. Using the ratios of species eliminates the volume from the calculation and may then be compared with experiment as a fit varying μ_i and T. The results of such are shown in figure 1.10. The fit produced the temperature for freeze out at $T = 163 \pm 4$ MeV and baryon chemical potential, $\mu_B = 24 \pm 4$ MeV. The quality of the fit is seen as an indication of thermal equilibrium of the fireball.

We have now described two aspects of the medium created at RHIC. It should be composed of strongly interacting constituents that equilibrate before producing hadrons. Moreover, there are several suggested signatures that we will not discuss. Theoretically, strange quark production should be enhanced due to the similarity
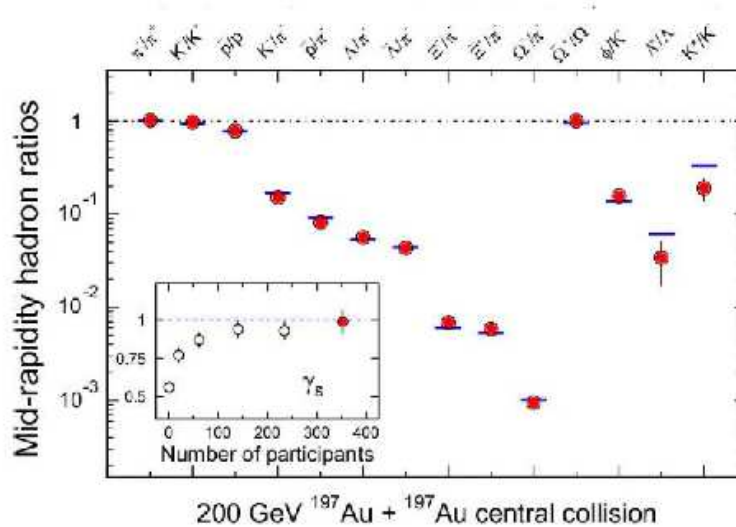
Figure 1.10: Thermal fit to particle species ratios at STAR.
Statistical model fit to measured particle ratios for $\sqrt{s_{NN}} = 200$GeV at STAR. The inset shows the equilibration (γ_s) of strange quarks vs. centrality. For most central collisions, it is one and fully equilibrated [2].

between the quarks mass and the deconfinement temperature. Alternatively, a J/Ψ meson will experience debye screening in the QGP and be suppressed.

The QGP aspect that is most closely related to this work is that of hydrodynamic flow of the fireball. In fact, this is the cornerstone discovery of RHIC. It was originally presumed the collision would create a weakly interacting gas but what was found was that the fireball behaves as a liquid [2]. This is thought to be due to the strong coupling between the constituents and is supported predominantly by the success of hydrodynamic data fitting for elliptic and radial flows. The initial anisotropy, eccentricity, of the beam influences the fireball after the collision. Whereas, if the plasma had a small coupling, the constituents would not feel the presence of each other and simply pass through without the propagation of anisotropy. Figure 1.11 shows a depiction of the geometry after the collision. Here a reaction plane is defined via the small axis of the amygdaloidal-shaped overlap region. After the nuclei pass through one another, the spectators continue along the beam's longitudinal direction, but the participants' interactions translate the anisotropy by way of a pressure gradient.

12

Hence a collective motion is observed and can be characterized by the elliptical and radial flows.

The most direct way to measure such a parameter is to look at the multiplicities and their azimuthal distribution throughout the detector. One can perform a harmonic expansion for the distribution of particles [13]

$$\frac{dN}{d(\phi - \psi_{RP})} = \frac{v_0}{2\pi} + \frac{v_1}{\pi} \cos(\phi - \psi_{RP}) + \frac{v_2}{\pi} \cos(2(\phi - \psi_{RP})) + \ldots \quad (1.3)$$

where ψ_{RP} is the reaction plane. The coefficients, v_i, are a function of the centrality and, when properly chosen events are used, the odd terms dissappear. The v_2 term is the elliptic flow and gives a quantitative view of the system's directional preference. This quantity comes from the initial spatial anisotropy. Therefore, when combined with the eccentricity of the system

$$\epsilon = \frac{\langle y^2 - x^2 \rangle}{\langle y^2 + x^2 \rangle}, \quad (1.4)$$
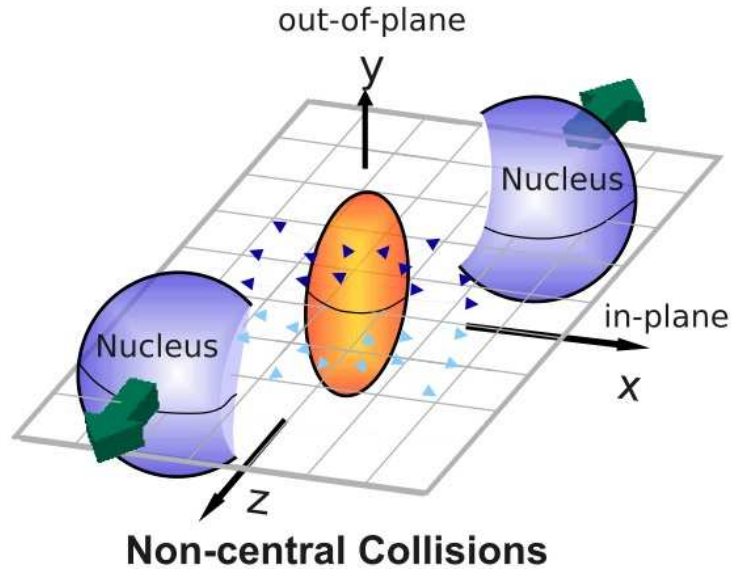
Figure 1.11: Geometry of a collision at RHIC.
The reaction plane is determined by the initial stage of the collision [12].

13

one can eliminate geometrical considerations of the collision, and the ratio provides insight into RHIC physics. However, there are still some issues in obtaining a proper measurement. This is due to defining the reaction plane [13] from the experimentally measurable event plane, as well as the initial participant geometry for the eccentricity averages via the phenomenological Glauber Model [14]. Further, there are difficulties from phenomenon such as jets, minijets, or resonances which will not be discussed.

As one of the most compelling arguments for RHIC's discovery of the fluid state, every detector performed tests on v_2 and its consequence. Figure 1.12 shows the elliptic flow versus transverse momentum and transverse mass, where transverse mass is given by $m_T = \sqrt{p_T^2 + m^2}$. There is a split between mesons and baryons, but when scaled by the number of quarks, the data coincides nicely. The scaling suggests quarks compose the degrees of freedom in the fireball, further strengthening the argument that the system is actually the QGP and not a hadron gas. In figure 1.13 the green lines represent the ideal hydrodynamic limits at AGS, SPS, and RHIC energies. The combination of v_2/ϵ versus $(1/S)dN_{ch}/dy$ allows for a comparison between different projectiles, energies, and centralities all in one plot with the elimination of geometry fluctuations. Moving left to right on the plot is understood as more and more central collisions. For RHIC's most central collisions, the bound is virtually saturated. This
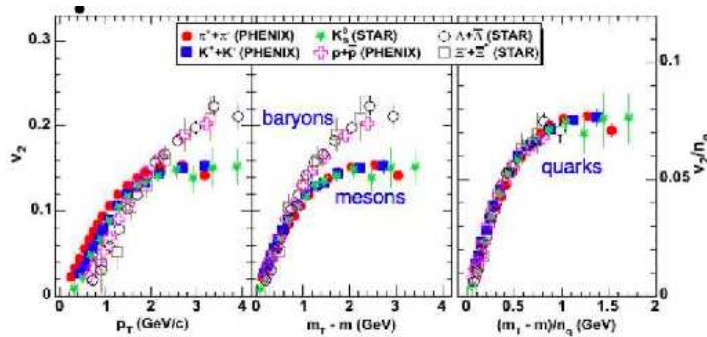
Figure 1.12: v_2 vs transverse momentum and transverse mass.
The success of quark scaling is an indication of QGP [15].

14
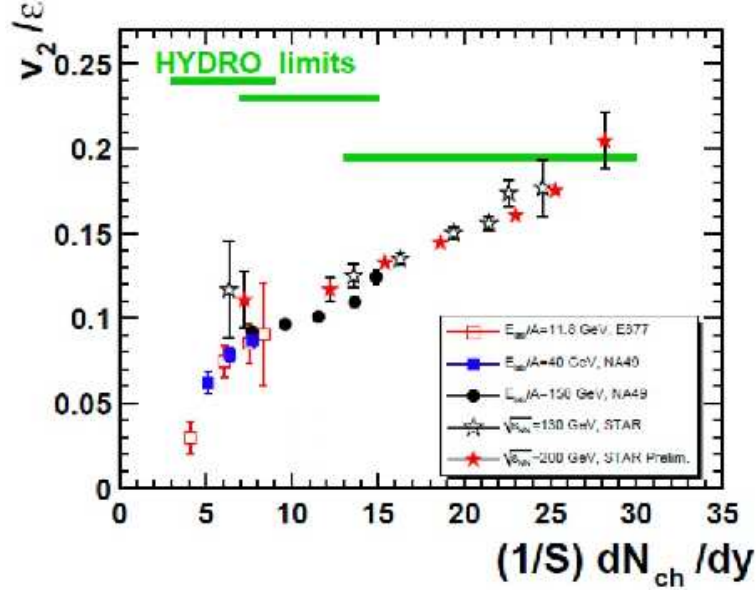
Figure 1.13: v_2/ϵ vs particle density per unit overlap area (S) at midrapidity. The saturation of the hydrodynamical limit is an indication of small viscosity. From left to right, the green lines represent the ideal hydrodynamical limits for AGS, SPS, and RHIC energies [16].

has been one of the strongest indications of the QGP possessing a hydrodynamic description with small dissipation.

There are several observables that can be used as a starting point to characterize the parameters of a hydrodynamical model for the RHIC fireball. However, the particle production rapidity density is a quick global measurement to make with multiplicity detectors and particle identification. BRAHMS, among the others, performed this measurement. Their findings for the most central collisions are shown in figure 1.14. The multiplicity distribution is sensitive to all stages of the collision and is characteristic of the expansion (discussed in Chapter 2). We note that in the central rapidity range, $|y| < 1$, the distribution drops slowly; however, it is well fit by a Gaussian outside the range. We will use this measurement as motivation for our theoretical framework to describe RHIC's fireball.

15
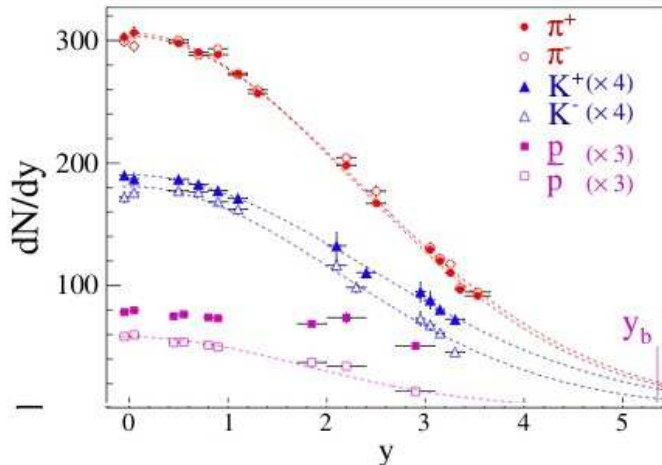
Figure 1.14: Particle rapidity density vs. rapidity from BRAHMS.
Data taken from Au-Au at $\sqrt{s_{NN}} = 200$ GeV. The particle rapidity density is an associated with the expansion of the fireball [17].

1.4 Outline of Chapter 2

We discuss the theoretical description for the fireball created at RHIC, starting with hydrodynamics for the macroscopic behavior. Bjorken hydrodynamics is presented as a model for the expansion; however, there are standard shortcomings of a purely phenomenological model. We also discuss the microscopic descriptions – perturbative QCD and lattice QCD, briefly, and the AdS/CFT correspondence. The AdS/CFT correspondence is argued to provide a working fit for the system and its applications are presented.

1.5 Outline of Chapter 3

We study an extension of the gravity dual to a perfect fluid model found by Janik and Peschanski [18]. By relaxing one of the constraints, namely invariance under reflection in the longitudinal direction, we introduce a metric ansatz which includes off-diagonal terms. We also include an R-charge following Bak and Janik [19]. We solve the Maxwell-Einstein equations and through holographic renormalization, we

16

show that the off-diagonal components of the bulk metric give rise to heat conduction in the corresponding CFT on the boundary [20].

1.6 Outline of Chapter 4

We consider a large black hole in asymptotically anti-de Sitter spacetime of arbitrary dimension with a Minkowski boundary. By performing an appropriate slicing as we approach the boundary, we obtain via holographic renormalization a gauge theory fluid obeying Bjorken hydrodynamics in the limit of large longitudinal proper time. The metric we obtain reproduces, to leading order, the metric found as a direct solution of the Einstein equations in five dimensions. Our results are also in agreement with exact results in three dimensions [21].

1.7 Outline of Chapter 5

We discuss the derivation of dissipative Bjorken hydrodynamics from a Schwarzschild black hole in asymptotically AdS spacetime of arbitrary dimension in the limit of large longitudinal proper time τ. Using a slicing near the boundary, we calculate the Schwarzschild metric to next-to-next-to-leading order in the large τ expansion, as well as the dual stress-energy tensor on the boundary. At next-to-next-to-leading order, it is necessary to perturb the Schwarzschild metric in order to maintain boost invariance. The perturbation has a power-law time dependence and leads to the same value of the ratio of viscosity to entropy density, $1/(4\pi)$, as in the case of sinusoidal perturbations. Our results are in agreement with known time-dependent asymptotic solutions of the Einstein equations in five dimensions [22].

1.8 Outline of Chapter 6

We analytically calculate the low-lying gravitational quasinormal modes of a topological AdS black hole of arbitrary dimension in the high temperature limit. We show that they are in agreement with corresponding results from the hydrodynamics of the gauge theory plasma on the boundary, as required by the AdS/CFT correspondence. For some of these modes, we obtain a lifetime, which is comparable to or longer than, the longest lifetime of perturbations of spherical black holes. Thus, these modes might play a significant role in the late-time behavior of the gauge theory plasma [23].

Chapter 2

Theoretical description

2.1 Macroscopics

In the first chapter, we provided some of the experimental evidence that the QGP created at RHIC can be described with hydrodynamics. We now lay out the prescription to do just this. Hydrodynamics is formulated with a stress-energy tensor and current which may be defined as a perfect fluid plus dissipative terms [24]

$$T^{\alpha\beta} = (\varepsilon + p)u^\alpha u^\beta + p\eta^{\alpha\beta} + t^{\alpha\beta}, \quad J^\alpha = \rho u^\alpha + j^\alpha. \tag{2.1}$$

The first two terms in $T^{\alpha\beta}$ should be recognized as an ideal fluid, as well as the first term in J^α, with $t^{\alpha\beta}$ and j^α dissipative corrections. Moreover, ε is the energy density, p the pressure, ρ the particle density, and u^α is the four velocity ($u^2 = -1$).

The governing equations for hydrodynamics is conservation of these two quantities,

$$\nabla_\alpha T^{\alpha\beta} = 0, \quad \nabla_\alpha J^\alpha = 0, \tag{2.2}$$

plus the standard thermodynamic relations

$$\varepsilon + p = Ts + \mu\rho, \quad d\varepsilon = Tds + \mu d\rho \ , \quad dp = sdT + \rho d\mu, \tag{2.3}$$

19

with temperature (T) and entropy density (s).

After defining a few parameters, initial conditions and transport coefficients, the equations are fully determined. For a RHIC-like scenario, these consist of the thermalization time, initial energy density and temperature, as well as an equation of state.

The local velocity and particle density can be chosen so that u^μ is orthogonal to the dissipative corrections,

$$u_\alpha t^{\alpha\beta} = u_\alpha j^\alpha = 0. \tag{2.4}$$

After requiring that entropy always increases, we find the general expression for the first order corrections as

$$t^{\alpha\beta} = -\eta[\nabla^\alpha u^\beta + u^\alpha u^\gamma \nabla_\gamma u^\beta + (\alpha \leftrightarrow \beta)] - \left(\zeta - \frac{2}{3}\eta\right)[\eta^{\alpha\beta} + u^\alpha u^\beta]\nabla_\gamma u^\gamma, \tag{2.5}$$

$$j^\alpha = -\varkappa(\partial^\alpha + u^\alpha u^\beta \partial_\beta)\frac{\mu}{T}, \tag{2.6}$$

in terms of the coefficient of thermal conductivity $\varkappa$ and shear and bulk viscosities, η and ζ, respectively. The dissipative components of the stress-energy tensor and current can be expanded to higher order in terms of derivatives of ε and u^μ [25].

This formalism also allows us to characterize fluctuation eigenmodes associated with the stress-energy tensor [26]. The first is the shear mode and is associated with transverse fluctuations of T^{0i}, with the eigenmode

$$\omega = -iDq^2, \quad D = \frac{\eta}{\varepsilon + p}, \tag{2.7}$$

where D is the diffusion constant of the dispersion relation. The other mode couples T^{00} and longitudinal modes of T^{0i}. The dispersion relation is given by

$$\omega = u_s - \frac{i}{2}\frac{1}{\varepsilon + p}\left(\zeta + \frac{4}{3}\eta\right)q^2, \quad u_s^2 = \frac{\partial p}{\partial \varepsilon} \tag{2.8}$$

and is dubbed the sound mode.

2.1.1 Longitudinal expansion

We now turn our attention to a hydrodynamical system that expands only in the longitudinal direction. Our motivation is to describe the expansion of the most central collisions seen at RHIC. To do so we must first discuss the variables that are important. The background must be that of four dimensional Minkowski space if we wish to describe a system seen in the lab. The metric is therefore given by

$$ds^2 = -dt^2 + (dx^1)^2 + (dx^\perp)^2, \tag{2.9}$$

where x^1 is the longitudinal direction and $x^\perp$ are the transverse directions (x^2, x^3). The fluid's rest frame follows from the kinematics. If the beam possesses energy (E) and longitudinal momentum (p_1), the proper time (τ) and rapidity (y) of the system

$$\tau = \sqrt{E^2 - p_1^2}, \quad y = \frac{1}{2} \ln \left(\frac{E + p_1}{E - p_1} \right) \tag{2.10}$$

can be used to define the rest frame, which is given by basic Special Relativity as $u^\alpha = (\cosh y, \sinh y, 0, 0)$.

The assumption of longitudinal expansion limits the *ideal* hydrodynamic equations to 1+1 dimensions expressed as

$$\partial_t T^{00} + \partial_1 T^{01} = 0, \quad \partial_t T^{01} + \partial_1 T^{11} = 0. \tag{2.11}$$

T^{22} and T^{33} will be determined with an equation of state. For our purposes, we assume conformal invariance

$$T^\mu_\mu = 0 \quad , \quad \varepsilon = 3p. \tag{2.12}$$

Sticking to convention, we would like to express the hydrodynamic equations in terms of lightcone coordinates

$$x^+ = t + x^1, \quad x^- = t - x^1. \tag{2.13}$$

With the help of (2.1), we can cast the stress-energy tensor's conservation in terms of two equations

$$\partial_+ \varepsilon + 2\partial_- \left(\varepsilon e^{-2y} \right) = 0, \quad \partial_- \varepsilon + 2\partial_+ \left(\varepsilon e^{2y} \right) = 0. \tag{2.14}$$

The solution to these equations, with initial conditions, will completely describe the hydrodynamical system. Several methods have been put forth, both analytical and numerical. The two most prominent analytical methods are the Landau and Bjorken models. The difference between the two pictures is how to handle the fireball's nuclear stopping power, or how the nuclei pass through one another.

Landau's description, developed in the 1950's, assumes full stopping power where the nuclei hit and progress only a small distance compared to the transverse size. Thermalization occurs very quickly and then the fireball evolves hydrodynamically. The picture assumes isentropic flow with no dissipative terms. One may calculate the rapidity distribution and obtain a Gaussian shape. For further discussion see the original text [24] or the more recent [27]. A comparison with data between the Landau Gaussian distribution, along with corrections, can be seen in figure 2.1. The edges are well fit, but the curvature in the $|y| < 1$ range should typically be more flat.

On the other hand, Bjorken's picture came thirty years later and assumed full transparency [28]. The nuclei pass through one another and expansion occurs homogeneously in the longitudinal direction. Thereby, a fluid element at x^1 distance from the collision is receding at velocity x^1/t, where t is the time since the collision. Another way of expressing the homogeneous nature of the expansion is to equate the spacetime rapidity with the fluid's kinetic rapidity

$$\tau = \sqrt{x^+ x^-} = \sqrt{t^2 - (x^1)^2}, \quad y = \frac{1}{2} \ln \frac{x^+}{x^-} = \frac{1}{2} \ln \left(\frac{t + x^1}{t - x^1} \right). \tag{2.15}$$

The observables, ε, T, s, ..., are all rapidity independent and become functions of only the proper time of the fluid. The hydrodynamical expansion occurs once the
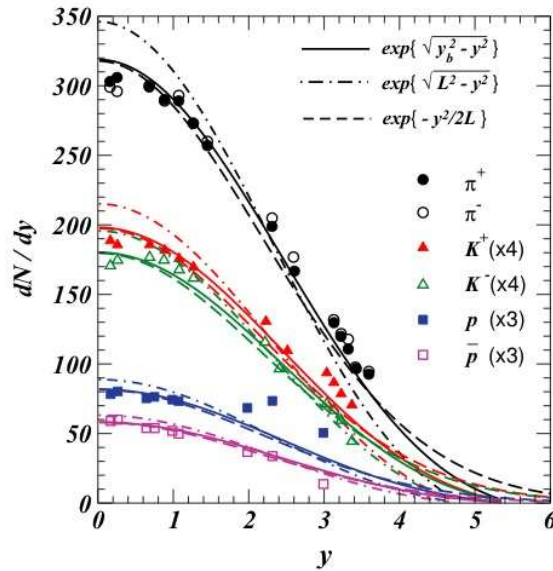
Figure 2.1: Gaussian fits to particle rapidity density data.
The Gaussian fits $|y| > 1$ well but overshoots the $|y| < 1$ range [27].

distance between nuclei is greater than their nuclear diameter. The characteristic behavior of Bjorken's particle production, shown in Section 2.1.2, is a constant. This works well with the data (figures 1.14,2.1) in the rapidity window $|y| < 1$. We will use Bjorken's picture for the rest of this work.

2.1.2 Bjorken hydrodynamics

Bjorken's hydrodynamical model for relativistic heavy ion collisions provided a simple description to data collected at CERN's SPS and ISR. The basic idea is to consider only the central rapidity region where particle distribution at large angles becomes independent of the rapidity in the center-of-mass frame. The homogeneous longitudinal expansion thereby forces the thermodynamic quantities to be dependent only on the proper time. A numerical solution accounting for being outside the central rapidity region and freeze out is shown in figure 2.2.

To properly understand the rapidity invariance it is convenient to change coordinates from Minkowski space to incorporate the rapidity y and proper time
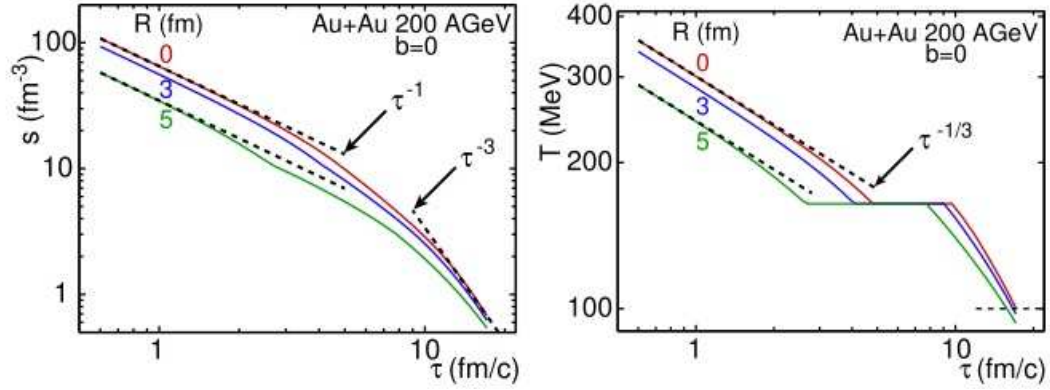
Figure 2.2: Entropy and temperature dependence on proper time at RHIC.
Entropy density and temperature numerically evaluated at different points from the center of the
beam (0, 3, and 5 fm). The dashed lines correspond to an initial one-dimensional expansion
followed by three-dimensional expansion after freezeout [29].

τ in the beam's longitudinal plane. We start with four-dimensional Minkowski space
(2.9) spanned by coordinates x^μ ($\mu = 0, 1, 2, 3$) and define

$$x^0 = t = \tau \cosh y, \qquad x^1 = \tau \sinh y. \tag{2.16}$$

The transverse coordinates are denoted by $x^\perp = (x^2, x^3)$ and the Minkowski space is
transformed to

$$ds^2 = -d\tau^2 + \tau^2 dy^2 + (dx^\perp)^2. \tag{2.17}$$

The stress tensor describing a fluid that follows rapidity invariance, $y \rightarrow -y$
invariance, translational and rotational symmetry in the transverse plane is of the
form

$$T^{\mu\nu} = \begin{pmatrix} T^{\tau\tau} & 0 & 0 & 0 \\ 0 & T^{yy} & 0 & 0 \\ 0 & 0 & T^{xx} & 0 \\ 0 & 0 & 0 & T^{xx} \end{pmatrix}. \tag{2.18}$$

24

From the local conservation law,

$$\nabla_\alpha T^{\alpha\beta} = \partial_\alpha T^{\alpha\beta} + \Gamma^\alpha_{\alpha\lambda} T^{\lambda\beta} + \Gamma^\beta_{\alpha\lambda} T^{\alpha\lambda} = 0, \tag{2.19}$$

and using the Christoffel symbols, $\Gamma^y_{y\tau} = \frac{1}{\tau} = \Gamma^y_{\tau y}$ and $\Gamma^\tau_{yy} = \tau$, we derive relations between the components of the stress tensor.

Choosing $\beta = \tau$, we obtain

$$\partial_\tau T^{\tau\tau} + \frac{1}{\tau} T^{\tau\tau} + \tau T^{yy} = 0. \tag{2.20}$$

One more relation is a consequence of conformal invariance. Demanding tracelessness, we obtain

$$- T^{\tau\tau} + \tau^2 T^{yy} + 2 T^{xx} = 0. \tag{2.21}$$

Solving for the components T^{yy} and T^{xx}, the stress-energy tensor in terms of $\varepsilon = T^{\tau\tau}$ (energy density) can be written as

$$T^{\mu\nu} = \begin{pmatrix} \varepsilon & 0 & 0 & 0 \\ 0 & -\frac{1}{\tau}\partial_\tau\varepsilon - \frac{1}{\tau^2}\varepsilon & 0 & 0 \\ 0 & 0 & \varepsilon + \frac{1}{2}\tau\partial_\tau\varepsilon & 0 \\ 0 & 0 & 0 & \varepsilon + \frac{1}{2}\tau\partial_\tau\varepsilon \end{pmatrix}. \tag{2.22}$$

We now compare this with the stress tensor for a perfect fluid in the rest frame $u^\mu = (1, 0, 0, 0)$

$$T^{\mu\nu} = (\varepsilon + p)u^\mu u^\nu + p\eta^{\mu\nu}, \tag{2.23}$$

where $\eta_{\mu\nu}$ corresponds to the metric (2.17). This allows us to deduce the system's energy density and pressure follow

$$\varepsilon, \; p \sim \frac{1}{\tau^{4/3}}. \tag{2.24}$$

25

Further, the entropy current of a perfect fluid is conserved

$$\nabla_\mu s^\mu = \nabla_\mu \left(\frac{\varepsilon + p}{T} u^\mu \right) = 0, \tag{2.25}$$

allowing for the entropy and temperature to be calculated as

$$s \sim \frac{1}{\tau}, \quad T \sim \frac{1}{\tau^{1/3}}. \tag{2.26}$$

The particle number is proportional to the entropy of the system. If we consider a slab in the x^1 direction at fixed time t_F (the time of hadronic freeze out), the entropy is given by

$$dS = su^0 dx^1 \Big|_{t=t_F} = \frac{t}{\cosh y} \frac{s_0}{\tau} dy \Big|_{t=t_F} = s_0 dy. \tag{2.27}$$

From this, it is clear

$$\frac{dN}{dy} \propto s_0, \tag{2.28}$$

and $\frac{dN}{dy}$ is independent of y. Thus, there is a plateau in the particle production for Bjorken's model.

We may continue the derivation to include viscous terms [30]. Starting with (2.1) and (2.5), conformal invariance of the plasma gives

$$T^\mu_\mu = -\varepsilon + 3p - 3\zeta \nabla_\lambda u^\lambda = 0, \tag{2.29}$$

which must be valid in all frames. This is accomplished only with $\varepsilon = 3p$ and zero bulk viscosity, $\zeta = 0$. We now wish to choose a local rest frame for a fluid that retains all of the symmetries of a perfectly boost-invariant system. In our coordinate system

26

(2.17), this remains $u^\mu = (1, 0, 0, 0)$. The stress tensor is then found as

$$T^{\mu\nu} = \begin{pmatrix} \varepsilon & 0 & 0 & 0 \\ 0 & \frac{1}{\tau^2}\left(p - \frac{4}{3}\frac{\eta}{\tau}\right) & 0 & 0 \\ 0 & 0 & p + \frac{2}{3}\frac{\eta}{\tau} & 0 \\ 0 & 0 & 0 & p + \frac{2}{3}\frac{\eta}{\tau} \end{pmatrix}$$

$$= \begin{pmatrix} \varepsilon & 0 & 0 & 0 \\ 0 & -\frac{1}{\tau}\partial_\tau\varepsilon - \frac{1}{\tau^2}\varepsilon & 0 & 0 \\ 0 & 0 & \varepsilon + \frac{1}{2}\tau\partial_\tau\varepsilon & 0 \\ 0 & 0 & 0 & \varepsilon + \frac{1}{2}\tau\partial_\tau\varepsilon \end{pmatrix}. \qquad (2.30)$$

Upon comparison we are led to an equation relating the energy density and shear viscosity

$$\partial_\tau\varepsilon + \frac{4}{3}\frac{\varepsilon}{\tau} - \frac{4}{3}\frac{\eta}{\tau^2} = 0. \qquad (2.31)$$

To solve this, we make an assumption on the behavior of η. For our purposes, we consider τ to be large compared to the relaxation time scale of the problem. This allows us to consider only powers of τ as solutions for η. For hydrodynamic theories built as the long-distance, low-frequency limit of an interacting theory, it has been suggested that $\eta \propto T^3$ [26]. With this in mind, we constrain

$$\eta = \frac{\eta_0}{\tau}, \qquad (2.32)$$

and find the solution to (2.31) as

$$\varepsilon = \frac{\varepsilon_0}{\tau^{4/3}} - \frac{2\eta_0}{\tau^2}. \qquad (2.33)$$

Even though we have found the energy density behavior with respect to the proper time (and pressure with the equation of state), there are limitations to our solution. The first is the determination of dissipative constant, η_0, or any dissipative process'

27

coefficient we may wish to study. A microscopic theory is required to determine a value. Hydrodynamics has nothing to say. Moreover, there is no good way to determine the temperature anymore. For the ideal fluid, we were able to use the thermodynamic relations and conservation of entropy, but for this system, entropy is created due to the shear viscosity. We may argue that the energy density and temperature should be related in a Stefan-Boltzmann way, but that is far from rigorous. To derive the entropy density, similar obstacles impede us. A stronger theory must be used, and for RHIC, this necessitates an understanding of the gauge theory that governs the fireball's constituents.

2.2 Microscopics

It was originally hoped that RHIC would provide enough energy to completely break QCD's confinement, and the quarks and gluons would no longer exist only in the hadronic bound states. Hence, the particles would be weakly interacting and the perturbative methods of QCD could be applied. However, this was not the case as the transition temperature, estimated at $T_C \sim 170$ MeV, is on the same order as RHIC. This regime, $T \sim T_C$, is where the strongly coupled quark-gluon plasma lives and the quarks and gluons, while no longer confined, continue to feel the presence of one another [29].

Lattice QCD developed as a means to handle the strongly interacting behavior. The quarks and gluons are placed on a Euclidean spacetime lattice and QCD is numerically calculated from the partition function

$$Z_{QCD} = \int \mathcal{D}[A] \prod_f \mathcal{D}[\psi_f]\mathcal{D}[\bar{\psi}_f] exp\left(-\int d^4x \mathcal{L}_{QCD}[A, \psi_f, \bar{\psi}_f]\right), \qquad (2.34)$$

which is a path integral over the gluon field A and quarks $\psi_f, \bar{\psi}_f$. The discrete spacetime provides a natural momentum cutoff (1/lattice spacing), thereby regularizing

the theory [31]. This has led to insights into the strongly coupled state of QCD, including a possible phase diagram shown in figure 2.3.

However, progress has been difficult to achieve in static scenarios and less is known for a dynamic plasma – especially near the transition temperature. One of the major features of the plasma at RHIC is the hydrodynamic behavior, and QCD fails to offer an explanation of why it is relevant from first principles. Extracting information for quantities like viscosity or heat conduction are acutely difficult from a QCD perspective, and other dynamic properties, such as jet quenching, are out of the question.

2.2.1 Anti-de Sitter space/conformal field theory correspondence

In an interesting fashion, string theory can play a major role in the promotion of physics at RHIC. One of the hallmarks of the theory has been the conception of an anti-de Sitter space/conformal field theory correspondence. It is a conjecture
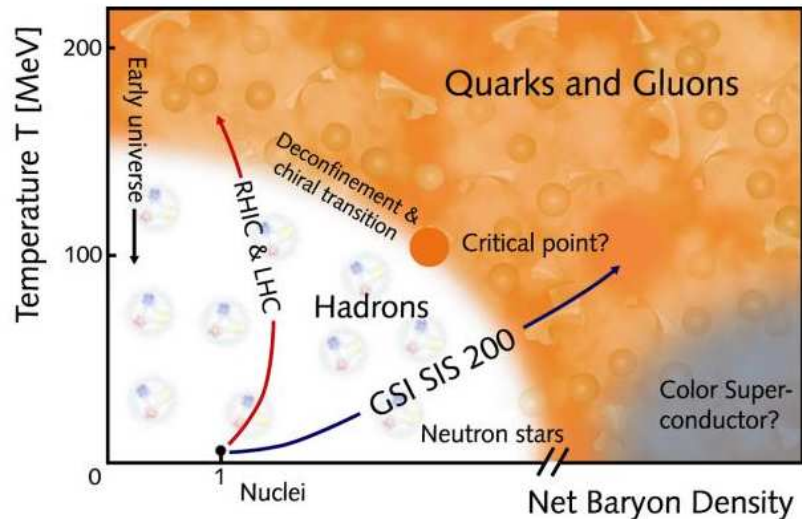
Figure 2.3: QCD phase diagram.
RHIC experiments are believed to follow the red line [32].

that states that a non-gravitational gauge theory has an equivalent formulation in terms of a quantum theory of gravity with extra dimensions [33, 34]. The best understood duality is between type IIB string theory in $\text{AdS}_5\times\text{S}^5$ and a maximally supersymmetric $\mathcal{N} = 4$ super Yang-Mills (SYM) gauge theory on the Minkowski space boundary of AdS_5. The $\mathcal{N} = 4$ SYM theory is certainly not QCD as there is no confinement among other aspects. However, once the limit of confinement is breached, $\mathcal{N} = 4$ SYM results seem to be relevant to QCD. In addition, the duality does not have to take place with an AdS_5 and 4D Minkowski space boundary. String theory also allows for dualities between other (warped) manifold's and their boundaries.

The correspondence was conjectured by Maldacena while studying the type IIB string theory in 10 dimensions [33]. A direct proof of the conjecture is not available, but arguments are highly refined and critically tested [34]. In this work, we will present a topical derivation. One may first see the connection between the theories by analyzing their symmetries. The $\mathcal{N} = 4$ SYM theory Lagrangian, with SU(N) gauge group, is uniquely given as (see Appendix A) [35]

$$
\begin{aligned}
\mathcal{L} &= -\frac{1}{2g_{YM}^2}Tr\Big\{\frac{1}{2}F^{\mu\nu}F_{\mu\nu} + D_\mu\phi^i D^\mu\phi^i + \frac{1}{2}[\phi^i,\phi^j][\phi^i,\phi^j] \\
&+ i(\bar{\lambda}_A\bar{\sigma}^\mu D_\mu\lambda^A + \lambda^A\sigma^\mu D_\mu\bar{\lambda}_A) + [\bar{\phi}_{AB},\lambda^A]\lambda^B - [\phi^{AB},\bar{\lambda}_A]\bar{\lambda}_B\Big\}. \quad (2.35)
\end{aligned}
$$

Here A_μ are the gauge fields, ϕ^i the scalars, and λ^A are Weyl spinors with $i = 1,\ldots,6$ and $A,B = 1,\ldots,4$. The global symmetry of the theory forms the projective special unitary group PSU(2,2|4), but the bosonic sector is reduced to SO(2,4)$\times$SO(6)$_R$. The bosonic symmetries can be seen as the combination of the theory's scale invariance, Poincaré symmetry, and six scalars.

The superstring theory living in $\text{AdS}_5\times\text{S}^5$ has the same global symmetry. Directly, one may note that the S^5 gives the SO(6)$_R$. The SO(2,4) is seen by realizing AdS_5 can be described as the five dimensional manifold

$$
-X_0^2 - X_1^2 + X_2^2 + X_3^2 + X_4^2 + X_5^2 = -L^2, \quad (2.36)
$$

which is a generalization of a hyperbola. This can be achieved with the coordinates

$$X_0 = \frac{r}{2L}\left(\frac{L^2}{r^2} + L^2 + \frac{x_2^2 + x_3^2 + x_4^2 - t^2}{L^2}\right), \qquad X_1 = \frac{tr}{L},$$

$$X_5 = \frac{r}{2L}\left(\frac{L^2}{r^2} - L^2 + \frac{x_2^2 + x_3^2 + x_4^2 - t^2}{L^2}\right), \qquad X^i = \frac{x^i r}{L}, \qquad (2.37)$$

and embedded in a six dimensional flat space

$$\begin{aligned}
ds_6^2 &= -dX_0^2 - dX_1^2 + dX_2^2 + dX_3^2 + dX_4^2 + dX_5^2 \\
&\to ds_{AdS}^2 = \frac{r^2}{L^2}\left(-dt^2 + dx_2^2 + dx_3^2 + dx_4^2\right) + \frac{L^2 dr^2}{r^2}. \qquad (2.38)
\end{aligned}$$

Therefore, the combined symmetry is SO(2,4)×SO(6)$_R$. One may perform a check using the massless fields in the string theory to realize the full PSU(2,2|4) (see [36] and references therein).

The connection between the two systems is made more clear with a stringy construction. This is realized as a stack of D-branes. D-branes are extended objects in string theory where fundamental strings end. The type we are concerned with are D3-branes which have three spatial dimensions. If N D3-branes are stacked on top of one another, the choice of brane where a string ends provides precisely the degrees of freedom to form an SU(N) gauge theory with the low energy theory described by an $\mathcal{N} = 4$ SYM theory. The characteristic scales of the theory are given by the string coupling g_s and string length l_s. The theories' couplings are related by

$$g_{YM}^2 = 4\pi g_s, \qquad (2.39)$$

where g_{YM} is the SYM coupling. The low energy theory is described by two separate types of excitations. The first being the SYM theory of open strings and the second that of closed strings away from the stack of branes.

The next step is to consider the amount of energy in the stack of branes. As more and more are taken into account by the scenario, the spacetime will begin to

warp. The warping should be in accordance to the equations of IIB supergravity. The solution to the supergravity equations was found in [37], assuming the stringy corrections are turned off ($g_{YM}^2 N >> 1$),

$$ds^2 = \frac{1}{\sqrt{1 + 4\pi g_s N l_s^4/r^4}}(-dt^2 + d\vec{x}^2) + \sqrt{1 + 4\pi g_s N l_s^4/r^4}(dr^2 + r^2 d\Omega_5^2). \quad (2.40)$$

The supergravity solution also contains a scalar field and a five form which are not pertinent for this discussion. This system has similar features to the first perspective, namely the two sets of excitations. It has those far away ($r \to \infty$) which are free closed strings and those near the horizon. One may examine the metric more closely in the near horizon limit,

$$ds^2 = \frac{r^2}{l_s^2\sqrt{4\pi g_s N}}(-dt^2 + d\vec{x}^2) + \frac{l_s^2\sqrt{4\pi g_s N}}{r^2}(dr^2 + r^2 d\Omega_5^2), \quad (2.41)$$

which is precisely AdS$_5\times$S^5 with the AdS and S^5 radii of $L^2 = l_s^2\sqrt{4\pi g_s N}$ as seen from (2.38).

The argument put forth by Maldacena was that these are two sides of the same coin. The first perspective of the brane system had SYM and closed string excitations, while the second has excitations described by anti-de Sitter space and closed string excitations. The closed string excitations should define the same theory. Therefore the conjecture is the equivalence between the two previously dissimilar theories – $\mathcal{N} = 4$ super Yang-Mills theory in four dimensions and IIB supergravity in 10 dimensional AdS$_5\times$S^5. Moreover, the correspondence may be built from near extremal D3-branes, which from a supergravity perspective, is black hole in AdS space. The duality then connects the black hole to a conformal field theory at non-zero temperature. This highly nontrivial prediction from string theory is perhaps its most significant result to date.

For many calculations the compact component of the 10 dimensional manifold decouples from the system and we are left with a direct correspondence between an

anti-de Sitter spacetime and a holographic conformal field theory on the boundary. This holds for several other combinations of geometries, such as a duality between AdS_d and conformal field theory in $d-1$ dimensions. The full AdS spacetime is referred to as the "bulk" and is where the Einstein equations must be satisfied. Figure 2.4 shows a visualization of the correspondence.

One finds the correspondence is particularly useful in certain regimes. The common procedure is take the 't Hooft limit

$$N \to \infty , \quad g_{YM}^2 N \gg 1. \tag{2.42}$$

Here $g_{YM}^2 N$ is the SYM coupling and we see this describes a strongly interacting gauge theory – similar to RHIC. Moreover, the quantum corrections in type IIB string theory are negligible and it simplifies to classical supergravity. Now via the AdS/CFT correspondence, we can answer any question about the strongly coupled SYM gauge theory by performing gravity calculations. Some of our concerns, in this text, come from a direct duality of the thermodynamic quantities. For example, when
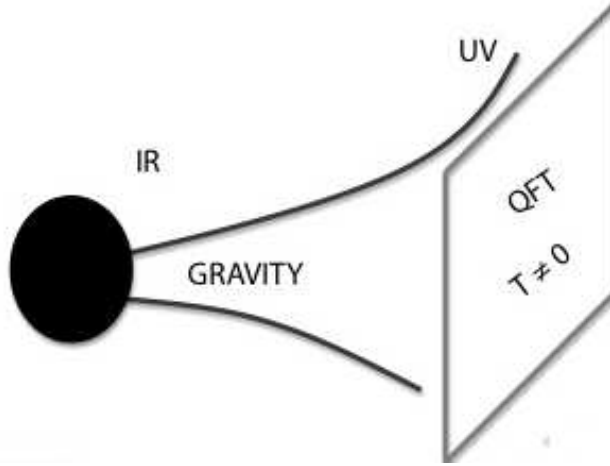
Figure 2.4: Visualization of the AdS/CFT correspondence.
Gravity exists in the bulk while the field theory lives on the boundary of the AdS space [38].

the AdS space contains a black hole with Hawking temperature T_H and entropy S, the dual gauge theory exists at temperature T_H and entropy S.

Furthermore, there are prescriptions for which fields in AdS are dual to which operators in the gauge theory, called the AdS/CFT dictionary, and are discussed in [33, 34]. The principal operator we are interested in is the stress-energy tensor. The correspondence relates the gravitational metric with the vacuum expectation value of the stress-energy tensor for the conformal field theory living on the boundary. This can be seen as the varying of the gravitational action with respect to the induced boundary metric ($\gamma_{\mu\nu}$)

$$\langle T^{\mu\nu} \rangle = \frac{2}{\sqrt{-\gamma}} \frac{\delta S_{grav}}{\delta \gamma_{\mu\nu}}. \tag{2.43}$$

To calculate a finite stress-energy tensor, one must introduce a series of boundary curvature invariants to the action [39, 40]. For AdS_d, this is accomplished with

$$S = -\frac{1}{16\pi G} \int_{\mathcal{M}} d^d x \sqrt{-g} \, (R - 2\Lambda_{AdS}) - \frac{1}{8\pi G} \int_{\partial\mathcal{M}} d^{d-1} \sqrt{-\gamma}\Theta + \frac{1}{8\pi G} S_{ct}(\gamma), \tag{2.44}$$

where Θ is the extrinsic curvature of the boundary and S_{ct} contains the curvature invariants regularizing the theory. A useful characteristic of the boundary comes in the form of a unit normal vector $\hat{n}^\mu$, defined as $\gamma_{\mu\nu}\hat{n}^\nu = 0$. The induced metric is a combination of the five dimensional gravity metric and the normal

$$\gamma_{\mu\nu} = g_{\mu\nu} - \hat{n}_\mu \hat{n}_\nu, \quad \gamma^{\mu\nu} = g^{\mu\alpha} g^{\nu\beta} \gamma_{\alpha\beta}. \tag{2.45}$$

The extrinsic curvature can then be written as

$$\Theta_{\mu\nu} = -\frac{1}{2}(\nabla_\mu \hat{n}_\nu + \nabla_\nu \hat{n}_\mu), \quad \Theta = g^{\mu\nu}\Theta_{\mu\nu}, \tag{2.46}$$

where ∇_μ is the covariant derivative for the induced metric. As for the counter term, the divergences' behavior changes depending on the dimension. For AdS_5, the term

is given as

$$S_{ct} = -3 \int_{\partial \mathcal{M}} d^{d-1} \sqrt{-\gamma} \left(1 - \frac{R}{12} \right), \tag{2.47}$$

where R is the four dimensional Ricci scalar. Once this is all in place, the action is varied to find the boundary stress-energy VEV,

$$\langle T^{\mu\nu} \rangle = \frac{1}{8\pi G} \left[\Theta^{\mu\nu} - \Theta\gamma^{\mu\nu} - 3\gamma^{\mu\nu} - \frac{1}{2} \left(R_{\mu\nu} - \frac{1}{2}R\gamma_{\mu\nu} \right) \right], \tag{2.48}$$

with all quantities in terms of the four dimensional boundary.

This work was advanced in Ref. [41], where it was promoted to express the boundary stress energy tensor in terms of the five dimensional gravity metric near the boundary. The procedure is referred to as holographic renormalization. The metric must first be brought to the form of a general asymptotically AdS metric in Fefferman-Graham coordinates

$$ds^2 = \frac{g_{\mu\nu}dx^\mu dx^\nu + dz_{FG}^2}{z_{FG}^2}. \tag{2.49}$$

Near the boundary at $z_{FG} = 0$, we may expand

$$g_{\mu\nu} = g_{\mu\nu}^{(0)} + z_{FG}^2 g_{\mu\nu}^{(2)} + \cdots + z_{FG}^{d-1} g_{\mu\nu}^{(d-1)} + h^{(d-1)} z_{FG}^{d-1} \ln z_{FG}^2 + \mathcal{O}(z_{FG}^d), \tag{2.50}$$

where $g_{\mu\nu}^{(0)} = \eta_{\mu\nu}$. For the metrics used in this work, $g_{\mu\nu}^{(d-1)}$ is proportional to the vacuum expectation value of the stress-energy tensor,

$$\langle T_{\mu\nu} \rangle = \frac{d-1}{16\pi G_d} g_{\mu\nu}^{(d-1)}, \tag{2.51}$$

where G_d is Newton's constant in the bulk.

Similar derivations may be done relating various supergravity fields with conformal field theory operators. One commonly used duality is between a scalar field in the supergravity (dilaton) and a nonzero expectation value for the trace of the CFT's field strength tensor squared. In this case, the mass of the dilaton determines the

operator's dimension. In Chapter 3 we turn on an electromagnetic gauge field in the supergravity and relate it to a conserved current in the hydrodynamic description of the CFT.

2.2.2 AdS/CFT correspondence applications

It might seem odd that we can take the limit $N \to \infty$ of a SYM theory and hope to describe a system like RHIC. To compare, QCD has $N = 3$ and is a chiral theory, and $\mathcal{N} = 4$ SYM does not contain quarks in the fundamental representation, is supersymmetric, and does not feature confinement.

However, when the energy scale approaches that at RHIC, there are qualities that QCD and $\mathcal{N} = 4$ SYM share. For example we may look at the ratio between the energy density at finite temperature and the energy density of a free gas shown in figure 2.5. Both ratios have a deficit of ~ 20 percent from unity – a common occurrence with QCD and SYM thermodynamic quantities in RHIC's range.

There is a dramatic rise to a plateau around the confining temperature T_C. Once this is crossed, confinement is broken and differences between QCD and $\mathcal{N} = 4$ SYM are tamed. In this regime QCD is no longer chiral and preliminary lattice calculations suggest scale invariance exists – both features of the SYM field. Moreover, once $T \neq 0$ the SYM's supersymmetry is broken. Additionally, for highly excited many body systems, differences at the microscopic level have small effects and the macroscopic behaviors will be similar between two strongly coupled theories.

These arguments, combined with the tractability of an AdS/CFT correspondence calculation, has motivated the use of SYM theories to approximate QCD. Furthermore, using the AdS/CFT correspondence, one can extract the information for numerous gauge theories from their gravitational duals, not just $\mathcal{N} = 4$ SYM. By warping the AdS space or adding D-branes, one may lessen the symmetries of the gauge field and/or alter fundamental characteristics. Models have been found that allow for confinement via a truncation of the AdS space[43]. By adding probe

D7-branes to the D3-brane system, quarks can be seen to exist in the fundamental representation [44]. Additionally, chiral symmetry breaking occurs in a D8 antiD8-brane setup [45].

One particular area of interest with respect to RHIC is jet quenching. Using a D7-brane as a probe to an AdS black hole, we may construct both quarks and mesons as strings with one end on the D7-brane and the other end on either the black hole's horizon or the D7-brane [46]. A quark's energy will dissipate into the black hole leading to jet quenching. The calculations may be performed in two different ways. One is to "kick" the string and see how it slows down to calculate the momentum rate of change. The other is to give the string a constant velocity through the plasma and calculate how much force it takes to keep it moving. The results, plus an appropriate scaling, are on the order of RHIC's data.

Another path is to search for universality between gauge theories. If a quantity is found to be true for a wide range of theories, then perhaps it is a characteristic for all
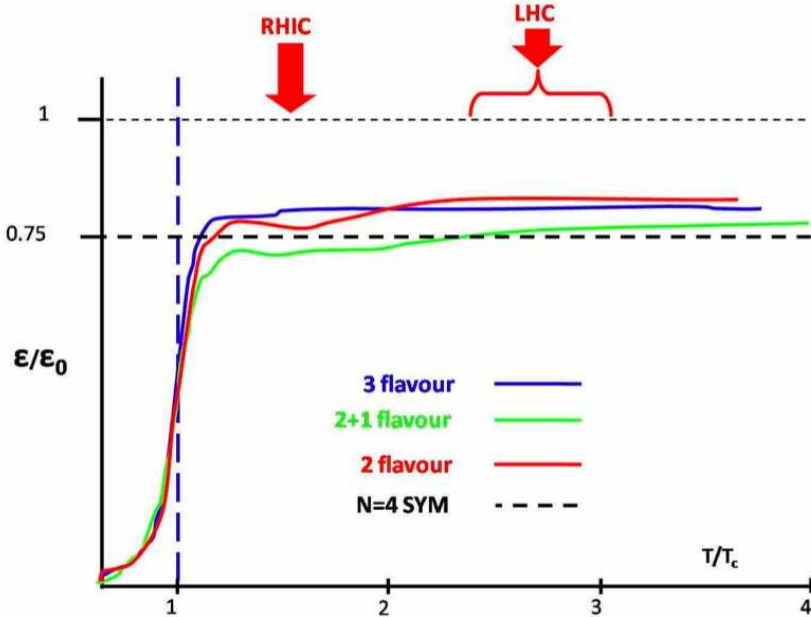
Figure 2.5: Energy density ratio between coupled gauge theories and free gas. The dotted line is the SYM ratio with the other representing lattice QCD calculations[42].

gauge theories, including QCD. One of the most intensely studied characteristics [26] has provided a new bound on the ratio of viscosity (a hydrodynamical quantity) to entropy density of a strongly interacting plasma. Originally accomplished using the AdS_5/CFT_4 correspondence by Policastro, Son and Starinets, it has been extended to incorporate several variations of the duality.

The physics behind hydrodynamics, thermodynamics and gravity have been known to be similar for a long time. A map has been created that translates quantities from gravity to hydrodynamics and thermodynamics [47], but the underlying principle remains a mystery. Qualitatively shear viscosity in a fluid plays the role of dampening. If the fluid is disturbed by a small perturbation, the constituents will feel a force between one another and transfer momentum until the system settles back to a steady state. This is the same behavior as a particle falling into a black hole. When a perturbative field is absorbed by a black hole, the horizon fluctuates, characterized by quasinormal modes, until it settles back to a static horizon. A quick illustration is shown in figure 2.6.
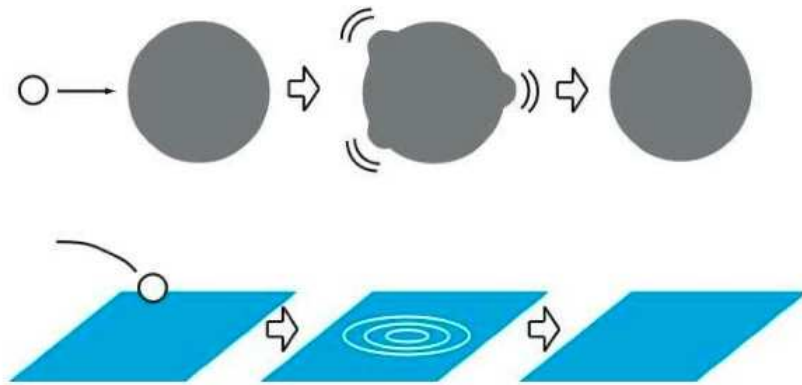
Figure 2.6: Perturbations acting on a fluid and a black hole.
The black hole and fluid both contain dampening [48].

38

The standard Kubo formula relates the shear viscosity of a fluid to the correlator of a transverse space-space component of the stress energy tensor as

$$\eta = \lim_{\omega \to 0} \frac{1}{2\omega} \int d^4 x e^{i\omega t} \langle [T_{x^2 x^3}(x), T_{x^2 x^3}(0)] \rangle. \tag{2.52}$$

Here ω is the frequency of the perturbation and $\langle \ldots \rangle$ is an average over the equilibrium thermal ensemble.

On the gravitational side, this is dual to the absorption of a graviton. The cross section of an AdS$_5$ black hole absorbing a transverse graviton, or equivalently for our purposes, a minimally coupled scalar, is given by

$$\sigma(\omega) = \frac{8\pi^5 L^8}{N^2} \frac{1}{2\omega} \int d^4 x e^{i\omega t} \langle [T_{x^2 x^3}(x), T_{x^2 x^3}(0)] \rangle. \tag{2.53}$$

We now note

$$\eta = \frac{N^2}{8\pi^5 L^8} \sigma(0). \tag{2.54}$$

The best feature of this derivation is that we do not have to calculate the strongly coupled theory's correlation functions. Instead, we turn our attention to the supergravity description of the graviton. We can take the AdS$_5 \times$S^5 background, given by

$$ds^2 = \frac{1}{\sqrt{1 + \frac{L^4}{r^4}}} \left(-(1 - \frac{r_0^4}{r^4}) dt^2 + d\vec{x}^2 \right) + \sqrt{1 + \frac{L^4}{r^4}} \left(\frac{dr^2}{1 - \frac{r_0^4}{r^4}} + r^2 d\Omega_5^2 \right), \tag{2.55}$$

and study the wave equation for a scalar perturbation

$$\partial_\mu (\sqrt{-g} g^{\mu\nu} \partial_\nu \phi) = \phi'' + \frac{5r^4 - r_0^4}{r(r^4 - r_0^4)} \phi' + \omega^2 \frac{r^4(r^4 + L^4)}{(r^4 - r_0^4)^2} \phi = 0. \tag{2.56}$$

The solution is found by matching the wave equation of three regions. The first is just outside the horizon, $r > r_0$, $r - r_0 \ll r_0$, the second at $r_0 < r \ll \frac{1}{\omega}$, and the third being $r \gg 1 \gg r_0$. The absorption probability (P) is related to the cross-section via

$\sigma = \frac{32\pi^2}{\omega^5}P$ and found as the ratio of the flux at r_0 to the flux of the incoming wave at large distances. The absorption probability is found as

$$P = \frac{\pi}{32}\omega^5 r_0^3 L^2, \tag{2.57}$$

and we can now express the shear viscosity in terms of the temperature (using $r_0 = \pi L^2 T$) as

$$\eta = \frac{\pi}{8}N^2 T^3. \tag{2.58}$$

The entropy can be calculated directly from the area of the black hole with the standard definition

$$S = \frac{A}{4G} = \frac{\pi^2}{2}N^2 T^3, \tag{2.59}$$

where we used $A = \pi^3 r_0^3 L^2$ and $G = \frac{\pi^4 L^8}{2N^2}$. Putting the two pieces together, we arrive at our goal,

$$\frac{\eta}{s} = \frac{1}{4\pi}. \tag{2.60}$$

Policastro, Son, and Starinets' result constitutes one of the most powerful calculations from string theory as related to experiment [26]. As stated before, this has been shown in a multitude of different systems with gravitational duals and is suggested to be universal. However, recent constructions using higher derivative corrections to the Einstein-Hilbert action or a hyperbolic AdS boundary have shown to slightly lower this bound [49], but these are suggested to violate causality [50].

Experiments have been performed at RHIC to test the viscosity-to-entropy-density ratio and it appears that the data is consistent with a near, if not full, saturation of this bound [29]. Moreover, accounting for viscosity constitutes far reaching affects in hydrodynamical extraction of physics from RHIC data due to a high sensitivity on η. When the ratio was first presented, there was no other theory that could reach this order of magnitude. This value provided enough motivation for the creation of the field applying gravity calculations to the physics at RHIC.

2.2.3 AdS/CFT correspondence and boost invariance

Now we may ask what the correspondence can say about a longitudinal expansion of a gauge theory plasma. This was the question posed by Janik and Peschanski in Ref. [18]. The course of action is to implement the same symmetries as discussed by Bjorken in his hydrodynamical model but to a five dimensional asymptotically AdS space. We will enforce these symmetries in an ansatz for the gravitational metric, solve the Einstein equations, and then extract the physics of the dual hydrodynamic system.

The five dimensional space is spanned by the same coordinates discussed in Bjorken's system – proper time (τ), rapidity (y) and transverse coordinates $(x^\perp = (x^2, x^3))$. Additionally, we have the fifth dimension that measures the distance away from the AdS boundary (z). We wish to implement boost invariance, symmetry under reflection in the longitudinal direction $(y \to -y)$, plus translational and rotational invariance. This is achieved with the ansatz

$$ds^2 = \frac{1}{z^2} \left[-e^{a(\tau,z)}d\tau^2 + \tau^2 e^{b(\tau,z)}dy^2 + e^{c(\tau,z)}dx^{\perp 2} + dz^2 \right], \tag{2.61}$$

with which will solve the Einstein equations (see Appendix B)

$$R_{\alpha\beta} - \frac{1}{2}g_{\alpha\beta}R + \Lambda g_{\alpha\beta} = 0, \tag{2.62}$$

where Λ is the standard AdS_5 cosmological constant, $\Lambda = -6$. Interestingly, if we introduce the scaling variable

$$v = \frac{z}{\tau^\sigma}, \tag{2.63}$$

the Einstein equations can be expressed as a power series in τ. This in turn constrains the functions in the ansatz to be expressed in an identical way

$$E_{\mu\nu} = E^{(0)}(v) + \tau^{-2/3}E^{(1)}(v) + \cdots = 0, \quad a(\tau, z) = a_0(v) + \tau^{-2/3}a_1(v) + \ldots,$$

$$b(\tau, z) = b_0(v) + \tau^{-2/3}b_1(v) + \ldots, \quad c(\tau, z) = c_0(v) + \tau^{-2/3}c_1(v) + \ldots . \tag{2.64}$$

The zeroth order equations can be solved by

$$a_0(v) = A(v) - 2m(v),$$

$$b_0(v) = A(v) + 2(4\sigma - 1)m(v),$$

$$c_0(v) = A(v) + 2(1 - 2\sigma)m(v), \tag{2.65}$$

where

$$A(v) = \frac{1}{2}\left[\ln(1 + \Delta v^4) + \ln(1 - \Delta v^4)\right],$$

$$m(v) = \frac{1}{4\Delta}\left[\ln(1 + \Delta v^4) + \ln(1 - \Delta v^4)\right], \tag{2.66}$$

with

$$\Delta = \sqrt{\frac{1}{3}(6\sigma^2 - 4\sigma + 1)}. \tag{2.67}$$

Upon further inspection of the curvature invariants, we find the Kretschmann scalar, $\mathcal{R}^2 = R^{\alpha\beta\mu\nu}R_{\alpha\beta\mu\nu}$ has a fourth order pole in $1 - \Delta^2 v^8$. The divergence is an indication of a breakdown of the theory. However, for a special choice of σ, the pole is exactly canceled. This corresponds to

$$\sigma = \frac{1}{3}, \tag{2.68}$$

thereby constraining the type of flow of the hydrodynamics on the boundary. Alternatively, we can place the constraint that the zeroth order solution should correspond to an ideal fluid; therefore, the entropy should be conserved and arrive at the same conclusion [51].

The hydrodynamic stress energy tensor can now be extracted using holographic renormalization (2.51) for $d = 5$, giving

$$T^{\mu\nu} = \begin{pmatrix} \frac{\varepsilon_0}{\tau^{4/3}} & 0 & 0 & 0 \\ 0 & \frac{1}{\tau^2}\frac{\varepsilon_0}{3\tau^{4/3}} & 0 & 0 \\ 0 & 0 & \frac{\varepsilon_0}{3\tau^{4/3}} & 0 \\ 0 & 0 & 0 & \frac{\varepsilon_0}{3\tau^{4/3}} \end{pmatrix}. \tag{2.69}$$

This is precisely what Bjorken found in the early 1980's (2.24). However, the AdS/CFT correspondence is a more powerful theory than hydrodynamics, and we may derive the transport coefficients. The microscopics are encoded in the subleading behavior of (2.64). Several people have contributed to solving the higher order equations which account for shear viscosity [30, 52]. The Einstein equations lead to

$$a_1(v) = 2\eta_0 \frac{(9 + v^4)v^4}{9 - v^8},$$
$$b_1(v) = -2\eta_0 \frac{v^4}{3 + v^4} + 2\eta_0 \ln \frac{3 - v^4}{3 + v^4},$$
$$c_1(v) = -2\eta_0 \frac{v^4}{3 + v^4} - \eta_0 \ln \frac{3 - v^4}{3 + v^4}, \tag{2.70}$$

and with holographic renormalization we find a stress-energy tensor that matches (2.30) and (2.33). Once again we find a divergence in the Kretschmann scalar, but at second order, not first. However, this is only a problem with the choice of FG coordinates. If instead we opted for Eddington-Finklestein, we would recover the violation at first order [53, 25, 40]. The divergence is exactly cancelled with a choice of η_0, something the hydrodynamical theory could not do. The parameter is given as

$$\eta_0 = \left(\frac{\sqrt{3}}{18}\right)^{1/2}. \tag{2.71}$$

This may also be used as an alternative derivation for (2.60).

43

The ability of the AdS/CFT correspondence to derive Bjorken hydrodynamics, a relativistic heavy ion collision model developed two decades previously, from a quantum theory is the major motivation for the rest of this text. We will use the scheme from this section to analyze adding off diagonal terms to account for thermal conductivity. Additionally, we develop a framework for the time-dependent temperature and entropy concepts and how these can be used to understand the subleading corrections to the Einstein equations.

Chapter 3

AdS/CFT correspondence with heat conduction

3.1 Introduction

In an interesting work, Janik and Peschanski [18] (Sec. 2.2.3) discussed a solution to the Einstein equations in the bulk AdS space in the limit $\tau \to \infty$, where τ is the proper time in the longitudinal plane. By demanding regularity in the bulk, they showed that the acceptable solution corresponds through holographic renormalization [41] to a perfect fluid on the boundary of AdS. The work was furthered by Bak and Janik [19] who studied the Maxwell-Einstein equations in the bulk with a conserved R-charge.

Here we extend the results of [18, 19] by relaxing the constraint of invariance under reflection in the longitudinal direction. This allows us to include off-diagonal terms in the bulk metric ansatz. We solve the Maxwell-Einstein equations in the bulk in the limit $\tau \to \infty$. We obtain an exact solution and show, through holographic renormalization, that it corresponds to a nonviscous fluid of nonvanishing chemical potential. The novel characteristic is a temperature gradient in the longitudinal direction. We study the thermodynamic properties of the fluid and their relation to the form of the bulk metric.

3.2 R-charged perfect fluid

We are interested in understanding the behavior of a fluid described by a gauge theory in a four-dimensional space spanned by coordinates x^μ ($\mu = 0, 1, 2, 3$). Following [28], we introduce the proper time τ and rapidity y on the longitudinal plane, defined by

$$x^0 = \tau \cosh y, \qquad x^1 = \tau \sinh y. \tag{3.1}$$

The transverse coordinates will be denoted by $x^\perp = (x^2, x^3)$. The gravity dual of the four-dimensional theory will be five-dimensional. Let z denote the fifth dimension. We shall solve the Maxwell-Einstein equations in the bulk

$$R_{\alpha\beta} + 4g_{\alpha\beta} + \frac{1}{12} F_{\mu\nu} F^{\mu\nu} g_{\alpha\beta} - \frac{1}{2} F^\mu_\alpha F_{\beta\mu} = 0, \tag{3.2}$$

$$\nabla_\alpha F^{\alpha\mu} - \frac{\sqrt{3}}{48\sqrt{-g}} \epsilon^{\mu\alpha\beta\gamma\delta} F_{\alpha\beta} F_{\gamma\delta} = 0. \tag{3.3}$$

Following [19], we adopt the metric and field strength tensor ansatz

$$ds^2 = \frac{1}{z^2} \left[-e^{a(\tau,z)} d\tau^2 + \tau^2 e^{b(\tau,z)} dy^2 + dx^{\perp 2} + e^{d(\tau,z)} dz^2 \right], \tag{3.4}$$

$$F_{z\tau} = K(\tau, z), \tag{3.5}$$

which is the most general bulk metric obeying boost invariance, symmetry under reflection in the longitudinal direction ($y \to -y$), plus translational and rotational invariance. It is convenient to introduce the coordinate

$$v = \frac{z}{\tau^\sigma} \tag{3.6}$$

in terms of which the metric (3.4) reads

$$ds^2 = \frac{1}{v^2\tau^{2\sigma}}\left[-(e^{a(\tau,v)} - e^{d(\tau,v)}\sigma^2v^2\tau^{2(\sigma-1)})d\tau^2 + \tau^2 e^{b(\tau,v)}dy^2 + dx^{\perp 2} + e^{d(\tau,v)}\tau^{2\sigma}dv^2\right]$$
$$+ 2\sigma e^{d(\tau,v)}\frac{dvd\tau}{v\tau}, \tag{3.7}$$
$$F_{v\tau} = F(\tau, v). \tag{3.8}$$

Substituting this ansatz into the Maxwell-Einstein equations, we obtain the leading behavior in the $\tau \to \infty$ limit [18, 19]

$$\sigma = 1/3, \qquad F(\tau, v) = \frac{qv}{\tau^{1/3}},$$
$$a(v) = \ln\left(1 + \alpha v^4 + \frac{q^2}{12}v^6\right), \quad b(v) = 0, \quad d(v) = -\ln\left(1 + \alpha v^4 + \frac{q^2}{12}v^6\right) \tag{3.9}$$

in terms of arbitrary parameters α and q.

The above bulk metric may be related to the vacuum expectation value of the stress-energy tensor of the corresponding gauge theory on the boundary through holographic renormalization [41], Section 2.2.1 and Eq. (2.49). It is can be seen from the form of $g_{\mu\nu}^{(4)}$, for the special value (3.9) of σ, that the stress-energy tensor corresponds to that of a perfect fluid

$$T_{\alpha\beta} = (\varepsilon + p)u_\alpha u_\beta + p\eta_{\alpha\beta} \tag{3.10}$$

obeying the equation of state $p = \frac{1}{3}\varepsilon$ (tracelessness due to conformal invariance). Further, from the explicit form of the metric it follows that the energy density and temperature fall off, respectively, as

$$\varepsilon = \frac{3N_c^2}{8\pi^2 v_h^4}\left(1 + \frac{q^2 v_h^6}{12}\right)\tau^{-4/3}, \tag{3.11}$$

$$T = T_H = \frac{1}{\pi v_h}\left(1 - \frac{q^2 v_h^6}{24}\right)\tau^{-1/3}, \tag{3.12}$$

where we used $N_c^2 = \frac{\pi}{2G_5}$, and v_h is the position of the horizon (obeying $1 + \alpha v_h^4 + q^2 v_h^6/12 = 0$).

After performing a detailed thermodynamic analysis one finds the entropy density (s), charge density (ρ), and chemical potential (μ), respectively,

$$s = \frac{S_{bulk}}{V_{brane}} = \frac{N_c^2}{2\pi v_h^3 \tau}, \quad \rho = \frac{D^{z\tau}}{V_{brane}} = \frac{N_c^2 q}{8\pi^2 \tau}, \quad \mu = A_\tau(z_h) - A_\tau(z = 0) = \frac{q v_h^2}{2\tau^{1/3}}. \quad (3.13)$$

Expressing the energy density in terms of s and ρ,

$$\varepsilon(s, \rho) = \frac{3 s^{4/3}}{2(2\pi N_c)^{2/3}} \left(1 + \frac{4\pi^2 \rho^2}{3s^2} \right), \quad (3.14)$$

one verifies that the chemical potential is conjugate to ρ ($\mu = \partial \varepsilon / \partial \rho$).

We must take note that that the geometry is evolving and exact notions of temperature and entropy are ill defined. However, it is assumed that the approximate notions still prevail. A discussion of dynamical horizons is given in [54].

3.3 An extension of the bulk metric

Next, we consider an extension of the bulk metric (3.4) which yielded the perfect fluid model discussed above. To this end, we relax one of the conditions which led to the general form of the metric, namely the requirement of invariance under reflection in the longitudinal direction, $y \to -y$. We may then add appropriate off-diagonal terms in the bulk metric (3.7) that will lead to new nonsingular solutions to the Maxwell-Einstein equations (3.2). We therefore consider the metric and gauge field

ansatz

$$
\begin{aligned}
ds^2 &= \frac{1}{v^2 \tau^{2\sigma}} \left[-(e^{a(v)} - e^{d(v)}\sigma^2 v^2 \tau^{2(\sigma-1)})d\tau^2 + \tau^2 e^{b(v)}dy^2 + dx^{\perp 2} + e^{d(v)}\tau^{2\sigma}dv^2 \right] \\
&+ 2\sigma e^{d(v)}\frac{dvd\tau}{v\tau} + 2v^{-2}\tau^{\lambda-2\sigma}h_{\parallel}(v)d\tau dy, \\
A_\tau &= \tau^{\xi_0}A_0(v), \\
A_y &= \tau^{\xi_1}A_1(v),
\end{aligned}
\tag{3.15}
$$

where the third line of the metric consists of the off-diagonal terms added to the "perfect fluid" ansatz (3.7). The exponents $-1 < \lambda - 2\sigma, \xi_0, \xi_1 \leq 0$ of τ, where bounds are placed so that the associated functions do not singularly dominate, and the functions, $a(v)$, $b(v)$, $d(v)$ and longitudinal coupling $h_{\parallel}(v)$ are to be determined by the Maxwell-Einstein equations (3.2).

Substituting the modified ansatz (3.15) into (3.2), we obtain coupled differential equations for the various functions parametrizing the ansatz. The task of extracting the leading contribution is complicated by the fact that we now have four parameters determining the order of the expansion, σ (which is present in the perfect fluid case) as well as λ, ξ_0, and ξ_1. For consistency of the expansion, we need

$$
0 < \sigma < 2/5
\tag{3.16}
$$

to be compared with the acceptable range $0 < \sigma < 1$ in the perfect fluid case. The restricted range still includes the special value (3.9).

Let us first consider the v and τ components of the Maxwell equations. They may be factored in powers of τ as

$$
\begin{aligned}
e^{a(v)+2b(v)}v^4 A_0'(v)\left(\xi_0 + 1 - 2\sigma\right) + \mathcal{O}(\tau^{2(\lambda-1)}, \tau^{\lambda+\xi_1-2-\xi_0}, \tau^{3\lambda+\xi_1-4-\xi_0}) &= 0, \\
e^{a(v)+2b(v)}v^3 \left[A_0'(v)(2 + va'(v) - vb'(v) + vd'(v)) - 2vA_0''(v) \right] & \\
+ \mathcal{O}(\tau^{2(\lambda-1)}, \tau^{\lambda+\xi_1-2-\xi_0}, \tau^{3\lambda+\xi_1-4-\xi_0}) &= 0,
\end{aligned}
\tag{3.17}
$$

The v component is satisfied by the choice of parameter

$$\xi_0 = 2\sigma - 1. \tag{3.18}$$

The τ component is solved by

$$A_0'(v) = qv \; e^{\frac{1}{2}(a(v)-b(v)+d(v))}, \tag{3.19}$$

where q is an arbitrary integration constant.

Turning attention to the y component of the Maxwell equations, we observe that the leading behavior is not unambiguously determined without further information on the parameters. Indeed, in addition to the manifestly $\mathcal{O}(\tau^0)$ term, there are two other terms in which the exponent of τ is not necessarily negative. The y component reads

$$e^{2a(v)+b(v)}v^3 \left[A_1'(v)\left(-2 + va'(v) - vb'(v) - vd'(v)\right) + 2vA_1''(v)\right]$$
$$-\tau^{\lambda-\xi_1-1/3}e^{a(v)+b(v)}v^3$$
$$\times \left[-2vA_0'(v)h_{||}'(v) + h_{||}(v)\left(A_0'(v)\left(2 + va'(v) + vb'(v) + vd'(v)\right) - 2vA_0''(v)\right)\right]$$
$$-\tau^{3\lambda-\xi_1-7/3}v^3h_{||}^3(v)\left[A_0'(v)(2 + vd'(v)) - 2vA_0''(v)\right]$$
$$+\mathcal{O}(\tau^{2(\lambda-1)}, \tau^{2(\sigma-1)}) = 0. \tag{3.20}$$

A similar ambiguity occurs in the $y\tau$ and vy components of the Einstein equations. They read, respectively,

$$\mathbf{c}_1(v)\tau^{6\sigma-2} + \mathbf{c}_2(v)\tau^{4\sigma+\xi_1-\lambda-1} + \mathbf{a}_1(v)h_{||}(v)$$
$$+\mathbf{a}_2(v)h_{||}'(v) + h_{||}''(v) + \mathcal{O}(\tau^{2(3\sigma+\lambda-2)}) = 0,$$
$$\mathbf{b}_0(v)\tau^{4\sigma+\xi_1-\lambda-1} + \mathbf{b}_1(v)h_{||}(v) + \mathbf{b}_2(v)h_{||}'(v) + h_{||}''(v) + \mathcal{O}(\tau^{2(\lambda-1)}) = 0, \tag{3.21}$$

where

$$\mathbf{c}_1 = \frac{v^2 e^{-a}}{3} h_{\|} A_0'^2, \quad \mathbf{c}_2 = v^2 A_0' A_1' , \qquad \mathbf{b}_0 = \frac{v A_0'}{\sigma} \left(v\sigma A_1' - \xi_1 A_1 \right),$$

$$\mathbf{a}_1 = \frac{8(1 - e^d)}{v^2} + \frac{d' - a' - b'}{v} + a'b' , \qquad \mathbf{b}_1 = \frac{b' \left(-\sigma + 1 + \lambda \right)}{v\sigma} + \frac{b'}{2} \left(a' + b' + d' \right) - b'',$$

$$\mathbf{a}_2 = \frac{-3}{v} - \frac{1}{2}(a' + b' + d') , \qquad \mathbf{b}_2 = \frac{\sigma - 1 - \lambda}{v\sigma} - \frac{1}{2}(a' + b' + d'). \qquad (3.22)$$

For consistency of the two equations (3.21), we must have $\mathbf{a}_2 = \mathbf{b}_2$, which leads to the constraint on the parameters

$$\lambda = 4\sigma - 1. \qquad (3.23)$$

The condition (3.23) is necessary for consistency but not sufficient. We need to ensure $\mathbf{a}_1 = \mathbf{b}_1$, as well. To this end, we turn to the diagonal components of the Einstein equations which will determine the parameters σ and ξ_1 as well as the functions $a(v)$, $b(v)$ and $d(v)$. As of now there is enough information to determine σ by demanding finiteness of the Maxwell scalar F^2. We have

$$F^2 = F_{\alpha\beta}F^{\alpha\beta} = -2q^2 v^6 e^{-b(v)} \tau^{6\sigma-2} + \mathcal{O}(\tau^{8\sigma+\xi_1-4}, \tau^{2(\sigma+\xi_1-2)}), \qquad (3.24)$$

which forces σ (and therefore λ on account of Eq. (3.23)) to take the special value

$$\sigma = \lambda = 1/3. \qquad (3.25)$$

The y component of the Maxwell equations may now be used to determine the remaining parameter ξ_1. Since $\xi_1 \leq 0$, the exponents of τ involving ξ_1 will be positive unless

$$\xi_1 = 0. \qquad (3.26)$$

With this choice, all terms shown explicitly in the y component of the Maxwell equations are $\mathcal{O}(\tau^0)$ (leading).

51

The rest of the Einstein equations are found to $\mathcal{O}(\tau^{-4/3})$ as

$$16(e^d - 1) + \frac{4}{3}e^{-a}v^4 A_0'^2 + 2v(4a' + b' - d') + v^2\left(-a'^2 - a'b' + a'd' - 2a''\right) = 0,$$

$$16(e^d - 1) - \frac{2}{3}e^{-a}v^4 A_0'^2 + 2v(a' + 4b' - d') + v^2\left(-a'b' - b'^2 + b'd' - 2b''\right) = 0,$$

$$8(e^d - 1) - \frac{1}{3}e^{-a}v^4 A_0'^2 + v(a' + b' - d') = 0,$$

$$16(e^d - 1) - \frac{4}{3}e^{-a}v^4 A_0'^2 + 2v(a' + b' - 4d')$$
$$+v^2\left(-a'^2 - b'^2 + a'd' + b'd' - 2a'' - 2b''\right) = 0,$$

$$16(e^d - 1) + \frac{4}{3}e^{-a}v^4 A_0'^2 + 2(4a' - b' - d') + v^2\left(-a'^2 - a'b' + a'd' - 2a''\right) = 0. \,(3.27)$$

To leading order, these are identical to the perfect fluid case and are solved by (3.9). The off-diagonal component $h_{||}(v)$ of the metric enters in the next-to-leading order. Once again, we note that the expansion is consistent for the restricted ranges of σ, ξ_0, ξ_1 and λ.

Turning back to the Eqs. (3.20) and (3.21), we observe that for the functions (3.9), the two Einstein equations coalesce and combined with the y Maxwell equation $A_1(v)$, $h_{||}(v)$ are uniquely determined at leading order. The resulting differential equations have regular solutions found after some straightforward algebra as

$$h_{||}(v) = \mathcal{A}\left(v^4 + \frac{q^2}{12\alpha}v^6\right) \tag{3.28}$$

and

$$A_1'(v) = -\frac{q\mathcal{A}}{\alpha}\,v, \tag{3.29}$$

where $\mathcal{A}$ is an arbitrary constant characterizing the departure from the symmetric state (under reflection in the longitudinal direction) discussed in [19].

3.4 Hydrodynamics

In order to understand the dynamics of the corresponding gauge theory on the boundary we invoke holographic renormalization [41]. To do this we must pass back to the Fefferman-Graham coordinates (2.49) and obtain the fourth order term in the expansion. Following the same procedure as in [19], we redefine

$$z = z_{FG} \left(1 + \frac{\alpha z_{FG}^4}{8\tau^{4/3}} + \dots \right), \tag{3.30}$$

which effectively flattens the z coordinate and from Eq. (2.51) we may determine the vacuum expectation value of the gauge theory stress-energy tensor. The diagonal components maintain the same form that led to the previous energy density and pressure (3.11). The off-diagonal component of the metric demands the vacuum expectation value of the gauge theory stress-energy tensor develop an off-diagonal component which behaves as

$$\langle T_{y\tau} \rangle = \frac{N_c^2}{2\pi^2} \frac{\mathcal{A}}{\tau}, \tag{3.31}$$

In order to understand how our solution relates to the gauge theory fluid, let us choose a stress-energy tensor which includes an arbitrary energy flux in the longitudinal direction, start by working with an arbitrary stress tensor with diagonal and τy components,

$$T^{\mu\nu} = \begin{pmatrix} T^{\tau\tau} & T^{\tau y} & 0 & 0 \\ T^{\tau y} & T^{yy} & 0 & 0 \\ 0 & 0 & T^{22} & 0 \\ 0 & 0 & 0 & T^{33} \end{pmatrix}. \tag{3.32}$$

Recalling our definition (3.1) of coordinates τ and y, the metric on the Minkowski space of the fluid reads

$$ds_4^2 = -d\tau^2 + \tau^2 dy^2 + (dx^\perp)^2. \tag{3.33}$$

From the local conservation law

$$\nabla_\alpha T^{\alpha\beta} = \partial_\alpha T^{\alpha\beta} + \Gamma^\alpha_{\alpha\lambda} T^{\lambda\beta} + \Gamma^\beta_{\alpha\lambda} T^{\alpha\lambda} = 0 \tag{3.34}$$

and using the Christoffel symbols $\Gamma^y_{y\tau} = \frac{1}{\tau} = \Gamma^y_{\tau y}$ and $\Gamma^\tau_{yy} = \tau$, we derive relations between the components of the stress tensor.

Choosing $\beta = \tau$, we obtain

$$\partial_\tau T^{\tau\tau} + \partial_y T^{\tau y} + \frac{1}{\tau} T^{\tau\tau} + \tau T^{yy} = 0. \tag{3.35}$$

Setting $\beta = y$, we deduce

$$\partial_\tau T^{\tau y} + \partial_y T^{yy} + \frac{3}{\tau} T^{\tau y} = 0. \tag{3.36}$$

One more relation is a consequence of conformal invariance. Demanding tracelessness, we obtain

$$- T^{\tau\tau} + \tau^2 T^{yy} + T^{22} + T^{33} = 0. \tag{3.37}$$

In order to match with the expected form of the stress-energy tensor from holographic renormalization, we observe that the components of the stress-energy tensor to the order we are considering should not depend on the rapidity y or the transverse coordinates $x^\perp$. We may then immediately solve for the energy flux component $T^{\tau y}$, obtaining

$$T^{\tau y} = \frac{\mathcal{C}}{\tau^3}, \quad T_{\tau y} = \frac{-\mathcal{C}}{\tau} \tag{3.38}$$

with $\mathcal{C}$ being an arbitrary constant. This behavior matches the prediction (3.31) of the gravity dual for $T^{\tau y}$.

Solving for the diagonal components T^{yy}, T^{ii} $(i = 2, 3)$, we obtain the stress-energy tensor in terms of $\varepsilon = T^{\tau\tau}$ (energy density) and the arbitrary constant $\mathcal{C}$ (determining

the energy flux),

$$T^{\mu\nu} = \begin{pmatrix} \varepsilon & \frac{\mathcal{C}}{\tau^3} & 0 & 0 \\ \frac{\mathcal{C}}{\tau^3} & -\frac{1}{\tau}\partial_\tau\varepsilon - \frac{1}{\tau^2}\varepsilon & 0 & 0 \\ 0 & 0 & \varepsilon + \frac{1}{2}\tau\partial_\tau\varepsilon & 0 \\ 0 & 0 & 0 & \varepsilon + \frac{1}{2}\tau\partial_\tau\varepsilon \end{pmatrix}. \tag{3.39}$$

The functional form of the energy density ε is obtained by demanding isotropy, $\tau^2 T^{yy} = T^{22} = T^{33}$. We deduce

$$\varepsilon \sim \frac{1}{\tau^{4/3}} \tag{3.40}$$

matching the perfect fluid behavior (3.11). The equation of state is also unchanged, $p = \frac{1}{3}\varepsilon$. For the energy flux, we obtain the velocity component

$$u^y \sim \tau \frac{T^{\tau y}}{T^{\tau\tau}} \sim \frac{1}{\tau^{2/3}}. \tag{3.41}$$

Summarizing, we have obtained the following behavior of the components of the stress-energy tensor,

$$\begin{aligned} T^{\tau\tau} &= \frac{\mathcal{B}}{\tau^{4/3}}, & T_{\tau\tau} &= \frac{\mathcal{B}}{\tau^{4/3}}, \\ T^{yy} &= \frac{\mathcal{B}}{3\tau^{10/3}}, & T_{yy} &= \frac{\mathcal{B}}{3}\tau^{2/3}, \\ T^{ii} &= \frac{\mathcal{B}}{3\tau^{4/3}}, & T_{ii} &= \frac{\mathcal{B}}{3\tau^{4/3}}, & (i = 2,3) \\ T^{\tau y} &= \frac{\mathcal{C}}{\tau^3}, & T_{\tau y} &= \frac{-\mathcal{C}}{\tau}. \end{aligned} \tag{3.42}$$

This behavior exactly matches that expected from the gravity dual. The constants $\mathcal{B}$ and $\mathcal{C}$ are related to the parameters of the bulk metric by

$$\mathcal{B} = \frac{3N_c^2}{8\pi^2 v_h^4}\left(1 + \frac{q^2 v_h^6}{12}\right), \quad \mathcal{C} = \frac{N_c^2}{2\pi^2}\mathcal{A}. \tag{3.43}$$

55

To gain further insight into the nature of this fluid, consider the general case of a dissipative relativistic fluid with stress-energy tensor and current discussed in Section 2.1 (Eqns (2.1)–(2.5)).

Assuming no particle transport, $\vec{J} = \vec{0}$, we deduce

$$\rho \vec{u} = \varkappa (\vec{\nabla} + \vec{u} u^\beta \partial_\beta) \frac{\mu}{T}, \tag{3.44}$$

where the vectors are three-dimensional. This can be solved as an expansion in the derivatives of μ/T,

$$\vec{u} = \frac{\varkappa}{\rho} \vec{\nabla} \frac{\mu}{T} + \dots . \tag{3.45}$$

This expansion is justified because local velocities are small ($|\vec{u}| \ll 1$). To match the behavior (3.42) of the stress-energy tensor, we assume no viscosity, thus setting

$$\eta = \zeta = 0. \tag{3.46}$$

Furthermore, the energy flow ought to be in the longitudinal direction, thus

$$u^\perp = 0. \tag{3.47}$$

We may determine the energy density and pressure (3.11) directly from the form of the bulk metric. The results are in agreement with the symmetric state considered in [19] (see section 5.2). The other thermodynamic quantities (temperature, entropy, charge density and chemical potential) acquire dependence on the longitudinal coordinate (as well as τ) due to the heat flux. Thus, we obtain corrections to the symmetric case (Eqs. (3.11) - (3.13)). Expanding in the y-coordinate, we may write

$$T = T_0 + y T_1 + \dots , \quad s = s_0 + y s_1 + \dots , \quad \rho = \rho_0 + y \rho_1 + \dots , \quad \mu = \mu_0 + y \mu_1 + \dots , \tag{3.48}$$

where the zeroth-order contributions are in agreement with their counterparts in the symmetric case. Higher-order corrections may be determined from the

thermodynamic relations and the form of the stress-energy tensor, where T_0 is the ideal system's temperature and T_1 is the first order correction. The remaining thermodynamic terms are similarly expanded.

Making use of (2.3) we obtain

$$\mu_1 = -T_1 \frac{s_0}{\rho_0}, \qquad \rho_1 = -s_1 \frac{T_0}{\mu_0}. \tag{3.49}$$

Combining with (3.45) we find

$$u^y = \frac{\varkappa}{\mu_0 \tau^2} \left(\frac{\mu_1}{T_0} - T_1 \frac{\mu_0}{T_0^2} \right) + \cdots = -\frac{\varkappa}{\rho_0 \tau^2} \left(\frac{s_0}{T_0 \rho_0} + \frac{\mu_0}{T_0^2} \right) T_1 + \ldots . \tag{3.50}$$

From (2.1), the energy flux in the longitudinal direction is

$$T^{\tau y} = (\varepsilon + p) u^\tau u^y. \tag{3.51}$$

To leading order, this is given by

$$T^{\tau y} = \frac{4}{3} \varepsilon u^y + \cdots = -\frac{4\varkappa \varepsilon}{3 \rho_0 \tau^2} \left(\frac{s_0}{T_0 \rho_0} + \frac{\mu_0}{T_0^2} \right) T_1 + \ldots, \tag{3.52}$$

where we used the equation of state $p = \frac{1}{3}\varepsilon$.

Upon comparison with Eqs. (3.11) - (3.13), (3.31), we deduce the temperature and chemical potential gradients,

$$T_1 = \frac{q^2 \mathcal{A} N_c^2}{32\pi^4 \varkappa} \frac{v_h^6 (1 - q^2 v_h^6/24)^2}{(1 + q^2 v_h^6/12)^2} \tau^{-1} \quad , \quad \mu_1 = \frac{q \mathcal{A} N_c^2}{8\pi^3 \varkappa} \frac{v_h^3 (1 - q^2 v_h^6/24)^2}{(1 + q^2 v_h^6/12)^2} \tau^{-1} \tag{3.53}$$

the entropy and charge density gradients may be found from the thermodynamic relation (3.14),

$$\begin{aligned}
s_1 &= \frac{q^2 \mathcal{A} N_c^4}{64\pi^4 \varkappa} \frac{v_h^4 (1 - q^2 v_h^6/24)^2}{(1 + q^2 v_h^6/12)^2 (1 + q^2 v_h^6/24)} \tau^{-5/3}, \\
\rho_1 &= -\frac{q \mathcal{A} N_c^4}{32\pi^5 \varkappa} \frac{v_h (1 - q^2 v_h^6/24)^3}{(1 + q^2 v_h^6/12)^2 (1 + q^2 v_h^6/24)} \tau^{-5/3}.
\end{aligned} \tag{3.54}$$

Finally, the energy flux may be written in terms of the temperature gradient (since the pressure gradient is of higher order) as

$$T^{\tau y} = -\kappa_T \partial_y T, \tag{3.55}$$

where κ_T is the standard definition of thermal conductivity in non-relativistic mechanics. We obtain [55]

$$\kappa_T = \varkappa \left(\frac{\varepsilon + p}{\tau \rho T} \right)^2. \tag{3.56}$$

To leading order, we have

$$\kappa_T = \frac{16\pi^2}{q^2 \tau^2} \frac{(1 + q^2 v_h^6/12)^2}{v_h^6 (1 - q^2 v_h^6/24)^2} \varkappa \tag{3.57}$$

and using the expression (3.53) for the temperature gradient, we easily see that the energy flux (3.55) matches (3.31).

3.5   Chapter 3 summary

We solved the Maxwell-Einstein equations in AdS_5 for long longitudinal proper time using a metric ansatz which was a generalization of the proposal of Ref. [19]. By relaxing the requirement of invariance under reflection in the longitudinal direction, we were able to add off-diagonal terms to the metric. We found an explicit solution by keeping leading terms in the Einstein equations. Through holographic renormalization, we showed that the bulk metric corresponded to a nonviscous gauge theory fluid with energy flux in the longitudinal direction. We studied its thermodynamic properties and calculated the standard coefficient of thermal conductivity and the temperature, chemical potential, entropy, and charge density gradients.

Chapter 4

Bjorken flow from an AdS Schwarzschild black hole

4.1 Introduction

In order to understand a flowing hydrodynamic description of the gauge field one must introduce time dependence into the dual AdS space. This was done in [18], where dependence on the proper time in the longitudinal plane of the collision was introduced into an AdS$_5$ space. Through the AdS/CFT correspondence it was found, in the late time limit, the boundary gauge field followed ideal Bjorken hydrodynamics [28]. The work has been furthered to understand the subleading terms in the expansion of the solution of the Einstein equations and the relation to dissipative hydrodynamics on the boundary [30, 56, 20, 52, 19].

In an interesting recent work, Kajantie, Louko and Tahkokallio [57] found a time-dependent solution in three dimensions that also produced a Bjorken flow in the boundary gauge theory. The time dependence of the solution could then be removed by a coordinate transformation to the standard AdS$_3$ Schwarzschild metric. Thus, a boost-invariant flow could be understood in terms of a static Schwarzschild black

hole. This is perhaps not surprising as three dimensions are special and results are not necessarily generalizable to higher dimensions.

Our aim is to show that the three-dimensional result of Kajantie, *et al.* [57], generalizes to arbitrary dimension. By performing an appropriate slicing near the boundary, we shall obtain a Bjorken flow from a static Schwarzschild black hole via holographic renormalization [41] to leading order in longitudinal proper time. In three dimensions, our results reduce to those of Ref. [57]. In five dimensions, we recover the metric of Janik and Peschanski [18]. Higher-order corrections can be calculated by a refinement of the slicing we perform here.

4.2   Schwarzschild black hole

We start with a short discussion of pertinent properties of an AdS_d Schwarzschild black hole. Although generally known, we cast them in a form that facilitates application to the non-static case. An AdS black hole is a solution of the Einstein equations

$$R_{\mu\nu} - \left(\frac{1}{2}R + \Lambda_d \right) g_{\mu\nu} = 0, \tag{4.1}$$

where $\Lambda_d = -\frac{(d-1)(d-2)}{2}$ is a negative cosmological constant. A large black hole has a flat horizon and may be found by substituting the ansatz

$$ds_{\mathrm{b.h.}}^2 = \frac{1}{z^2} \left(-e^{a(z)}dt^2 + d\vec{x}^2 + e^{b(z)}dz^2 \right), \tag{4.2}$$

where $\vec{x} \in \mathbb{R}^{d-2}$, in the Einstein equations. They reduce to the two independent equations

$$a' + b' = 0, \quad zb' + (d-1)(1 - e^b) = 0, \tag{4.3}$$

whose solution is

$$a(z) = -b(z) = \ln\left(1 - 2\mu z^{d-1}\right), \tag{4.4}$$

where μ is an integration constant. The horizon is at

$$z_+ = (2\mu)^{-\frac{1}{d-1}} \tag{4.5}$$

and the boundary of the asymptotically AdS space is at $z = 0$.

The Hawking temperature of the hole is

$$T_H = \frac{d-1}{4\pi z_+}. \tag{4.6}$$

This solution is related to a gauge theory on the boundary via holographic renormalization [41], discussed in Section 2.2.1. To find the stress-energy tensor corresponding to the hole, we write the radial distance in the bulk as

$$z = z_{FG}\left[1 - \frac{\mu}{d-1}z_{FG}^{d-1} + \mathcal{O}(z_{FG}^{2(d-1)})\right] \tag{4.7}$$

so that the metric (4.2) is of the Fefferman-Graham form (2.49). We obtain

$$g_{tt}^{(d-1)} = \frac{d-2}{d-1}2\mu, \qquad g_{ij}^{(d-1)} = \frac{2\mu}{d-1}\delta_{ij} \tag{4.8}$$

$(i, j = 1, \ldots, d-2)$ leading to energy density and pressure of the gauge theory fluid on the boundary, respectively,

$$\varepsilon = \langle T^{tt} \rangle = (d-2)\frac{\mu}{8\pi G_d} \quad, \qquad p = \langle T^{ii} \rangle = \frac{\mu}{8\pi G_d} \tag{4.9}$$

obeying $p = \frac{1}{d-2}\varepsilon$, as expected for a conformal fluid. With the temperature given by (4.6), we obtain the equation of state

$$p = \frac{1}{16\pi G_d}\left(\frac{4\pi T_H}{d-1}\right)^{d-1} \tag{4.10}$$

and the energy and entropy densities, respectively, as functions of the temperature

$$\varepsilon = \frac{d-2}{16\pi G_d}\left(\frac{4\pi T_H}{d-1}\right)^{d-1}, \quad s = \frac{dp}{dT} = \frac{1}{4G_d}\left(\frac{4\pi T_H}{d-1}\right)^{d-2}. \tag{4.11}$$

4.3 Bjorken hydrodynamics

Having understood the case of a static gauge theory fluid on $(d-1)$-dimensional Minkowski space, we turn our attention to boost-invariant hydrodynamics in order to understand heavy ion collisions, following a suggestion by Bjorken [28]. The gauge theory fluid will still be on a $(d-1)$-dimensional Minkowski space as in the static case, but to distinguish it from the boundary of the large AdS_d Schwarzschild black hole, we shall denote its coordinates by $\tilde{x}^\mu$ ($\mu = 0, 1, \ldots, d-2$) and assume that the colliding beams are along the $\tilde{x}^1$ direction. As seen in Section 2.1.2, but now generalized to $d-1$ dimensions, it is convenient to choose coordinates τ, y (proper time and rapidity in the longitudinal plane, respectively), where

$$\tilde{x}^0 = \tau \cosh y, \quad \tilde{x}^1 = \tau \sinh y. \tag{4.12}$$

The $(d-1)$-dimensional Minkowski metric takes the form

$$d\tilde{s}^2 = d\tilde{x}_\mu d\tilde{x}^\mu = -d\tau^2 + \tau^2 dy^2 + (d\tilde{x}^\perp)^2, \tag{4.13}$$

where $\tilde{x}^\perp = (\tilde{x}^2, \ldots, \tilde{x}^{d-2})$ represents the transverse coordinates.

For the stress-energy tensor let us assume one which satisfies boost invariance, symmetry under reflection in the longitudinal direction ($y \to -y$), plus translational and rotational invariance [18],

$$T^{\mu\nu} = \mathrm{diag}\left(\begin{array}{cccc} \varepsilon(\tau) & p(\tau)/\tau^2 & \ldots & p(\tau) \end{array}\right). \tag{4.14}$$

Using the local conservation law for the stress-energy tensor,

$$\nabla_\alpha T^{\alpha\beta} = \partial_\alpha T^{\alpha\beta} + \Gamma^\alpha_{\alpha\lambda} T^{\lambda\beta} + \Gamma^\beta_{\alpha\lambda} T^{\alpha\lambda} = 0 \tag{4.15}$$

with the Christoffel symbols $\Gamma^y_{y\tau} = \frac{1}{\tau} = \Gamma^y_{\tau y}$ and $\Gamma^\tau_{yy} = \tau$, we derive relations between the components of the stress tensor.

Choosing $\beta = \tau$, we obtain

$$\partial_\tau \varepsilon + \frac{1}{\tau}(\varepsilon + p) = 0. \tag{4.16}$$

Demanding tracelessness, a consequence of conformal invariance, we obtain another constraint on the stress-energy tensor

$$-\varepsilon + (d-2)p = 0. \tag{4.17}$$

Solving the above equations, we deduce

$$\varepsilon = (d-2)p = \frac{\varepsilon_0}{\tau^{\frac{d-1}{d-2}}} \tag{4.18}$$

The temperature of the system may be found as a consequence of a perfect fluid's entropy conservation [28]

$$T = \frac{T_0}{\tau^{1/(d-2)}}. \tag{4.19}$$

The constants ε_0 and T_0 represent the initial values of the energy density and temperature, respectively, (at $\tau = 1$).

The entropy density is

$$s = \frac{\dot{p}}{\dot{T}} = \frac{s_0}{\tau}, \qquad s_0 = \frac{d-1}{d-2} \frac{\varepsilon_0}{T_0}. \tag{4.20}$$

Notice that the energy and entropy densities have the same dependence on the temperature as in the static case (4.11). If we identify initial data with their

corresponding values in the static case,

$$T_0 = T_H, \quad \varepsilon_0 = \frac{(d-2)\mu}{8\pi G_d}, \quad (4.21)$$

then Eq. (4.11), with T_H replaced by T (Eq. (4.19)), describes the evolution of the energy and entropy densities in a Bjorken flow.

To find the solution of the Einstein equations (4.1) which follows the same symmetries as that of the stress-energy tensor, we shall adopt the ansatz

$$ds^2_{\text{Bjorken}} = \frac{-e^A d\tau^2 + \tau^2 dy^2 + e^C (d\tilde{x}^\perp)^2 + e^B d\tilde{z}^2}{\tilde{z}^2}, \quad (4.22)$$

where A, B, C are all functions of $\tilde{z}$ and τ, following [18, 19]. For the perfect fluid solution we also imposed the condition of isotropy $\frac{1}{\tau^2} g_{yy} = g_{ii}$. The coordinates need to be brought into the Fefferman-Graham form (2.49) so the hydrodynamics may be derived via holographic renormalization [41].

The Einstein equations will couple the dependence of A, B, C on z and τ, but this problem is eliminated by introducing a variable v which is kept fixed as $\tau \to \infty$,

$$v = \frac{\tilde{z}}{\tau^{1/(d-2)}}. \quad (4.23)$$

Assuming that the functions $A(\tilde{z}, \tau), \ B(\tilde{z}, \tau), \ C(\tilde{z}, \tau)$ become functions of only v,

$$A = A_0(v) + \ldots, \quad B = B_0(v) + \ldots, \quad C = C_0(v) + \ldots, \quad (4.24)$$

where the dots represent terms that vanish in the $\tau \to \infty$ limit, the Einstein equations (4.1) are then reduced to the three independent equations

$$A_0' + B_0' = C_0' = 0, \quad vB_0' + (d-1)(1 - e^{B_0}) = 0, \quad (4.25)$$

64

which are of the same form as Eq. (4.3) in the static case. They are solved by

$$A_0(v) = -B_0(v) = \ln\left(1 - 2\mu v^{d-1}\right), \quad C_0(v) = 1, \tag{4.26}$$

where, again, μ is an integration constant (*cf.* with Eq. (4.4)).

In order to gain information of the gauge theory on the boundary, we use holographic renormalization [41]. The metric (4.22) needs to be expressed in Fefferman-Graham coordinates (Eq. (2.49)). To leading order in τ, this is achieved by the transformation

$$\tilde{z} = \tilde{z}_{FG}\left[1 - \frac{\mu}{d-1}\frac{\tilde{z}_{FG}^{d-1}}{\tau^{(d-1)/(d-2)}} + \mathcal{O}(\tilde{z}_{FG}^{2(d-1)})\right], \tag{4.27}$$

which is similar to the static case (4.7). For the metric (4.22) we may read off

$$\varepsilon = \langle T^{\tau\tau}\rangle = \frac{\varepsilon_0}{\tau^{\frac{d-1}{d-2}}} \quad, \quad p = \tau^2\langle T^{yy}\rangle = \langle T^{ii}\rangle = \frac{\varepsilon}{d-2}, \tag{4.28}$$

where ε_0 is given by (4.21). In comparison with (4.18) we see that the geometry is the dual of Bjorken hydrodynamics. However, the assignment of temperature and entropy is a little murky, because the bulk metric does not possess a static horizon. The null surface at $v = (2\mu)^{-1/(d-1)} = z_+$ cannot be used for a rigorous definition of the temperature, because the bulk metric (4.22) with $A = A_0$ and $B = B_0$ (Eq. (4.26)) is not an exact solution of the Einstein equations; it is only the leading term in a $1/\tau$ expansion placing the null surface at the boundary of the region of validity of the expansion. Nevertheless, if one blindly follows the arguments in the static case [18, 19], one obtains from (4.6)

$$T = \frac{d-1}{4\pi\tilde{z}_+} = \frac{T_H}{\tau^{1/(d-2)}} \tag{4.29}$$

where we used (4.23), in agreement with the result (4.19) from Bjorken hydrodynamics with initial data (4.21). Knowing T, we may deduce the entropy density as in (4.20).

65

Our goal now turns to understanding the bulk geometry in terms of a static AdS black hole and shed some light on the validity of the assignment of temperature (4.29).

4.4 Static to flowing

In order to produce a flow on the boundary of the static black hole, instead of approximating the boundary with $z = $ const. hypersurfaces (as $z \to 0$), we shall make a different choice of slicing.

Near the boundary, the two metrics (4.2) and (4.22) may be approximated, respectively, by

$$
\begin{aligned}
ds^2_{\text{b.h.}} &\to \frac{1}{z^2}\left(-dt^2 + d\vec{x}^2 + dz^2\right), \\
ds^2_{\text{Bjorken}} &\to \frac{1}{\tilde{z}^2}\left(-d\tau^2 + \tau^2 dy^2 + (d\tilde{x}^\perp)^2 + d\tilde{z}^2\right).
\end{aligned}
\tag{4.30}
$$

While the former is the asymptotic form of an exact solution of the Einstein equations, the latter is only valid in the large τ limit. We are interested in finding a transformation which relates the two asymptotic forms in this limit. To be precise, we define the $\tau \to \infty$ limit as follows: let

$$
\tau = \tau_0 + \tau',
\tag{4.31}
$$

where τ_0 is a constant. We assume $\tau_0 \gg 1$ and $\tau' \sim \mathcal{O}(1)$ so that $d\tau = d\tau' \sim \mathcal{O}(1)$. Also $\tilde{x}^\perp \sim \mathcal{O}(1)$ and $v \sim \mathcal{O}(1)$. The latter implies $\tilde{z} \sim \mathcal{O}(\tau_0^{1/(d-2)})$. By defining

$$
\tilde{z} = \tilde{z}_0 \tau_0^{1/(d-2)} + \tilde{z}'
\tag{4.32}
$$

and demanding $\tilde{z}_0, \tilde{z}' \sim \mathcal{O}(1)$, we ensure $d\tilde{z} = d\tilde{z}' \sim \mathcal{O}(1)$. Of course, as we approach the boundary, we need to let both $\tilde{z}_0, \tilde{z}' \to 0$. The remaining term in the metric will

be $\mathcal{O}(1)$ provided we choose $y' \sim \mathcal{O}(1)$, where we defined

$$y = \frac{y'}{\tau_0}, \tag{4.33}$$

Having thus defined the limit $\tau \to \infty$, it is not hard to see that the following transformation performs the desired task of relating the two metrics (4.30),

$$t = \frac{d-2}{d-3}\tau^{\frac{d-3}{d-2}} \quad , \qquad x^1 = \tau^{\frac{d-3}{d-2}}y,$$

$$x^\perp = \frac{\tilde{x}^\perp}{\tau^{1/(d-2)}} \quad , \qquad z = \frac{\tilde{z}}{\tau^{1/(d-2)}}. \tag{4.34}$$

Then, instead of the $z = $ const slicing, we shall approach the boundary on $\tilde{z} = $ const hypersurfaces (as $z, \tilde{z} \to 0$). The latter coincide 'initially' (at $\tau = 1$), but "flow" as the new coordinates describing the black hole metric are τ-dependent.

Applying the transformation (4.34) to the exact black hole metric (4.2) (more precisely, to a patch which includes the boundary $z \to 0$), we obtain

$$ds_{\text{b.h.}}^2 \;=\; \frac{1}{\tilde{z}^2}\left[-\left(1 - 2\mu\frac{\tilde{z}^{d-1}}{\tau^{\frac{d-1}{d-2}}}\right)d\tau^2 + \tau^2 dy^2 + (d\tilde{x}^\perp)^2 \right.$$

$$\left. + \frac{d\tilde{z}^2}{1 - 2\mu\frac{\tilde{z}^{d-1}}{\tau^{(d-1)/(d-2)}}}\right] + \mathcal{O}(\tau^{-(d-3)/(d-2)}), \tag{4.35}$$

which matches the bulk metric of Bjorken flow (Eqs. (4.22), (4.24) and (4.26)) to leading order in $1/\tau$. Thus, the gauge theory fluid on the boundary of the Schwarzschild black hole which is approached with $\tilde{z} = $ const. hypersurfaces as $\tilde{z} \to 0$ obeys Bjorken hydrodynamics in the large τ limit.

In addition to the standard derivation of the energy density and pressure (4.28), we may now address the issue of the temperature of the gauge theory fluid. The horizon is static and the Hawking temperature is well-defined because the exact geometry giving rise to the approximate expression (4.35) is a Schwarzschild black hole. The Hawking temperature T_H is the temperature of the static gauge theory fluid on the

hypersurface $z \to 0$ whose metric is

$$ds^2_{z \to 0} = -dt^2 + d\vec{x}^2. \tag{4.36}$$

On the other hand, the $\tilde{z} \to 0$ hypersurface has metric

$$ds^2_{\tilde{z} \to 0} = -d\tau^2 + \tau^2 dy^2 + (d\tilde{x}^\perp)^2. \tag{4.37}$$

This Bjorken metric (*cf.* with Eq. (4.13)) is related to the metric (4.36) in the large τ limit by a conformal transformation which is obtained by restricting the transformation (4.34) to these hypersurfaces,

$$t = \frac{d-2}{d-3} \tau^{\frac{d-3}{d-2}}, \qquad x^1 = \tau^{\frac{d-3}{d-2}} y, \qquad x^\perp = \frac{\tilde{x}^\perp}{\tau^{1/(d-2)}}. \tag{4.38}$$

The two metrics (4.36) and (4.37) are related by

$$ds^2_{z \to 0} = \tau^{-\frac{2}{d-2}} \left[ds^2_{\tilde{z} \to 0} + \mathcal{O}(1/\tau) \right] \tag{4.39}$$

showing that the Euclidean proper time period of thermal Green functions on the Bjorken boundary (4.37) scales as $\tau^{1/(d-2)}$. Since the period is inversely proportional to the temperature, the latter scales as $\tau^{-1/(d-2)}$, in agreement with expectations (Eq. (4.29)). The two hypersurfaces coincide at $\tau = 1$ at which time $T = T_H$.

Let us also check that the transformation (4.34) reduces to the transformation found in [57] for $d = 3$. To do this we must proceed with a little care. For the time coordinate we must add an appropriate constant term so that the limit $d \to 3$ is well-defined. Then as $d \to 3$, we obtain

$$t = \ln \tau, \qquad x^1 = y, \qquad z = \frac{\tilde{z}}{\tau}. \tag{4.40}$$

The transformation to Fefferman-Graham coordinates can be found exactly in this case,

$$z = \frac{\tilde{z}_{FG}}{\tau} \left(1 + \frac{\mu}{2} \frac{\tilde{z}_{FG}^2}{\tau^2} \right)^{-1}, \tag{4.41}$$

which matches the result of [57] in the large black hole limit. It also agrees with the general expression (4.27) to first order.

Higher-order corrections to Bjorken flow dictated by the black hole may be found by refining the transformation (4.34). This entails introducing corrections which are of $o(1/\tau)$ and making sure that the application of the transformation to the metric (4.2) does not introduce dependence of the metric on the rapidity and the transverse coordinates. This can be done systematically at each order in the $1/\tau$ expansion and will be reported on elsewhere.

4.5   Chapter 4 summary

We discussed the possibility of obtaining Bjorken hydrodynamics [28] on a $(d-1)$-dimensional Minkowski space from a large AdS_d Schwarzschild black hole (of flat horizon). The latter is normally considered dual to a static gauge theory fluid on the boundary whose temperature coincides with the Hawking temperature. By introducing an appropriate set of coordinates in a patch of the hole which included the boundary, we obtained a generalization of the metric of Janik and Peschanski [18] to arbitrary dimensions in the late time limit. Thus, we obtained Bjorken hydrodynamics on the boundary in the limit of longitudinal proper time $\tau \to \infty$. This was effectively achieved by a slicing near the boundary of the black hole consisting of "flowing" hypersurfaces related to the standard static hypersurfaces by a time-dependent conformal transformation. The conformal factor also provided a justification for determining the temperature. Our results coincided with those of Ref. [57] in the large black hole limit in three dimensions.

Chapter 5

Dissipative Bjorken hydrodynamics from an AdS Schwarzschild black hole

5.1   Introduction

The aim of this Chapter is to extend our result in Chapter 4, [21], by including subleading corrections in the large τ expansion. We show that next-to-leading-order corrections correspond to viscosity in the gauge theory plasma. At this level the coefficient of viscosity η is arbitrary, in agreement with results in five dimensions based on an asymptotic time-dependent solution to the Einstein equations [30]. At next-to-next-to-leading order we find that the Schwarzschild metric yields a flow which is not boost invariant, no matter how one chooses the slicing near the AdS boundary. Boost invariance is recovered after the Schwarzschild metric is perturbed by a power-law, τ-dependent perturbation. We show that the perturbed metric is nonsingular in the bulk, provided

$$\frac{\eta}{s} = \frac{1}{4\pi} \tag{5.1}$$

where s is the entropy density, in agreement with asymptotic time-dependent solutions in five dimensions [52]. This special value of the ratio η/s is also in agreement with the case of sinusoidal perturbations of an AdS Schwarzschild black hole [26].

Our discussion starts with a review of dissipative Bjorken hydrodynamics in Section 5.2. In Section 5.3 we discuss the time-dependent slicing we perform near the boundary in order to reproduce Bjorken hydrodynamics, including next-to-next-to-leading-order contributions in the large τ expansion. We also introduce the perturbation to the Schwarzschild metric which is necessary to maintain boost invariance at the order we are interested in. We show that demanding the absence of singularities in the bulk metric leads to the standard value (5.1) of the viscosity-to-entropy-density ratio. Finally Section 5.4 contains our summary.

5.2 Dissipative Bjorken hydrodynamics

In extending the results of Section 2.1.2, let us consider a gauge theory fluid on a $(d-1)$-dimensional flat Minkowski space spanned by coordinates $\tilde{x}^\mu$ ($\mu = 0, 1, \ldots, d-2$). (We shall reserve the notation x^μ for the coordinates of a static gauge theory fluid; $\tilde{x}^\mu$ will span the Minkowski space of the Bjorken fluid in order to avoid confusion.) With the colliding beams along the $\tilde{x}^1$ direction, it is convenient to work with the coordinates τ (longitudinal proper time) and y (rapidity), defined by

$$\tilde{x}^0 = \tau \cosh y, \quad \tilde{x}^1 = \tau \sinh y, \tag{5.2}$$

The $(d-1)$-dimensional Minkowski metric takes the form

$$ds^2_{\text{Bjorken}} = d\tilde{x}_\mu d\tilde{x}^\mu = -d\tau^2 + \tau^2 dy^2 + (d\tilde{x}^\perp)^2, \tag{5.3}$$

where $\tilde{x}^\perp = (\tilde{x}^2, \ldots, \tilde{x}^{d-2})$ represents the transverse coordinates.

For the stress-energy tensor we use the standard notions and enforce conservation and conformal invariance via

$$
\begin{aligned}
T^{\mu\nu} &= (\varepsilon + p)u^\mu u^\nu + pg^{\mu\nu} - \zeta \triangle^{\mu\nu}\nabla_\lambda u^\lambda \\
&\quad -\eta\left(\triangle^{\mu\lambda}\nabla_\lambda u^\nu + \triangle^{\nu\lambda}\nabla_\lambda u^\mu - \frac{2}{d-2}\triangle^{\mu\nu}\nabla_\lambda u^\lambda\right), \\
\nabla_\mu T^{\mu\nu} &= 0, \\
T^\mu_\mu &= 0, \tag{5.4}
\end{aligned}
$$

where $\triangle_{\mu\nu} = g_{\mu\nu} + u_\mu u_\nu$ and ε, p, η and ζ represent the energy density, pressure, shear viscosity and bulk viscosity, respectively, of the fluid. Two constraints immediately follow from Eq. (6.46),

$$
\varepsilon = (d-2)p, \quad \zeta = 0, \tag{5.5}
$$

In the rest frame of the conformal fluid, the velocity field is given by $u^\mu = (1, \vec{0})$. The stress-energy tensor simplifies to

$$
T^{\mu\nu} = \begin{pmatrix}
\varepsilon(\tau) & 0 & \dots & 0 \\
0 & \frac{p(\tau)}{\tau^2} - 2\frac{d-3}{d-2}\frac{\eta(\tau)}{\tau^3} & \dots & 0 \\
 & & \ddots & \\
0 & 0 & \dots & p(\tau) + \frac{2}{d-2}\frac{\eta(\tau)}{\tau}
\end{pmatrix}. \tag{5.6}
$$

Choosing $\nu = \tau$ in the conservation equation of (6.46), we obtain

$$
\partial_\tau \varepsilon + \frac{d-1}{d-2}\frac{\varepsilon}{\tau} - 2\frac{d-3}{d-2}\frac{\eta}{\tau^2} = 0. \tag{5.7}
$$

Assuming the viscosity to be a subleading effect, we deduce from (5.7) the leading behavior of the energy density

$$
\varepsilon \approx \frac{\varepsilon_0}{\tau^{(d-1)/(d-2)}} \tag{5.8}
$$

72

and hence of the pressure, temperature (from the Stefan-Boltzmann law in $d-1$ dimensions, $\varepsilon \sim T^{d-1}$) and entropy density, respectively,

$$p = \frac{\varepsilon}{d-2} \approx \frac{\varepsilon_0}{d-2} \frac{1}{\tau^{(d-1)/(d-2)}}, \quad T \approx \frac{T_0}{\tau^{1/(d-2)}}, \quad s = \frac{dp}{dT} \approx \frac{s_0}{\tau}, \quad s_0 = \frac{d-1}{d-2} \frac{\varepsilon_0}{T_0}. \quad (5.9)$$

The constants ε_0 and T_0 represent the initial values of the energy density and temperature, respectively (at $\tau = 1$).

At high temperatures we expect the viscosity to have the same dependence on the temperature as the entropy density (which is known to be true in the case of sinusoidal perturbations of the static $\mathcal{N} = 4$ SYM plasma in five dimensions [26]) so that the ratio η/s asymptotes to a constant. Therefore, we shall assume

$$\eta(\tau) \approx \frac{\eta_0}{\tau} \quad (5.10)$$

where η_0 is a constant. We may then solve Eq. (5.7) and obtain a subleading correction to the energy density,

$$\varepsilon = \frac{\varepsilon_0}{\tau^{\frac{d-1}{d-2}}} - \frac{2\eta_0}{\tau^2} + \dots, \quad (5.11)$$

yielding corresponding corrections to the temperature and entropy density,

$$\begin{aligned} T &= T_0 \left(\frac{1}{\tau^{1/(d-2)}} - \frac{2\eta_0}{(d-1)\varepsilon_0 \tau} + \dots \right), \\ s &= \frac{dp}{dT} = s_0 \left(\frac{1}{\tau} - \frac{2(d-2)\eta_0}{(d-1)\varepsilon_0} \frac{1}{\tau^{\frac{2d-5}{d-2}}} + \dots \right). \end{aligned} \quad (5.12)$$

Note that to leading order we obtain the ratio

$$\frac{\eta}{s} = \frac{\eta_0}{s_0} = \frac{(d-2)\eta_0 T_0}{(d-1)\varepsilon_0}. \quad (5.13)$$

This ratio is known to take the value $1/(4\pi)$ (Eq. (5.1)) if the gauge theory fluid is dual to a perturbed AdS Schwarzschild black hole [26]. We shall show that the above Bjorken fluid also admits a gravity dual which is an appropriately perturbed AdS

Schwarzschild black hole leading to the same value (5.1) of the viscosity-to-entropy-density ratio.

5.3   AdS Schwarzschild black hole

The procedure to transform a Schwarzschild black hole to incorporate Bjorken flow was developed in Chapter 4. We will continue in this direction, and produce subleading corrections to the metric dual to ideal flow. Curvature invariants of the AdS black hole become important in this discussion. We have already seen R^2 employed to constrain the type of flow and transport coefficients in Section 2.2.3. In order to produce the dissipative corrections from a Schwarzschild black hole we will need a more sophisticated way of finding the invariants.

The leading-order metric (4.35) can be seen to be regular in the bulk. Indeed, the Kretschmann scalar

$$\mathcal{R}^2 = R_{\mu\nu\alpha\beta}R^{\mu\nu\alpha\beta} \tag{5.14}$$

is found to be

$$\mathcal{R}^2 = 2(d-1)\left[d + 2(d-2)^2(d-3)\mu^2 v^{2(d-1)}\right] + \mathcal{O}(1/\tau^{(d-3)/(d-2)}) \tag{5.15}$$

whose only singularity is obtained in the limit $z \to \infty$.

Moreover, one can construct invariants which are linear combinations of the components of the Riemann tensor. For the geometry to be regular, these invariants

must also be free of singularities [40]. Introducing the vielbein

$$e_a^\alpha = \left\{ \begin{pmatrix} \tilde{z}/\sqrt{1-2\mu v^{d-1}} \\ 0 \\ 0 \\ 0 \\ 0 \end{pmatrix}, \begin{pmatrix} 0 \\ \tilde{z}/\tau \\ 0 \\ 0 \\ 0 \end{pmatrix}, \begin{pmatrix} 0 \\ 0 \\ \tilde{z} \\ 0 \\ 0 \end{pmatrix}, \ldots, \begin{pmatrix} 0 \\ 0 \\ 0 \\ 0 \\ \sqrt{1-2\mu v^{d-1}}/\tilde{z} \end{pmatrix} \right\}$$
(5.16)

with $a = 0, \ldots, d-1$ spanning a local Minkowski space such that $g_{\alpha\beta}e_a^\alpha e_b^\beta = \eta_{ab}$, the Riemann tensor invariants are

$$\mathcal{R}_{abcd} = R_{\alpha\beta\gamma\delta}e_a^\alpha e_b^\beta e_c^\gamma e_d^\delta.$$
(5.17)

Even though the individual components of the Riemann tensor have singularities, the invariants (5.17) are all regular. The nonvanishing components are found to be

$$\mathcal{R}_{1010} = \mathcal{R}_{2020} = \cdots = \mathcal{R}_{(d-2)0(d-2)0} = 1 + (d-3)\mu v^{d-1} + \mathcal{O}(1/\tau^{(d-3)/(d-2)}),$$

$$\mathcal{R}_{1212} = \cdots = \mathcal{R}_{(d-2)1(d-2)1} = \cdots = \mathcal{R}_{(d-3)(d-2)(d-3)(d-2)}$$
$$= -1 + 2\mu v^{d-1} + \mathcal{O}(1/\tau^{(d-3)/(d-2)}),$$

$$\mathcal{R}_{(d-1)1(d-1)1} = \cdots = \mathcal{R}_{(d-1)(d-2)(d-1)(d-2)}$$
$$= -1 - (d-3)\mu v^{d-1} + \mathcal{O}(1/\tau^{(d-3)/(d-2)}),$$

$$\mathcal{R}_{(d-1)0(d-1)0} = 1 - (d-3)(d-2)\mu v^{d-1} + \mathcal{O}(1/\tau^{(d-3)/(d-2)}), \quad (5.18)$$

together with those obtained using the symmetries of the Riemann tensor.

5.3.1 Next-to-leading order

To extend the transformation to next-to-leading order ($\mathcal{O}(1/\tau^{(d-3)/(d-2)})$), let us add a correction to (4.30) so that it reads

$$
\begin{aligned}
t &= \tau^{\frac{d-3}{d-2}}\left(\frac{d-2}{d-3} + \frac{(d-3)\tau^2 y^2 - (\tilde{x}^\perp)^2}{2(d-2)\tau^2(1-2\mu v^{d-1})}\right) - \mathcal{C}_1 \ln\tau + \frac{f_1(v)}{\tau^{(d-3)/(d-2)}}, \\
x^1 &= \tau y\left(\frac{1}{\tau^{1/(d-2)}} - \frac{\mathcal{C}_1 + b_1(v)}{\tau}\right), \quad x^\perp = \tilde{x}^\perp\left(\frac{1}{\tau^{1/(d-2)}} - \frac{\mathcal{C}_1 + c_1(v)}{\tau}\right), \\
z &= \tilde{z}\left(\frac{1}{\tau^{1/(d-2)}} - \frac{\mathcal{C}_1}{\tau}\right),
\end{aligned}
\tag{5.19}
$$

where $\mathcal{C}_1$ is an arbitrary constant, v is defined in (4.23) and $b_1(v)$, $c_1(v)$ and $f_1(v)$ are functions which vanish at the boundary ($v = 0$), so that they do not alter the boundary behavior of the metric obtained at leading order above.

The function $f_1(v)$ is determined by the requirement that the $\tau\tilde{z}$ component of the metric vanish at the order we are interested in. We obtain the constraint

$$
v + (d-2)\left(1 - 2\mu v^{d-1}\right)^2 f_1'(v) = 0
\tag{5.20}
$$

whose unique solution (with $f_1(0) = 0$) may be written in terms of a hypergeometric function,

$$
\begin{aligned}
f_1(v) &= \frac{-v^2(d-3)}{2(d-2)(d-1)}F\left(1, \frac{2}{d-1}; \frac{d+1}{d-1}; 2\mu v^{d-1}\right) \\
&\quad - \frac{v^2}{(d-2)(d-1)(1-2\mu v^{d-1})}.
\end{aligned}
\tag{5.21}
$$

With this choice of $f_1(v)$, under the transformation (5.19) the black hole metric (4.2) turns into

$$
\begin{aligned}
ds_{\text{b.h.}}^2 &= \frac{1}{\tilde{z}^2}\Bigg[-\left(1 - 2\mu v^{d-1} + \frac{2(d-1)\mu\mathcal{C}_1 v^{d-1}}{\tau^{(d-3)/(d-2)}}\right)d\tau^2 + \left(1 - \frac{2b_1(v)}{\tau^{(d-3)/(d-2)}}\right)\tau^2 dy^2 \\
&\quad + \left(1 - \frac{2c_1(v)}{\tau^{(d-3)/(d-2)}}\right)(d\tilde{x}^\perp)^2 + \frac{d\tilde{z}^2}{1 - 2\mu v^{d-1} + \frac{2(d-1)\mu\mathcal{C}_1 v^{d-1}}{\tau^{(d-3)/(d-2)}}} + \dots\Bigg]
\end{aligned}
\tag{5.22}
$$

where the dots represent higher-order terms in the large τ expansion.

The Einstein equations at next-to-leading order yield two independent equations for the functions $b_1(v)$, $c_1(v)$,

$$
\begin{aligned}
b_1'(v) + (d-3)c_1'(v) &= 0, \\
-\mu\mathcal{C}_1 v^{d-2} + \frac{\mu v^{d-2}}{d-2}\left[b_1(v) + (d-3)c_1(v)\right] + \frac{1 - 2\mu v^{d-1}}{(d-1)(d-3)}b_1'(v) &= 0 \quad (5.23)
\end{aligned}
$$

whose unique solution (with the boundary conditions $b_1(0) = c_1(0) = 0$) is

$$
b_1(v) = -\frac{(d-3)\mathcal{C}_1}{2}\ln\left(1 - 2\mu v^{d-1}\right), \quad c_1(v) = \frac{\mathcal{C}_1}{2}\ln\left(1 - 2\mu v^{d-1}\right). \quad (5.24)
$$

Using (5.24), the metric (5.22) can be written as

$$
\begin{aligned}
ds^2_{\text{b.h.}} = \frac{1}{\tilde{z}^2}\Bigg[&-\left(1 - 2\mu v^{d-1} + \frac{2(d-1)\mu\mathcal{C}_1 v^{d-1}}{\tau^{(d-3)/(d-2)}}\right)d\tau^2 \\
&+ \left(1 - 2\mu v^{d-1}\right)^{(d-3)\mathcal{C}_1/\tau^{(d-3)/(d-2)}} \tau^2 dy^2 + \left(1 - 2\mu v^{d-1}\right)^{-\mathcal{C}_1/\tau^{(d-3)/(d-2)}}(d\tilde{x}^{\perp})^2 \\
&+ \frac{d\tilde{z}^2}{1 - 2\mu v^{d-1} + \frac{2(d-1)\mu\mathcal{C}_1 v^{d-1}}{\tau^{(d-3)/(d-2)}}} + \cdots \Bigg], \quad (5.25)
\end{aligned}
$$

which includes $\mathcal{O}(1/\tau^{(d-3)/(d-2)})$ corrections to the leading-order expression (4.35). The next-to-leading-order expression (5.25) for the metric has no dependence on the rapidity y and transverse coordinates $\tilde{x}^{\perp}$, therefore it leads to a Bjorken flow for the gauge theory fluid on the boundary.

We may now use holographic renormalization (Section 2.2.1) to calculate the VEV of the stress-energy tensor of the dual gauge theory. The transformation to Fefferman-Graham coordinates (2.49) is

$$
\tilde{z} = z_{FG}\left[1 - \mu\left(\frac{1}{d-1} - \frac{\mathcal{C}_1}{\tau^{(d-3)/(d-2)}}\right)\frac{z_{FG}^{d-1}}{\tau^{\frac{d-1}{d-2}}} + \mathcal{O}(z_{FG}^{2(d-1)})\right], \quad (5.26)
$$

correcting the leading-order transformation (4.27). The form of the boundary metric is unaltered by design whereas the first nonvanishing correction away from the

boundary reads

$$g_{\tau\tau}^{(d-1)} = \frac{2\mu(d-2)}{d-1}\left(\frac{1}{\tau^{(d-1)/(d-2)}} - \frac{(d-1)\mathcal{C}_1}{\tau^2}\right), \qquad g_{ii}^{(d-1)} = \frac{2\mu}{d-1}\frac{1}{\tau^{(d-1)/(d-2)}}$$

$$\frac{1}{\tau^2}g_{yy}^{(d-1)} = \frac{2\mu}{d-1}\left(\frac{1}{\tau^{(d-1)/(d-2)}} - \frac{(d-1)(d-2)\mathcal{C}_1}{\tau^2}\right), \tag{5.27}$$

correcting the leading-order expression.

Using Eq. (2.51), we obtain a stress-energy tensor for the conformal fluid in agreement with Bjorken hydrodynamics (Eqs. (5.10) and (5.11)) with ε_0, as before (Eq. (4.21)) and

$$\eta_0 = \frac{(d-1)\mathcal{C}_1\varepsilon_0}{2}, \tag{5.28}$$

matching the result of Ref. [30] for $d = 5$.

The temperature of the gauge theory fluid can also be determined through the conformal factor relating the static metric (4.36) to the Bjorken metric (5.3), as before. Applying the restriction of the transformation (5.19) on the boundary,

$$t = \frac{d-2}{d-3}\tau^{\frac{d-3}{d-2}} - \mathcal{C}_1\ln\tau, \quad x^1 = \tau y\left(\frac{1}{\tau^{1/(d-2)}} - \frac{\mathcal{C}_1}{\tau}\right), \quad x^\perp = \tilde{x}^\perp\left(\frac{1}{\tau^{1/(d-2)}} - \frac{\mathcal{C}_1}{\tau}\right), \tag{5.29}$$

we obtain at next-to-leading order in τ,

$$ds_{\text{static}}^2 = \left(\frac{1}{\tau^{1/(d-2)}} - \frac{\mathcal{C}_1}{\tau}\right)^2\left[ds_{\text{Bjorken}}^2 + \ldots\right] \tag{5.30}$$

which yields the τ-dependent temperature

$$T = T_H\left(\frac{1}{\tau^{1/(d-2)}} - \frac{\mathcal{C}_1}{\tau}\right), \tag{5.31}$$

correcting the leading-order result (4.6) and in agreement with the hydrodynamic result (5.12) with $T_0 = T_H$. The correct expression for the entropy density also

follows, and we obtain the ratio

$$\frac{\eta}{s} = \frac{(d-1)(d-2)}{8\pi} \, \mathcal{C}_1 (2\mu)^{1/(d-1)}. \tag{5.32}$$

There is no constraint on this ratio at this order because the truncated metric (5.25) is regular in the bulk [30]. This can be seen by a calculation of the Kretschmann scalar (5.14). With the metric (5.25), we obtain

$$\mathcal{R}^2 = 2(d-1) \left[d + 2(d-2)^2(d-3)\mu^2 v^{2(d-1)} \left(1 - \frac{2(d-1)\mathcal{C}_1}{\tau^{(d-3)/(d-2)}} \right) \right] + \dots \ . \tag{5.33}$$

Equation (5.33) corrects the leading-order result (5.15), showing that to this order the Kretschmann scalar is regular.

However, the metric (5.25) leads to singular Riemann invariants (5.17). Indeed, we obtain explicitly, e.g., for $d = 5$,

$$\mathcal{R}_{0101} = 1 + 2\mu v^4 + \frac{32\mathcal{C}_1 \mu^2 v^8}{\tau^{2/3}} \frac{1}{1 - 2\mu v^4} + \dots, \tag{5.34}$$

exhibiting a simple pole at $v = (2\mu)^{-1/4}$. This singularity should be absent, since our metric comes from a Schwarzschild black hole which has no singularities except as $z \to \infty$. We obtained a pole because we have not included all contributions at order $\mathcal{O}(1/\tau^{(d-3)/(d-2)})$. There are additional contributions from next-order $(\mathcal{O}(1/\tau))$ terms are in the metric (5.25). Including them, the corrected metric reads

$$\begin{aligned}
ds^2_{\text{b.h.}} &= \frac{1}{\tilde{z}^2} \Bigg[- \left(1 - 2\mu v^{d-1} + \frac{2(d-1)\mu\mathcal{C}_1 v^{d-1}}{\tau^{(d-3)/(d-2)}} \right) d\tau^2 \\
&\quad + \left(1 - 2\mu v^{d-1} \right)^{(d-3)\mathcal{C}_1/\tau^{(d-3)/(d-2)}} \tau^2 dy^2 + \left(1 - 2\mu v^{d-1} \right)^{-\mathcal{C}_1/\tau^{(d-3)/(d-2)}} (d\tilde{x}^{\perp})^2 \\
&\quad + \frac{d\tilde{z}^2}{1 - 2\mu v^{d-1} + \frac{2(d-1)\mu\mathcal{C}_1 v^{d-1}}{\tau^{(d-3)/(d-2)}}} + 2\mathcal{A}_\mu d\tilde{x}^\mu d\tilde{z} + 2\mathcal{B}_\mu d\tilde{x}^\mu d\tau + \dots \Bigg]
\end{aligned} \tag{5.35}$$

where the off-diagonal elements are

$$\mathcal{A}_\tau = 0 \;, \quad \mathcal{A}_y = -\frac{(d-1)(d-3)\mathcal{C}_1\mu\tau y v^{d-2}}{1-2\mu v^{d-1}} \;, \quad \mathcal{A}_{\tilde{x}^\perp} = \frac{(d-1)\mathcal{C}_1\mu\tilde{x}^\perp v^{d-2}}{\tau(1-2\mu v^{d-1})}. \qquad (5.36)$$

These corrections do not lead to a Bjorken flow. However, the metric (5.35) satisfies the Einstein equations at this order. The Kretschmann scalar (5.33) is unaltered, and the Riemann invariants (5.17) are corrected with the corrections cancelling all singularities. For example, the invariant (5.34) for $d = 5$ is corrected to

$$\mathcal{R}_{0101} = 1 + 2\mu v^4 - \frac{8\mathcal{C}_1\mu v^4}{\tau^{2/3}} + \dots \qquad (5.37)$$

which is a regular expression.

5.3.2 Next-to-next-to-leading order

Extending the above results to next-to-next-to-leading order requires calculations which are considerably involved. We shall therefore restrict our attention to the physically interesting case of five dimensions, setting $d = 5$, and employ Mathematica for the lengthy algebraic manipulations. The generalization to an arbitrary dimension is straightforward but adds little to the main results.

Let us augment the transformation (5.19) for $d = 5$ with appropriate $\mathcal{O}(1/\tau^{4/3})$ terms as follows,

$$\begin{aligned}
t &= \frac{3}{2}\tau^{2/3}\left[1 + \frac{2\tau^2 y^2 - (\tilde{x}^\perp)^2}{9(1-2\mu v^4)\tau^2}\right] - \mathcal{C}_1\ln\tau + \frac{f_1(v) - \frac{3}{2}\mathcal{C}_2}{\tau^{2/3}} + \frac{f_2(v)}{\tau^{4/3}}, \\
x^1 &= \tau^{2/3}y\left(1 - \frac{\mathcal{C}_1 + b_1(v)}{\tau^{2/3}} + \frac{b_2(v) + \mathcal{C}_2}{\tau^{4/3}}\right), \\
x^\perp &= \frac{\tilde{x}^\perp}{\tau^{1/3}}\left(1 - \frac{\mathcal{C}_1 + c_1(v)}{\tau^{2/3}} + \frac{c_2(v) + \mathcal{C}_2}{\tau^{4/3}}\right), \\
z &= v\left(1 - \frac{\mathcal{C}_1}{\tau^{2/3}} + \frac{a_2(v) + \mathcal{C}_2}{\tau^{4/3}}\right), \qquad (5.38)
\end{aligned}$$

where v is defined in (4.23). The constant $\mathcal{C}_1$ is once again related to the viscosity coefficient (Eq. (5.28)), but to understand $\mathcal{C}_2$ one must employ second order hydrodynamics [25], whereby it is understood to be related to the relaxation time. The functions $f_1(v)$ and $b_1(v), c_1(v)$ have already been determined at first perturbative order (Eqs. (5.21) and (5.24), respectively, with $d = 5$). The new functions $f_2(v)$ and $a_2(v), b_2(v), c_2(v)$ ought to vanish at the boundary ($v = 0$) so as not to contribute to the boundary metric.

As with $f_1(v)$, demanding that the $\tau\tilde{z}$ component of the metric vanish at the order we are interested in yields the constraint on $f_2(v)$,

$$3(1 - 2\mu v^4)^3 f_2'(v) - \mathcal{C}_1 v(3 + 10\mu v^4) = 0 \tag{5.39}$$

which has the unique solution (with $f_2(0) = 0$)

$$f_2(v) = -\mathcal{C}_1 f_1(v) + \frac{\mathcal{C}_1 v^2}{3(1 - 2\mu v^4)^2}. \tag{5.40}$$

With this choice of $f_2(v)$, the application of the transformation (5.38) to the black hole metric (4.2) with $d = 5$ turns the latter into the form

$$
\begin{aligned}
ds^2_{\text{b.h.}} \;=\; \frac{1}{\tilde{z}^2}\Bigg[& -\left(1 - 2\mu v^4 + \frac{8\mu\mathcal{C}_1 v^4}{\tau^{2/3}} + \frac{A_2(v)}{\tau^{4/3}}\right) d\tau^2 \\
& +\left(1 - \frac{2b_1(v)}{\tau^{2/3}} + \frac{B_2(v)}{\tau^{4/3}}\right)\tau^2 dy^2 + \left(1 - \frac{2c_1(v)}{\tau^{2/3}} + \frac{C_2(v)}{\tau^{4/3}}\right)(d\tilde{x}^\perp)^2 \\
& +\frac{d\tilde{z}^2}{1 - 2\mu v^4 + \frac{8\mu\mathcal{C}_1 v^4}{\tau^{2/3}} - \frac{d_2(v)}{\tau^{4/3}}} + 2\mathcal{A}_\mu d\tilde{x}^\mu d\tilde{z} + \dots \Bigg]
\end{aligned}
\tag{5.41}
$$

where the dots represent higher-order terms.

The off-diagonal elements are

$$\mathcal{A}_\tau = \frac{4\mu v^3((\tilde{x}^\perp)^2 - 2\tau^2 y^2)}{3(1 - 2\mu v^4)\tau^{4/3}}, \quad \mathcal{A}_y = -\frac{8\mathcal{C}_1\mu\tau y v^3}{1 - 2\mu v^4}, \quad \mathcal{A}_{\tilde{x}^\perp} = \frac{4\mathcal{C}_1\mu\tilde{x}^\perp v^3}{\tau(1 - 2\mu v^4)} \tag{5.42}$$

and we have defined

$$
\begin{aligned}
A_2(v) &= \frac{v^2}{9(1 - 2\mu v^4)} - 4\mu v^4 (3\mathcal{C}_1^2 + 2\mathcal{C}_2) - \frac{4}{3}(1 - 2\mu v^4)f_1(v) - 2(1 + 2\mu v^4)a_2(v), \\
B_2(v) &= b_1^2(v) - 2\mathcal{C}_1 b_1(v) - 2a_2(v) + 2b_2(v), \\
C_2(v) &= c_1^2(v) - 2\mathcal{C}_1 c_1(v) - 2a_2(v) + 2c_2(v), \\
d_2(v) &= 4\mu v^4 (3\mathcal{C}_1^2 + 2\mathcal{C}_2 + 2a_2(v)) + 2v(1 - 2\mu v^4)a_2'(v) - \frac{v^2}{9(1 - 2\mu v^4)}.
\end{aligned}
\tag{5.43}
$$

Evidently, the metric depends on the rapidity as well as the transverse coordinates at next-to-next-to-leading order. This dependence cannot be eliminated by any choice of the functions which are yet to be determined. One may try to modify the transformation (5.38) to eliminate the off-diagonal terms which depend on y and $\tilde{x}^\perp$, but this only shifts the dependence on these coordinates to other components of the metric. If we insist on reproducing Bjorken flow on the boundary, we must perturb the Schwarzschild metric (4.2). Let the perturbed metric be

$$
ds^2_{\text{perturbed}} = ds^2_{\text{b.h.}} - \frac{1}{\tilde{z}^2}\left[\frac{v^2 \mathcal{A}(v)}{\tau^{4/3}}d\tilde{z}^2 + 2\mathcal{A}_\mu d\tilde{x}^\mu d\tilde{z}\right]
\tag{5.44}
$$

where, apart from the off-diagonal elements, we are also modifying the $\tilde{z}\tilde{z}$ component of the black hole metric by an amount proportional to an arbitrary function $\mathcal{A}(v)$. It turns out that, even though we have certain freedom in the choice of $\mathcal{A}(v)$ (gauge freedom), this function cannot vanish.

Using Eqs. (5.41) and (5.44), the $\tilde{z}\tilde{z}$ component of the perturbed metric can be expanded as

$$
g_{\tilde{z}\tilde{z}} = \frac{1}{\tilde{z}^2}\left[\frac{1}{1 - 2\mu v^4} - \frac{8\mu\mathcal{C}_1 v^4}{\tau^{2/3}(1 - 2\mu v^4)^2} + \frac{v^2 D_2(v)}{\tau^{4/3}} + \dots\right]
\tag{5.45}
$$

where

$$
D_2(v) = \frac{d_2(v)}{v^2(1 - 2\mu v^4)^2} + \frac{64\mu^2 \mathcal{C}_1^2 v^6}{(1 - 2\mu v^4)^3} - \mathcal{A}(v).
\tag{5.46}
$$

82

Demanding that the perturbed metric satisfy the Einstein equations at the order we are interested in yields four constraints on the four functions $A_2(v), B_2(v), C_2(v), D_2(v)$,

$$3(1 - 2\mu v^4)^2(3 - 2\mu v^4)(B_2' + 2C_2') - 3v(1 - 2\mu v^4)^3(B_2'' + 2C_2''')$$
$$-9v^2(1 - 2\mu v^4)^4 D_2' + 18v(1 + 6\mu v^4)(1 - 2\mu v^4)^3 D_2$$
$$+8\mu v^5\left[-1 + 36C_1^2\mu v^2\left(11 - 6\mu v^4 - 2(1 - 2\mu v^4)\ln(1 - 2\mu v^4)\right)\right] = 0,$$

$$9v(1 - 2\mu v^4)^3 A_2'' - 9(3 - 10\mu v^4)(1 - 2\mu v^4)^2 A_2' + 288\mu^2 v^7(1 - 2\mu v^4)A_2$$
$$+9v^2(3 - 2\mu v^4)(1 - 2\mu v^4)^4 D_2' - 18v(3 + 8\mu v^4 - 12\mu^2 v^8)(1 - 2\mu v^4)^3 D_2$$
$$+18v(1 - 2\mu v^4)^4 C_2''' - 18(3 + 2\mu v^4)(1 - 2\mu v^4)^3 C_2'$$
$$-8\mu v^5\left[7 + 2\mu v^4 + 36C_1^2\mu v^2(9 + 44\mu v^4 + 4\mu^2 v^8)\right] = 0,$$

$$9v(1 - 2\mu v^4)^3 A_2'' - 9(3 - 10\mu v^4)(1 - 2\mu v^4)^2 A_2' + 288\mu^2 v^7(1 - 2\mu v^4)A_2$$
$$+9v(1 - 2\mu v^4)^4(B_2'' + C_2''') - 9(3 + 2\mu v^4)(1 - 2\mu v^4)^3(B_2' + C_2')$$
$$+9v^2(3 - 2\mu v^4)(1 - 2\mu v^4)^4 D_2' - 18v(3 + 8\mu v^4 - 12\mu^2 v^8)(1 - 2\mu v^4)^3 D_2$$
$$-8\mu v^5\left[1 + 14\mu v^4 + 36C_1^2\mu v^2(39 - 28\mu v^4 + 28\mu^2 v^8)\right] = 0,$$

$$-9(1 - 2\mu v^4)^2 A_2' - 72\mu v^3(1 - 2\mu v^4)A_2$$
$$-3(1 - 2\mu v^4)^2(3 - 2\mu v^4)(B_2' + 2C_2') - 36v(1 - 2\mu v^4)^3 D_2 + 8\mu v^5$$
$$+8\mu v^3\left[18C_1^2\left(14\mu v^4 + 4\mu^2 v^8 - (1 - 2\mu v^4)(3 - 2\mu v^4)\ln(1 - 2\mu v^4)\right)\right] = 0,(5.47)$$

coming from the $\tau\tau$, yy, xx, and zz components of the Einstein equations, respectively. This system of equations does not completely determine the four functions. Keeping $A_2(v)$ arbitrary (gauge degree of freedom), the other three

functions are determined to be

$$B_2'(v) = \left(\frac{A_2(v)}{1 + 2\mu v^4}\right)'$$

$$+\frac{2\mu v^3}{9(1 - 4\mu^2 v^8)^2}\left\{-4v^2(3 + 4\mu v^4 + 4\mu^2 v^8) - 72\mathcal{C}_1^2(1 - 24\mu v^4 - 20\mu^2 v^8)\right.$$

$$-8(1 - 2\mu v^4)(1 + \mu v^4 + 2\mu^2 v^8)\frac{1}{\sqrt{2\mu}}\tanh^{-1} v^2\sqrt{2\mu}$$

$$-72\mathcal{C}_1^2(5 + 2\mu v^4 + 8\mu^2 v^8)(1 - 2\mu v^4)\ln(1 - 2\mu v^4)$$

$$\left.+\mathcal{C}_3(1 - 2\mu v^4)^2 - \mathcal{C}_4(1 - 2\mu v^4)(3 + 4\mu^2 v^8)\right\},$$

$$C_2'(v) = \left(\frac{A_2(v)}{1 + 2\mu v^4}\right)'$$

$$+\frac{2\mu v^3}{9(1 - 4\mu^2 v^8)^2}\left\{-2v^2(3 - 4\mu v^4 - 4\mu^2 v^8)\right.$$

$$-2(1 - 10\mu v^4 + 12\mu^2 v^8 + 8\mu^3 v^{12})\frac{1}{\sqrt{2\mu}}\tanh^{-1} v^2\sqrt{2\mu}$$

$$-36\mathcal{C}_1^2(11 - 6\mu v^4 + 20\mu^2 v^8 + 24\mu^3 v^{12})$$

$$-36\mathcal{C}_1^2(7 - 22\mu v^4 + 20\mu^2 v^8 - 8\mu^3 v^{12})\ln(1 - 2\mu v^4)$$

$$\left.+\mathcal{C}_3(1 - 2\mu v^4)^2 + \mathcal{C}_4(-\frac{3}{2} + 9\mu v^4 - 10\mu^2 v^8 - 4\mu^3 v^{12})\right\},$$

$$D_2(v) = -\frac{1}{v(1 - 4\mu^2 v^8)}A_2'(v) + \frac{4\mu v^2(1 - 6\mu v^4)}{(1 - 4\mu^2 v^8)^2}A_2(v)$$

$$+\frac{\mu v^2(3 - 2\mu v^4)}{9(1 - 2\mu v^4)(1 + 2\mu v^4)^2}\left\{\frac{2}{\sqrt{2\mu}}\tanh^{-1} v^2\sqrt{2\mu}\right.$$

$$\left.+108\mathcal{C}_1^2\ln(1 - 2\mu v^4) - \frac{\mathcal{C}_3}{2} + \mathcal{C}_4\right\}$$

$$+\frac{2\mu v^2}{9(1 - 4\mu^2 v^8)^2(1 - 2\mu v^4)}\left\{-v^2(7 + 4\mu^2 v^8)\right.$$

$$\left.+72\mathcal{C}_1^2(3 - 6\mu v^4 + 20\mu^2 v^8 + 24\mu^3 v^{12})\right\}. \tag{5.48}$$

The functions $B_2(v)$ and $C_2(v)$ are found by integrating the first two equations, respectively. No arbitrary integration constants are introduced because $B_2(0) =$

$C_2(0) = 0$. Notice also that apart from the arbitrary function $A_2(v)$, the above functions contain arbitrary parameters $\mathcal{C}_3$ and $\mathcal{C}_4$.

Constraints on the parameters are obtained by demanding regularity of the perturbed metric in the bulk. After some algebra, the Kretschmann scalar (5.14) is found as an asymptotic expansion in τ,

$$
\begin{aligned}
\mathcal{R}^2 &= 8(5 + 36\mu^2 v^8) - \frac{2304\mathcal{C}_1\mu^2 v^8}{\tau^{2/3}} + \frac{96\mu^2 v^8}{9(1 + 2\mu v^4)\tau^{4/3}} \Bigg\{ -108 A_2 \\
&\quad + \frac{v^2(-14 + 8\mu v^4 - 24\mu^2 v^8) + 72\mathcal{C}_1^2(3 + 24\mu v^4 - 44\mu^2 v^8 + 32\mu^3 v^{12})}{(1 - 2\mu v^4)^2} \\
&\quad + \left(\frac{3}{2} - 3\mu v^4\right)\mathcal{C}_3 - 3(1 - 2\mu v^4)\mathcal{C}_4 \\
&\quad - 6(1 - 2\mu v^4)\left[\frac{1}{\sqrt{2\mu}}\tanh^{-1} v^2\sqrt{2\mu} + 54\mathcal{C}_1^2 \ln(1 - 2\mu v^4)\right] \Bigg\} + \dots, \quad (5.49)
\end{aligned}
$$

correcting the lower order expression (5.33) for $d = 5$. At this order, we have a double pole at $v = 1/(2\mu)^{1/4}$. Demanding regularity of the Kretschmann scalar, we obtain two constraints. One fixes the parameter $\mathcal{C}_1$ (which is related to the viscosity coefficient),

$$
\mathcal{C}_1 = \frac{1}{6(2\mu)^{1/4}}, \quad (5.50)
$$

and the other fixes the residue of the function $A_2(v)$ (which ought to have a simple pole at $v = 1/(2\mu)^{1/4}$). Near the pole, we obtain

$$
A_2(v) \approx \frac{v^2}{9(1 - 2\mu v^4)}, \quad (5.51)
$$

Thus, $A_2(v)$ cannot vanish; however, other than the simple pole at $v = 1/(2\mu)^{1/4}$, it is arbitrary. Finally, there are no constraints on the parameters $\mathcal{C}_3$ and $\mathcal{C}_4$.

The Riemann invariants (5.17) are singular, as in lower order (Eq. (5.34)). Their singularities are canceled by higher-order contributions to the metric (5.44) which, however, spoil boost invariance (*cf.* with the corrected expression (5.37) due to the corrected metric (5.35)).

Having obtained an explicit expression for the metric, we may now use holographic renormalization to compute the stress-energy tensor of the dual gauge theory. This is a tedious task. However, note that the temperature is easy to deduce from the restriction of the transformation (5.38) to the boundary,

$$
\begin{aligned}
t &= \frac{3}{2}\tau^{2/3}\left[1 + \frac{2\tau^2 y^2 - (\tilde{x}^\perp)^2}{9\tau^2}\right] - \mathcal{C}_1 \ln \tau - \frac{3\mathcal{C}_2}{2\tau^{2/3}}, \\
x^1 &= \tau^{2/3}y\left(1 - \frac{\mathcal{C}_1}{\tau^{2/3}} + \frac{\mathcal{C}_2}{\tau^{4/3}}\right), \quad x^\perp = \frac{\tilde{x}^\perp}{\tau^{1/3}}\left(1 - \frac{\mathcal{C}_1}{\tau^{2/3}} + \frac{\mathcal{C}_2}{\tau^{4/3}}\right),
\end{aligned}
\tag{5.52}
$$

with a new correction dependent on $\mathcal{C}_2$. The metric perturbation does not change the argument we employed at lower orders because the perturbation vanishes at the boundary. From the conformal factor relating the static and Bjorken metrics in the next-to-next-to-leading order, we may obtain the temperature as

$$
T = T_H\left(\frac{1}{\tau^{1/3}} - \frac{\mathcal{C}_1}{\tau} + \frac{\mathcal{C}_2}{\tau^{5/3}}\right).
\tag{5.53}
$$

The Stefan-Boltzmann law may be used to calculate the other thermodynamic quantities in the next-to-next-to-leading order. In particular, the viscosity-to-entropy-density ratio is still given by (5.32) with $d = 5$, but with $\mathcal{C}_1$ constrained by (5.50). It follows that this ratio is given by

$$
\frac{\eta}{s} = \frac{1}{4\pi}
\tag{5.54}
$$

which is the same value one obtains from sinusoidal perturbations of the AdS Schwarzschild metric [26]. This is also in agreement with the conclusion reached by considering time-dependent asymptotic solutions of the Einstein equations [52].

5.4 Chapter 5 summary

We discussed the possibility of obtaining viscous Bjorken hydrodynamics on a $(d-1)$-dimensional Minkowski space from a large AdS_d Schwarzschild black hole

(of flat horizon). The latter is normally considered dual to a static gauge theory fluid on the boundary whose temperature coincides with the Hawking temperature. By appropriately modifying the boundary conditions, we obtained viscous Bjorken hydrodynamics on the boundary in the limit of large longitudinal proper time ($\tau \to \infty$) at next-to-leading order. Our results are in agreement with those obtained by considering time-dependent asymptotic solutions of the Einstein equations in five dimensions [18, 30, 56]. Moreover, since our bulk space consisted of a Schwarzschild black hole, we were able to determine the temperature of the conformal fluid on the boundary in terms of the Hawking temperature of the hole. At next-to-next-to-leading order, we saw that no choice of boundary conditions could lead to a boost-invariant flow. In order to obtain a dual Bjorken flow at that order, we had to perturb the black hole metric. This led to a constraint on the viscosity coefficient, and the viscosity-to-entropy-density ratio was fixed to the value $1/(4\pi)$ as in the case of sinusoidal perturbations [26]. This was in agreement with a next-to-next-to-leading-order calculation of a time-dependent asymptotic solution [52].

It may also be worthwhile, albeit tedious, to go beyond the perturbative order considered here. It has already been observed that the supergravity Fefferman-Graham metrics dual to boost-invariant hydrodynamics suffer from singularities of the curvature invariants near the reputed black hole horizon [53]. This occurs at the third perturbative order it the large τ expansion and cannot be canceled by an appropriate choice of transport coefficients as has been done at second order. However, by working with Eddington-Finkelstein instead of Fefferman-Graham coordinates, an expansion in the new time coordinate was shown to lead to nonsingular solutions at all orders with the correct choice of transport coefficients [40, 58]. It would be interesting to investigate the connection of the AdS Schwarzschild black hole metric with these Eddington-Finkelstein-type solutions of the Einstein equations.

Chapter 6

Low-lying quasinormal modes of topological AdS black holes and hydrodynamics

6.1 Introduction

The simplest AdS solution to study is the Schwarzschild metric, which has a dual static CFT on the boundary. This may be extended by looking at small deformations of the Schwarzschild metric, i.e., quasinormal modes which dictate the late-time behavior of the black hole [59]. Calculating these modes has been held in high importance and thereby studied in vast detail (see [60] and references therein). According to the AdS/CFT correspondence, the lowest frequency modes govern the hydrodynamic behavior of the conformal field theory on the boundary [26]. However, these modes are difficult to find and may be missed by some quasinormal mode techniques [61].

In [59, 62] the lowest-lying gravitational quasinormal modes for an AdS Schwarzschild solution were numerically calculated in four and five dimensions and were shown to be in agreement with hydrodynamic perturbations of the gauge theory plasma on the

AdS boundary. For AdS$_5$ this was understood as a finite "conformal soliton flow" after the spherical AdS$_5$ boundary one obtains in global coordinates was conformally mapped to the physically relevant flat Minkowski spacetime. The perturbations also allowed for calculations of the elliptic flow of the plasma and its thermalization time – two of the observables at RHIC. While there is still work to be done, the calculations compared well with what has been found experimentally.

An alternative to a spherical AdS black hole would be to choose one with a hyperbolic horizon [63, 64, 65, 66, 67]. They are usually referred to as topological AdS black holes because they possess topologically nontrivial horizons. Our aim is to elucidate their effect on the gauge theory plasma on the AdS boundary. By studying gravitational perturbations, we shall show that they possess quasinormal modes whose lifetime is comparable to or longer than their counterparts in the case of horizons with positive curvature (spherical black holes). These results are in agreement with those obtained by studying the hydrodynamics of the gauge theory plasma on the boundary. Therefore, topological AdS black holes might have a significant effect on the behavior of the quark-gluon plasma in heavy ion collisions at RHIC and the LHC via the AdS/CFT correspondence.

In Section 6.2 we discuss the scalar, vector, and tensor gravitational perturbations of a topological AdS black hole in d dimensions. We calculate analytically the lowest lying quasinormal modes using the procedure of Ref. [61]. In section 6.3 we study the hydrodynamics of a gauge theory plasma on a hyperbolic space in $d - 1$ dimensions extending the results of Ref. [62]. We show that the frequencies obtained from hydrodynamics are in agreement with their counterparts obtained from black hole perturbations in Section 6.2. We summarize our conclusions in Section 6.4.

6.2 Topological AdS black holes

The Einstein equations for vacuum anti-de Sitter space allows for three separate maximally symmetric solutions parameterized with a single parameter K taking the

values $0, \pm 1$. For $K = 0$ we have a flat horizon whereas for $K = +1$ the horizon is a compact sphere. The case $K = -1$ yields a horizon which is a hyperbolic space and has been much less studied. Nevertheless, in the context of the AdS/CFT correspondence all solutions to the Einstein equations should be taken into account. Here we concentrate on the case of black holes with a hyperbolic horizon ($K = -1$) aiming at elucidating their effect on the gauge theory plasma on the AdS boundary.

The metric of an AdS black hole with $K = -1$ in d spacetime dimensions takes the form

$$ds^2 = -f(r)dt^2 + \frac{dr^2}{f(r)} + r^2 d\Sigma_{d-2}^2, \quad f(r) = r^2 - 1 - \frac{2\mu}{r^{d-3}}, \tag{6.1}$$

where we have chosen units in which the AdS radius is $R = 1$. The horizon radius is found from

$$2\mu = r_H^{d-1}\left(1 - \frac{1}{r_H^2}\right). \tag{6.2}$$

The Hawking temperature is

$$T_H = \frac{(d-1)r_H^2 - (d-3)}{4\pi r_H}. \tag{6.3}$$

The area of the horizon is rendered finite by introducing identifications in the hyperbolic space which make the horizon topologically nontrivial. Thus $\Sigma_{d-2} = \mathbb{H}^{d-2}/\Gamma$ where Γ is a discrete group of isometries of the hyperbolic space $\mathbb{H}^{d-2}$. Various choices of Γ were eagerly studied in the late nineties in preparation for the Wilkinson Microwave Anisotropy Probe as it was thought to possibly describe the type of universe we live in [68]. For example, in $d = 4$ the boundary may be compactified with periodic boundaries around an octagon specified by Γ; in higher dimensions the fundamental domain becomes a generalization of the octagon.

The mass and entropy of the hole are given, respectively, by [66]

$$M = (d-2)(r_H^2 - 1)\frac{r_H^{d-3}}{16\pi G}V_{d-2}, \quad S = \frac{r_H^{d-2}}{4G}V_{d-2}, \tag{6.4}$$

where V_{d-2} is the volume of the hyperbolic space Σ_{d-2}.

Through the AdS/CFT correspondence, the black hole is mapped onto a gauge theory fluid on the boundary of AdS which in this case is the open Einstein static universe, $\Sigma_{d-2} \times \mathbb{R}$. On the other hand, the quark-gluon plasma created in heavy ion collisions lives in Minkowski space ($\mathbb{R}^{d-2,1}$, for $d = 5$). To understand experimental results, we need to choose a different foliation near the boundary of AdS consisting of hypersurfaces which become asymptotically flat. This is achieved through an appropriate coordinate transformation in the bulk which amounts to a conformal transformation between part of the open static universe, $\Sigma_{d-2} \times \mathbb{R}$, and the Minkowski space, $\mathbb{R}^{d-2,1}$. This transforms the static plasma on $\Sigma_{d-2} \times \mathbb{R}$ to a flow of finite extent (soliton) on $\mathbb{R}^{d-2,1}$. In the case of a spherical horizon, this flow was dubbed "conformal soliton flow" [59]. Understanding the behavior of the plasma in our case would entail numerical techniques due to the complexity of $\Sigma_{d-2} \times \mathbb{R}$. We shall leave such a detailed calculation for future work.

Here we concentrate on perturbations of the conformal soliton whose characteristic frequencies and lifetimes are determined by the quasinormal modes of the black hole (real and imaginary parts, respectively).

For the study of perturbations, we need to understand the behavior of harmonic functions on Σ_{d-2}. In general, they obey

$$\left(\nabla^2 + k^2 \right) \mathbb{T} = 0. \tag{6.5}$$

Without identifications (i.e., in $\mathbb{H}^{d-2}$), the spectrum is continuous. We obtain [69]

$$k^2 = \xi^2 + \left(\frac{d-3}{2} \right)^2 + \delta, \tag{6.6}$$

where ξ is arbitrary and $\delta = 0, 1, 2$ for scalar, vector and tensor perturbations, respectively. When a compactification scheme is chosen, the spectrum becomes discrete. Depending on the choice of Γ, the discretized eigenvalues ξ may be made

as small as desired, i.e., zero is an accumulation point of the spectrum of ξ [68]. As $\xi \to 0$, the complexity of the set of isometries Γ increases and the volume V_{d-2} of the hyperbolic space Σ_{d-2} diverges (hence also the mass and entropy of the hole). This ought to be studied numerically for a detailed comparison with experimental data in heavy ion collisions at RHIC through a generalization of the approach of [59].

Having understood the harmonics on Σ_{d-2}, we may write the wave equation for gravitational perturbations in the general Schrödinger-like form [70]

$$-\frac{d^2\phi}{dr_*^2} + V[r(r_*)]\phi = \omega^2\phi \qquad (6.7)$$

in terms of the tortoise coordinate r_* defined by

$$\frac{dr_*}{dr} = \frac{1}{f(r)} \qquad (6.8)$$

where $f(r)$ is defined in (6.1). The potential takes different forms for different types of perturbation. We shall study each case separately.

6.2.1 Vector perturbations

The vector potential is given by

$$V_V = \frac{f(r)}{r^2}\left(k_V^2 - 1 + \frac{(d-2)(d-4)}{4}(r^2 - 1) - \frac{3(d-2)^2\mu}{r^{d-3}}\right), \qquad (6.9)$$

where k_V^2 is an eigenvalue of a vector harmonic (Eq. (6.6) with $\delta = 1$).

It is convenient to introduce the variable

$$u = \left(\frac{r_H}{r}\right)^{d-3}. \qquad (6.10)$$

The wave equation (6.7) takes the form

$$-(d-3)^2 u^{\frac{d-4}{d-3}}\hat{f}(u)\partial_u\left(u^{\frac{d-4}{d-3}}\hat{f}(u)\partial_u\phi\right) + \hat{V}_V(u)\phi = \hat{\omega}^2\phi, \qquad (6.11)$$

where

$$\hat{V}_V(u) = \hat{f}(u)\left[\hat{k}_V^2 + \frac{(d-2)(d-4)}{4}u^{\frac{2}{3-d}} - \frac{3(d-2)^2}{4}u\right.$$
$$\left. - \frac{1}{r_H^2}\left(1 + \frac{(d-2)(d-4)}{4} - \frac{3(d-2)^2}{4}u\right)\right],$$
$$\hat{f}(u) = \frac{f(r)}{r^2} = 1 - u^{\frac{2}{d-3}}\left(u + \frac{1-u}{r_H^2}\right), \quad \hat{\omega}^2 = \frac{\omega^2}{r_H^2}, \quad \hat{k}_V^2 = \frac{k_V^2}{r_H^2}. \quad (6.12)$$

With $\hat{\omega}$ and $\hat{k}_V$ fixed, to leading order in $1/r_H$ this is the same equation as the case of a flat horizon studied in [26] and also coincides with the leading-order equation in the case of spherical horizon studied in [61]. The curvature of the horizon only comes into play at $\mathcal{O}(1/r_H^2)$, as expected, since the horizon becomes flat in the limit $r_H \to \infty$. Following the perturbative analysis performed in [61], we shall solve the wave equation in the $r_H \to \infty$ limit and add the $\mathcal{O}(1/r_H^2)$ contributions as perturbative corrections (treating $\hat{\omega}, \hat{k}_V^2 \sim \mathcal{O}(1/r_H^2)$).

Factoring out the behavior of ϕ as it approaches the horizon ($u = 1$),

$$\phi(u) = (1-u)^{-i\frac{\hat{w}}{d-1}}F(u) \qquad (6.13)$$

so that the wave equation in the large r_H limit (including $\mathcal{O}(1/r_H^2)$ contributions) becomes

$$\mathcal{H}F \equiv \mathcal{A}F'' + \mathcal{B}F' + \mathcal{C}F = 0, \qquad (6.14)$$

where

$$\mathcal{A} = -(d-3)^2 u^{\frac{2d-8}{d-3}}\left(1-u^{\frac{d-1}{d-3}}\right) + \frac{2(d-3)^2}{r_H^2}u^2(1-u),$$

$$\mathcal{B} = -(d-3)[d-4-(2d-5)u^{\frac{d-1}{d-3}}]u^{\frac{d-5}{d-3}} - 2(d-3)^2\frac{i\hat{\omega}}{d-1}\frac{u^{\frac{2d-8}{d-3}}(1-u^{\frac{d-1}{d-3}})}{1-u}$$
$$+\frac{d-3}{r_H^2}u\left[(d-3)(2-3u)-(d-1)\frac{1-u}{1-u^{\frac{d-1}{d-3}}}u^{\frac{d-1}{d-3}}\right],$$

$$\mathcal{C} = \hat{k}_V^2 + \frac{(d-2)[d-4-3(d-2)u^{\frac{d-1}{d-3}}]}{4}u^{-\frac{2}{d-3}}$$
$$-(d-3)\frac{i\hat{\omega}}{d-1}\frac{[d-4-(2d-5)u^{\frac{d-1}{d-3}}]u^{\frac{d-5}{d-3}}}{1-u} - (d-3)^2\frac{i\hat{\omega}}{d-1}\frac{u^{\frac{2d-8}{d-3}}(1-u^{\frac{d-1}{d-3}})}{(1-u)^2}$$
$$-\frac{d-2}{2r_H^2}\left[d-4-(2d-5)u-(d-1)\frac{1-u}{1-u^{\frac{d-1}{d-3}}}u^{\frac{d-1}{d-3}}\right]. \tag{6.15}$$

Expanding the wave function,

$$F = F_0 + F_1 + \ldots \tag{6.16}$$

we may solve the wave equation (6.14) perturbatively.

The zeroth order wave equation,

$$\mathcal{H}_0 F_0 = 0 \tag{6.17}$$

is obtained in the limit $\hat{\omega}, \hat{k}_v, 1/r_H^2 \to 0$. Explicitly,

$$\mathcal{H}_0 F_0 = \mathcal{A}_0 F_0'' + \mathcal{B}_0 F_0' + \mathcal{C}_0 F_0, \tag{6.18}$$

where

$$\mathcal{A}_0 = -(d-3)^2 u^{\frac{2d-8}{d-3}}\left(1-u^{\frac{d-1}{d-3}}\right),$$

$$\mathcal{B}_0 = -(d-3)[d-4-(2d-5)u^{\frac{d-1}{d-3}}]u^{\frac{d-5}{d-3}},$$

$$\mathcal{C}_0 = \frac{(d-2)[d-4-3(d-2)u^{\frac{d-1}{d-3}}]}{4}u^{-\frac{2}{d-3}}. \tag{6.19}$$

94

The zeroth order wave equation (6.17) has the two exact solutions

$$F_0 = u^{\frac{d-2}{2(d-3)}}, \quad \check{F}_0 = u^{-\frac{d-4}{2(d-3)}} \, _2F_1\left(1, -\frac{d-3}{d-1}, \frac{2}{d-1}; u^{\frac{d-1}{d-3}}\right). \tag{6.20}$$

The former is well behaved at both the horizon $(u \to 1)$ and the boundary $(u \to 0)$ but the latter diverges at both ends, therefore it is unacceptable.

The constraint for $\hat{\omega}$ comes from the first order equation which accounts for the $\mathcal{O}(1/r_H^2)$ terms in (6.14)

$$\mathcal{H}_0 F_1 + \mathcal{H}_1 F_0 = 0 \tag{6.21}$$

solved by

$$F_1 = -F_0 \int \frac{\check{F}_0 \mathcal{H}_1 F_0}{\mathcal{A}_0 \mathcal{W}_0} + \check{F}_0 \int \frac{F_0 \mathcal{H}_1 F_0}{\mathcal{A}_0 \mathcal{W}_0} \tag{6.22}$$

where $\mathcal{W}_0$ is the zeroth order Wronskian

$$\mathcal{W}_0 = \frac{1}{u^{\frac{d-4}{d-3}}\left(1 - u^{\frac{d-1}{d-3}}\right)}. \tag{6.23}$$

The second term in the expression for F_1 is ill-behaved at both the boundary and the horizon. If we choose one of the limits of integration at the boundary $(u = 0)$, then the second term becomes regular there. However, at the horizon it diverges due to the behavior of $\check{F}_0$. This is avoided if the coefficient of $\check{F}_0$ vanishes as $u \to 1$. This requirement yields the constraint

$$\int_0^1 \frac{F_0 \mathcal{H}_1 F_0}{\mathcal{A}_0 \mathcal{W}_0} = 0, \tag{6.24}$$

which is a linear equation in $\hat{\omega}$ whose solution is

$$\hat{\omega} = -i \frac{\hat{k}_V^2 + \frac{d-3}{r_H^2}}{d-1}. \tag{6.25}$$

This is the frequency of the lowest-lying vector quasinormal mode. It can be written as

$$\omega = -i\frac{\xi^2 + \left(\frac{d-1}{2}\right)^2}{(d-1)r_H}.$$ (6.26)

This mode is inversely proportional to the radius of the horizon and will dictate the hydrodynamics of the dual gauge theory. We obtain an upper bound for the lifetime of this mode which may be written in terms of the temperature $T_H \approx \frac{d-1}{4\pi} r_H$ (Eq. (6.3) in the large r_H limit and in units in which the AdS radius is $R = 1$),

$$\tau = \frac{1}{|\omega|} < \frac{16\pi}{(d-1)^2} T_H.$$ (6.27)

In the physically interesting case of $d = 5$, this reads $\tau < \pi T_H$. To compare this with the case of a spherical horizon, note that the frequency is given by [61]

$$\omega^{S^{d-2}} = -i\frac{(l+d-2)(l-1)}{(d-1)r_H}.$$ (6.28)

which yields a maximum lifetime

$$\tau_{\max}^{S^{d-2}} = \frac{4\pi}{d} T_H$$ (6.29)

and in the case $d = 5$, we obtain an upper bound of $\frac{4\pi}{5} T_H$ which is lower than the upper bound in the hyperbolic case (πT_H).

To assess the relevance of this result to heavy ion collisions, one ought to relate the lifetime (6.27) to the thermalization time of the plasma which lives on flat Minkowski space $\mathbb{R}^{d-2,1}$. For spherical horizons, the latter is roughly half the former [59]. In our case, the relationship will be determined once the conformal map from part of the open Einstein static universe $\Sigma_{d-2} \times \mathbb{R}$ onto $\mathbb{R}^{d-2,1}$ is found. As discussed earlier, this will require the use of numerical techniques and is deferred to future work. Nevertheless, the large value of the lifetime (6.27) indicates that these modes may play a role in determining the behavior of the quark-gluon plasma.

6.2.2 Scalar perturbations

We now turn our attention to scalar perturbations for which the master equation can be cast into the same form as (6.11) but with a new potential,

$$
\begin{aligned}
\hat{V}_S(u) &= \frac{u^{-\frac{2}{d-3}} - u - \frac{1}{r_H^2}(1-u)}{4(\hat{m}+u)^2}\Bigg\{ (-6+d)(-4+d)\hat{m}^2 - 6(-4+d)(-2+d)\hat{m}u \\
&+ (-2+d)du^2 - 3(-6+d)(-2+d)\hat{m}^2 u^{\frac{d-1}{d-3}} + 2(-2+d)(-1+d)\hat{m}^3 u^{\frac{2}{-3+d}} \\
&+ 2(18+d(-11+2d))\hat{m}u^{\frac{2(d-2)}{d-3}} + (-2+d)^2 u^{\frac{3d-7}{d-3}} \\
&- \frac{u^{\frac{2}{d-3}}}{r_H^2}[(-2+d)\hat{m}^2(d+2(-1+d)\hat{m}) - 3(-2+d)\hat{m}(-8-6\hat{m}+d(2+\hat{m}))u \\
&+ (24+36\hat{m}+d(-10+d-22\hat{m}+4d\hat{m}))u^2 + (-2+d)^2 u^3]\Bigg\}, \tag{6.30}
\end{aligned}
$$

where

$$
\hat{m} = 2\frac{k_S^2 + d - 2}{(d-1)(d-2)(r_H^2 - 1)} \tag{6.31}
$$

and k_S^2 is an eigenvalue of a scalar harmonic (Eq. (6.6) with $\delta = 0$).

A new singularity at $u = -\hat{m}$ arises in the scalar potential. It is best to factor out the behavior at this point in addition to the behavior at the horizon and boundary. We see again that the effect of the curvature enters at $\mathcal{O}(1/r_H^2)$ and the wave equation matches the spherical case [61] at leading order first in $1/r_H$.

Defining

$$
\phi(u) = (1-u)^{-i\frac{\hat{w}}{d-1}}\frac{u^{\frac{d-4}{2(d-3)}}}{\hat{m}+u}F(u) \tag{6.32}
$$

as in the vector case we obtain a wave equation for F which may be solved perturbatively. In the vector case, we had $\hat{\omega}, \hat{k}_V^2 \sim \mathcal{O}(1/r_H^2)$, so keeping terms to $\mathcal{O}(1/r_H^2)$ we could drop terms which were quadratic in $\hat{\omega}$. In the scalar case, the frequency has a real part which is related to the speed of sound in the gauge theory fluid [26]. In a conformal fluid, the speed of sound is $\frac{1}{\sqrt{d-2}}$. Therefore, in the limit $r_H \to \infty$ we expect $\omega \sim \mathcal{O}(1)$, consequently terms which are quadratic in $\hat{\omega} = \frac{\omega}{r_H}$ must be kept and will contribute at first order in $1/r_H^2$.

The zeroth-order wave equation ought to coincide with the case of a spherical horizon, because the curvature plays no role at leading order. Following [61], we choose

$$\mathcal{H}_0 F_0 = \mathcal{A}_0 F_0'' + \mathcal{B}_0 F_0' + \mathcal{C}_0 F_0 = 0, \tag{6.33}$$

where

$$
\begin{aligned}
\mathcal{A}_0 &= -(d-3)^2 u^{\frac{2d-8}{d-3}}(1 - u^{\frac{d-1}{d-3}}), \\
\mathcal{B}_0 &= -(d-3)u^{\frac{2d-8}{d-3}}(1 - u^{\frac{d-1}{d-3}})\left[\frac{d-4}{u} - \frac{2(d-3)}{\hat{m}+u}\right] \\
&\quad - (d-3)[d-4 - (2d-5)u^{\frac{d-1}{d-3}}]u^{\frac{d-5}{d-3}}, \\
\mathcal{C}_0 &= 0. \tag{6.34}
\end{aligned}
$$

This zeroth order wave equation has two linearly independent solutions,

$$F_0 = 1, \tag{6.35}$$

which is well-behaved at all points and a singular one which can be written in terms of the Wronskian,

$$\check{F}_0 = \int \mathcal{W}_0 \,, \quad \mathcal{W}_0 = \frac{(\hat{m}+u)^2}{u^{\frac{2d-8}{d-3}}(1 - u^{\frac{d-1}{d-3}})}. \tag{6.36}$$

Care must be exercised in the case $d = 4$ where $\check{F}_0$ does not lead to a singularity at the boundary; however, the boundary conditions ought to be altered to Robin boundary conditions [61, 62].

Proceeding as with vector perturbations, a constraint similar to (6.24) is found by including terms up to $\mathcal{O}(1/r_H^2)$ which also account for the contributions of $\hat{m} \sim \mathcal{O}(1/r_H^2)$ and $\hat{\omega} \sim \mathcal{O}(1/r_H)$. After some tedious algebra, we arrive at a quadratic equation for $\hat{\omega}$,

$$\frac{d-1}{2}\frac{1 + (d-2)\hat{m}}{(1+\hat{m})^2} - \frac{1}{r_H^2}\left(\frac{1}{\hat{m}} + \mathcal{O}(1)\right) - i\hat{\omega}\frac{d-3}{(1+\hat{m})^2} - \hat{\omega}^2\left(\frac{1}{\hat{m}} + \mathcal{O}(1)\right) = 0. \tag{6.37}$$

98

The two solutions for small $\hat{m}$ are

$$\hat{\omega} = \pm\sqrt{\frac{d-1}{2}\hat{m} - \frac{1}{r_H^2}} - i\frac{d-3}{2}\hat{m}, \tag{6.38}$$

which may also be written as

$$\omega_0 = \pm\frac{k_S}{\sqrt{d-2}} - i\frac{d-3}{(d-1)(d-2)r_H}\left[k_S^2 + d - 2\right]. \tag{6.39}$$

The real part gives the correct speed of sound $(\frac{1}{\sqrt{d-2}})$ whereas the imaginary part yields the lifetime

$$\tau = \frac{1}{|\Im\omega|} = \frac{4\pi(d-2)}{(d-3)(\xi^2 + \left(\frac{d-1}{2}\right)^2)} T_H. \tag{6.40}$$

This is bounded by

$$\tau < \frac{16\pi(d-2)}{(d-3)(d-1)^2} T_H \tag{6.41}$$

to be compared with the maximum lifetime of a scalar mode in the spherical horizon case [61]

$$\tau_{\max}^{S^{d-2}} = \frac{4(d-2)\pi}{(d-3)d} T_H. \tag{6.42}$$

In the physically interesting case $d = 5$, the bound for a hyperbolic horizon is $\frac{3\pi}{2} T_H$ which is higher than the maximum lifetime for a spherical horizon, $\frac{6\pi}{5} T_H$, as well as the upper bounds of vector modes.

These modes may be important in understanding the quark-gluon plasma, but again, as with vector modes, their significance will be determined after one computes their relationship to the thermalization time of the quark-gluon plasma. These modes correspond to perturbations of a static fluid on the open Einstein universe $\Sigma_{d-2} \times \mathbb{R}$ and need to be transformed to the Minkowski space ($\mathbb{R}^{d-2,1}$, where $d = 5$ for comparison with experimental data) in which the quark-gluon plasma lives.

6.2.3 Tensor perturbations

The remaining quasinormal modes come from tensor perturbations. Following [70], the wave equation may be cast in the same form as (6.11) with the potential in the large r_H limit,

$$\hat{V}_T(u) = \frac{d-2}{4}\left(du^{-\frac{2}{d-3}} - (d-2)u^{\frac{2(d-2)}{d-3}} - 2u\right) + \hat{k}_T^2\left(1 - u^{\frac{d-1}{d-3}}\right), \qquad (6.43)$$

where $\hat{k}_T = k_T/r_H$ and k_T is the tensor harmonic eigenvalue given by Eq. (6.6) with $\delta = 2$.

The zeroth order wave equation can be solved as in the spherical case [61] to find the two independent solutions

$$\phi_0 = u^{-\frac{d-2}{2(d-3)}}, \quad \hat{\phi}_0 = u^{-\frac{d-2}{2(d-3)}}\ln\left(1 - u^{\frac{d-1}{d-3}}.\right) \qquad (6.44)$$

Both can be seen to diverge at the boundary $(u \to 0)$ and the horizon $(u \to 1)$. Therefore, there are no low frequency tensor modes. The lowest modes are expected to have frequencies $\omega \sim \mathcal{O}(r_H)$ and cannot be found using the same perturbative technique as with vector and scalar modes. We are not interested in finding the tensor modes in this case because they do not contribute to the hydrodynamic behavior of the gauge theory plasma.

6.3 Hydrodynamics

In the previous section we calculated the lowest lying quasinormal modes whose imaginary part was inversely proportional to the radius of the horizon (and therefore their lifetime was proportional to the Hawking temperature of the black hole). Based on the analysis in [60], the overtones do not exhibit this behavior; their frequencies are all proportional to the radius of the horizon for large black holes. This leads to the interpretation of the lowest-lying modes corresponding to the hydrodynamics on

the dual gauge theory plasma [26], and the subsequent overtones to its microscopic behavior. In this section, we study the hydrodynamics in the linearized regime of a $d-1$ dimensional fluid with dissipative effects taken into account, similar to Section 2.1. The fluid lives on the boundary with topology $\mathbb{R} \times \Sigma_{d-2}$ where $\Sigma_{d-2} = \mathbb{H}^{d-2}/\Gamma$, i.e., the quotient of the hyperbolic space $\mathbb{H}^{d-2}$ with the discrete group of isometries Γ. We thus extend earlier results for a spherical boundary [62].

Using μ, ν running over the boundary with metric

$$ds^2_{\text{boundary}} = -dt^2 + d\Sigma^2_{d-2} \tag{6.45}$$

and i, j over only the hyperbolic space Σ_{d-2}, the hydrodynamic equations for the conformal fluid follow in a standard manner,

$$
\begin{aligned}
T^{\mu\nu} &= (\epsilon + p)u^\mu u^\nu + p g^{\mu\nu} - \zeta \triangle^{\mu\nu} \nabla_\lambda u^\lambda \\
&\quad - \eta \left(\triangle^{\mu\lambda} \nabla_\lambda u^\nu + \triangle^{\nu\lambda} \nabla_\lambda u^\mu - \frac{2}{d-2} \triangle^{\mu\nu} \nabla_\lambda u^\lambda \right), \\
\nabla_\mu T^{\mu\nu} &= 0, \\
T^\mu_\mu &= 0,
\end{aligned}
\tag{6.46}
$$

where $\triangle_{\mu\nu} = g_{\mu\nu} + u_\mu u_\nu$ and ϵ, p, η and ζ represent the energy density, pressure, shear viscosity and bulk viscosity, respectively, of the conformal field theory. Two constraints on the parameters immediately follow,

$$\epsilon = (d-2)p, \quad \zeta = 0, \tag{6.47}$$

u^μ is the velocity field of the conformal fluid. The reference frame is chosen so that $u^\mu u_\mu = -1$. In the rest frame of the fluid, $u^\mu = (1, 0, 0, 0)$. Perturbations introduce small disturbances,

$$u^\mu = (1, u^i), \tag{6.48}$$

where u^i is small and also allow for small corrections to the pressure so that

$$p = p_0 + \delta p. \tag{6.49}$$

Applying (6.46), we obtain the set of hydrodynamic equations

$$
\begin{aligned}
0 &= \nabla_\mu T^{\mu t} = (d-2)\partial_t \delta p + (d-1)p_0 \nabla_i u^i, \\
0 &= \nabla_\mu T^{\mu i} = (d-1)p_0 \partial_t u^i + \partial^i \delta p \\
&\quad - \eta \left[\nabla^j \nabla_j u^i - (d-3)u^i + \frac{d-4}{d-2}\partial^i(\nabla_j u^j) \right],
\end{aligned}
\tag{6.50}
$$

where we used $R_{ij} = -(d-3)g_{ij}$.

Looking first at vector perturbations of the fluid, the appropriate ansatz is [62]

$$\delta p = 0, \quad u^i = \mathcal{A}_V e^{-i\Omega t} \mathbb{V}^i, \tag{6.51}$$

where $\mathbb{V}^i$ is a vector harmonic.

The first hydrodynamic equation is trivially satisfied and the second becomes

$$-i\Omega(d-1)p_0 + \eta \left[k_V^2 + d - 3 \right] = 0 \tag{6.52}$$

This can be solved for the frequency Ω characterizing the deviation from a perfect fluid. The solution may be written in terms of the parameters of the dual black hole. Using Eqs. (6.4) and (6.47), we obtain

$$\frac{\eta}{p_0} = \frac{4\pi\eta}{s}\frac{r_H}{r_H^2 - 1}, \tag{6.53}$$

where s is the entropy density. With $\frac{\eta}{s} = \frac{1}{4\pi}$ [26] and for large r_H we arrive at the expression for the frequency of vector perturbations

$$\Omega = -i\frac{k_V^2 + d - 3}{(d-1)r_H}. \tag{6.54}$$

102

This is in agreement with the frequency of vector modes of the black hole, Eq. (6.26), on account of the definition (6.6).

Turning now to scalar hydrodynamic perturbations, we should allow for deviations in pressure as well as the velocity field. The appropriate ansatz is [62]

$$u^i = \mathcal{A}_S e^{-i\Omega t} \partial^i \mathbb{S}, \quad \delta p = \mathcal{B}_S e^{-i\Omega t} \mathbb{S}, \tag{6.55}$$

where $\mathbb{S}$ is a scalar harmonic. The hydrodynamic equations become

$$(d-2)i\Omega \mathcal{B}_S + (d-1)p_0 k_S^2 \mathcal{A}_S = 0,$$
$$\mathcal{B}_S + \mathcal{A}_S \left[-i\Omega(d-1)p_0 + 2(d-3)\eta + 2\eta k_S^2 \frac{d-3}{d-2} \right] = 0. \tag{6.56}$$

This is a linear system of homogeneous equations. To be compatible, their determinant must vanish,

$$\det \begin{pmatrix} (d-2)i\Omega & (d-1)p_0 k_S^2 \\ 1 & -i\Omega(d-1)p_0 + 2(d-3)\eta + 2\eta k_S^2 \frac{d-3}{d-2} \end{pmatrix} = 0, \tag{6.57}$$

which imposes a constraint on the frequency Ω. Working along the same lines as for the vector perturbation, we arrive at the expression for Ω,

$$\Omega = \pm \frac{k_S}{\sqrt{d-2}} - i \frac{d-3}{(d-1)(d-2)r_H} \left[k_S^2 + d - 2 \right], \tag{6.58}$$

which is in exact agreement with the quasinormal frequency of scalar gravitational perturbations (6.39).

Finally, an ansatz cannot be built to describe tensor perturbations with the associated harmonics because of the tracelessness and zero divergence of tensor spherical harmonics. This is in consistent with the negative conclusion reached in Section 6.2 on tensor modes of gravitational perturbations of the black hole.

103

6.4 Chapter 6 summary

We analytically calculated the low-lying quasinormal modes of topological AdS black holes in arbitrary dimension in the high temperature limit. These are black holes with hyperbolic horizons of nontrivial topology. We considered all three different types of perturbations (scalar, vector and tensor) and solved the wave equation [70] in each case by applying the method of Ref. [61]. We obtained quasinormal frequencies which were in agreement with the frequencies obtained by considering perturbations of the gauge theory fluid on the boundary, thus extending results obtained in the case of black holes with spherical horizons [62].

In the physically interesting case of five dimensions, we showed that the lifetimes of some of these modes exceed the longest lifetime of the modes of a black hole with spherical horizon [59, 61]. Therefore, they play an important role in the late time behavior of the gauge theory fluid and may contribute to the properties of the quark-gluon plasma produced in heavy ion collisions.

Chapter 7

Conclusion and Outlook

In this dissertation, we started with a discussion of relativistic heavy ion collisions. Some of the data from RHIC, supporting the quark-gluon plasma existing in a fluid state, was presented with the major component being a collective motion of the constituents characterized by the elliptic flow. Hydrodynamical theory was developed as a description of the fireball. Bjorken's model, which implements homogeneous longitudinal expansion, could then be used to derive the thermodynamic quantities $(\varepsilon, p, \rho, \dots)$ associated with the collision. However, hydrodynamics has no ability to derive the transport coefficients for dissipation. To do this, one needs a microscopic theory that incorporates the interactions of quarks and gluons.

The AdS/CFT correspondence was presented as doing just that. There are two perspectives to consider with the correspondence. The first is a strongly coupled gauge theory with the second focusing on supergravity. The gauge theory is $\mathcal{N} = 4$ SYM, but, in RHIC's regime, the difference between SYM and QCD is softened. The AdS/CFT correspondence was shown to be the most attractive when studying dissipative processes. We then reproduced Bjorken hydrodynamics but with the shear viscosity determined.

In the subsequent chapters, we discussed our contribution to the field applying the AdS/CFT correspondence to hydrodynamically flowing systems. In line with

studying viscosity, we turned the system around to study energy transfer by means of the conductivity coefficient. The supergravity equations constrained the conductivity to fall as a power-law in the longitudinal propertime as well as creating a temperature gradient.

In Chapters 4 and 5, we developed the framework to derive the time-dependent temperature and entropy. This was achieved by taking a static Schwarzschild black hole and foliating it with time-dependent slices. When the transformation was constrained correctly, we produced the time-dependent black hole that is dual to Bjorken hydrodynamics. The temperature and entropy are found by the conformal transformation between the static Minkowski space boundary and the time-dependent boundary.

Lastly, we turned our attention to quasinormal modes. These were found for gravitational perturbations of a topological black hole. The frequencies are related to the hydrodynamic lifetimes of a strongly coupled plasma. Whereas much work has been done for flat and spherical boundaries, hyperbolic boundaries have received somewhat less. However, we showed that the hyperbolic hydrodynamic modes can exist for longer than the other two.

A few possible directions for work directly related to the material in the Chapters is discussed in the following.

Chapter 3:

It would be interesting to relax the assumption of rapidity invariance of the bulk metric and consider more general forms by including dependence on transverse spatial coordinates. That would lead to a more complicated energy flow by introducing viscosity in combination with conduction.

Chapter 4:

Interesting results might be found if the AdS_d Schwarzschild metric (or other exact solutions of the Einstein equations) are used to study subleading terms, aside from viscosity, in the τ expansion of time-dependent solutions of the Einstein equations. This would encode the effects of dissipation of the gauge theory fluid on the boundary.

Chapter 5:

If we do not perturb the black hole metric, deviations from Bjorken flow are found, which are a subleading effect at late times. It might be worth exploring the connection of such deviations (coming from a dual Schwarzschild black hole) to experimental data.

Chapter 6:

Further work is required for a detailed comparison with experimental data which will determine how a topological AdS black hole scenario is applicable to RHIC and the LHC. Following the analysis of [59], one needs to map the hyperbolic boundary of the topological black holes onto flat Minkowski space via a conformal map and study the resulting flow of the gauge theory fluid. Unlike in the case of a spherical boundary, this procedure cannot be carried out analytically for topological AdS black holes owing to the complexity of the (topologically nontrivial) boundary [68]. Instead, one needs to resort to numerical techniques.

There is still more work to be done with flowing hydrodynamical duals. The more refined dualities which feature flavor, confinement, or any number of interesting characteristics have largely not been applied to time-dependent systems. With respect to heavy ion collisions, there is the matter of rapidity dependence in a supergravity setting. A gravitational dual that incorporates this loss of symmetry might help us to gain some insight via the observable particle distributions from RHIC. Additionally, the framework developed in Chapters 2 and 3 could be used for studying the elliptic flow structure, thermalization, and quark drag of a strongly coupled plasma in a time dependent setting. The drag calculations are considered a candidate for quantitatively comparing the use of holographic constructions and perturbative QCD at the Large Hadron Collider [71].

Bibliography

Bibliography

[1] H. D. Politzer, "Reliable perturbvative results for strong interactions?," Phys. Rev. Lett. **30**, 1346 (1973); 2

H. D. Politzer, "Asymptotic freedom: an approach to strong interactions," Phys. Rept. **14**, 129 (1974);

D. J. Gross and F. Wilczek, "Asymptotically free gauge theories I," Phys. Rev. D **8**, 3633 (1973);

D. J. Gross and F. Wilczek, "Asymptotically free gauge theories II," Phys. Rev. D **9**, 980 (1974).

[2] I. Arsene et al. [BRAHMS Collaboration], "Quarkgluon plasma and color glass condensate at RHIC? The perspective from the BRAHMS experiment," Nucl. Phys. **A757**, 1 (2005); 2, 12

B. B. Back et al. [PHOBOS Collaboration], "The PHOBOS perspective on discoveries at RHIC," Nucl. Phys. **A757**, 28 (2005);

J. Adams et al. [STAR Collaboration], "Experimental and theoretical challenges in the search for the quarkgluon plasma: The STAR Collaboration's critical assessment of the evidence from RHIC collisions," Nucl. Phys. **A757**, 102 (2005);

K. Adcox et al. [PHENIX Collaboration], "Formation of dense partonic matter in relativistic nucleusnucleus collisions at RHIC: Experimental evaluation by the PHENIX Collaboration," Nucl. Phys. **A757**, 184 (2005).

[3] Jeffery Mitchell, Brookhaven National Lab - RHIC Animations http://www.phenix.bnl.gov/WWW/software/luxor/ani/ 3

[4] Bartels, J. and others, "Proceedings of the 38th international symposium on multiparticle dyanmics (ISMD08)," [arXiv:0902.0377]. 4

[5] Brookhaven National Lab - RHIC, http://www.bnl.gov/rhic/complex.asp 5

[6] K. H. Ackermann et al., "STAR detector overview," Nucl. Instrum. Meth. A **499**, 624 (2003). 7

[7] PHOBOS Detector, http://www.phobos.bnl.gov/index_12_12_05.htm 8

[8] BRAHMS Detector, http://www.bnl.gov/rhic/PHOBOS_BRAHMS.asp 9

[9] B. Sahlmueller, "Photons at RHIC," PoS (High-pT physics09), (2009), [arXiv:0904.4764] 10

[10] J. Adams et al. [STAR Collaboration], "Evidence from d+Au measurements for final-state suppression of high-pT hadrons in Au+Au collisions at RHIC," Phys. Rev. Lett. **91**, 072304, (2003). 11

[11] S. Wheaton and J. Cleymans, "THERMUS: A thermal model package for ROOT," Comput. Phys. Commun. **180**, 84, (2009), [arXiv:hep-ph/0407174]. 10

[12] M. Kaneta, "π^0 and photon v_2 study in $\sqrt{s_{NN}} = 200$GeV Au+Au collisions," "Collective flow and QGP properties," RIKEN-BNL workshop, (2003) 13

[13] E. Shuryak, "Why does the quark gluon plasma at RHIC behave as a nearly ideal fluid?," Prog. Part. Nucl. Phys. **53**, 273 (2004), [arXiv:hep-ph/0312227]; 13, 14

S. A. Voloshin, A. M. Poskanzer, and R. Snellings, "Collective phenomena in non-central nuclear collisions," (2008), [arxiv:0809.2949].

[14] M. L. Miller, K. Reygers, S. Sanders, M. L. Miller, and P. Steinberg, "Glauber modeling in high energy nuclear collisions," Ann. Rev. Nucl. Part. Sci. **57**, 205 (2007), [arXiv:nucl-ex/0701025] 14

[15] A. Adare et al. [PHENIX Collaboration], "Scaling properties of azimuthal anisotropy in Au+Au and Cu+Cu collisions at $\sqrt{s_{NN}} = 200$ GeV" Phys. Rev. Lett. **98**, 162301 (2007), [arXiv:nucl-ex/0608033]. 14

[16] P. F. Kolb, J. Sollfrank and U. W. Heinz, "Anisotropic transverse flow and the quark-hadron phase transition," Phys. Rev. C **62**, 054909 (2000), [arXiv:hep-ph/0006129]. 15

[17] M. Murray, for the BRAHMS Collaboration, "Scanning the phases of QCD with BRAHMS," J. Phys. G. **30**, S667 (2004), [arXiv:nucl-ex/0404007]. 16

[18] R. A. Janik and R. Peschanski, "Asymptotic perfect fluid dynamics as a consequence of AdS/CFT," Phys. Rev. D **73**, 045013 (2006) [arXiv:hep-th/0512162]. 16, 41, 45, 47, 59, 60, 62, 64, 65, 69, 87

[19] D. Bak and R. A. Janik "From static to evolving geometries–R-charged hydrodynamics from supergravity," Phys. Lett. B **645**, 303 (2007) [arXiv:hep-th/0611304]. 16, 45, 46, 47, 52, 53, 56, 58, 59, 64, 65

[20] J. Alsup, G. Siopsis and C. Middleton, "AdS/CFT correspondence with heat conduction," Phys. Lett. B **654** (2007) [arXiv:hep-th/0607139]. 17, 59

[21] J. Alsup and G. Siopsis, "Bjorken flow from an AdS Schwarzschild black hole," Phys. Rev. Lett. **101**, 031602 (2008) [arXiv:0712.216]. 17, 70

[22] J. Alsup and G. Siopsis, "Dissipative Bjorken hydrodynamics from an AdS Schwarzschild black hole" Phys. Rev. D **79** 066011; [arXiv:0812.1818]. 17

[23] J. Alsup and G. Siopsis, "Low-lying quasinormal modes of topological AdS black holes and hydrodynamics" Phys. Rev. D **78** 086001; [arXiv:0805.0287]. 18

[24] L.D. Landau and E.M. Lifshitz, *Fluid Mechanics*, Pergamon Press, NewYork, 1987, 2nd ed. 19, 22

[25] R. Baier, P. Romatschke, D. T. Son, A. O. Starinets and M. A. Stephanov, "Relativistic viscous hydrodynamics, conformal invariance, and holography," JHEP **0804**, 100 (2008) [arXiv:0712.2451]. 20, 43, 81

[26] G. Policastro, D. T. Son and A. O. Starinets, "The shear viscosity of strongly coupled $N = 4$ supersymmetric Yang-Mills plasma," Phys. Rev. Lett. **87**, 081601 (2001) [arXiv:hep-th/0104066]; 20, 27, 38, 40, 71, 73, 86, 87, 88, 93, 97, 101, 102

G. Policastro, D. T. Son and A. O. Starinets, "From AdS/CFT correspondence to hydrodynamics," JHEP **0209**, 043 (2002) [arXiv:hep-th/0205052];

D. T. Son, and A. .O. Starinets, "Minkowski-space correlators in AdS/CFT correspondence: recipe and applications," JHEP **09**, 042 (2002) [arXiv:hep-th/0205051];

P. Kovtun, D. T. Son and A. O. Starinets, "Viscosity in strongly interacting quantum field theories from black hole physics," Phys. Rev. Lett. **94**, 111601 (2005) [arXiv:hep-th/0405231];

A. Buchel and J. T. Liu, "Universality of the shear viscosity in supergravity," Phys. Rev. Lett. **93**, 090602 (2004) [arXiv:hep-th/0311175].

[27] C. Y. Wong, "Landau hydrodynamics reexamined," Phys. Rev. C **78**, 054902 (2008), [arXiv:0808.1294v3]. 22, 23

[28] J. D. Bjorken, "Highly relativistic nucleus-nucleus collisions: the central rapidity region," Phys. Rev. D **27**, 140 (1983). 22, 46, 59, 62, 63, 69

[29] B. Muller and J. L. Nagle, "Results from the relativistic heavy ion collider," Ann. Rev. Nucl. Part. Sci. **56**, 93 (2006) [arXiv:nucl-th/0602029]; 24, 28, 40

P. F. Kolb and U. W. Heinz, "Hydrodynamic description of ultrarelativistic heavy-ion collisions," [arXiv:nucl-th/0305084].

[30] S. Nakamura and S.-J. Sin, "A holographic dual of hydrodynamics," JHEP **0609**, 020 (2006) [arXiv:hep-th/0607123]. 26, 43, 59, 70, 78, 79, 87

[31] C. Davies, "Lattice QCD," "Heavy flavour physics," Scottish Grad. Text. Ser., Inst. of Phys. (2002) arXiv:hep-ph/0205181 29

[32] S. Scherer HHLR-Nutzerkolloquium, Darmstadt (2003) http://th.physik.uni-frankfurt.de/ scherer/vortrag/HHLR/ 29

[33] J. M. Maldacena, "The large-N limit of superconformal field theories and supergravity," Adv. Theor. Math. Phys. **2**, 231 (1998) [Int. J. Theor. Phys. **38**, 1113 (1999)] [arXiv:hep-th/9711200]; 30, 34

S. S. Gubser, I. R. Klebanov and A. M. Polyakov, "Gauge theory correlators from non-critical string theory," Phys. Lett. B **428**, 105 (1998) [arXiv:hep-th/9802109];

E. Witten, "Anti-de Sitter space and holography," Adv. Theor. Math. Phys. **2**, 253 (1998) [arXiv:hep-th/9802150].

[34] O. Aharony, S. S. Gubser, J. M. Maldacena, H. Ooguri and Y. Oz, "Large-N field theories, string theory and gravity," Phys. Rept. **323**, 183 (2000) [arXiv:hep-th/9905111]. 30, 34

[35] M. Bianchi, "Trieste lectures on AdS/CFT," (2003). 30, 121

[36] R. Haag, J. Lopuszanski and M. Sohnius, "All possible generators of supersymmetries of the S-Matrix," Nucl. Phys. B **88**, 257 (1975); 31

W. Siegel, "AdS/CFT in superspace," (2010) [arXiv:1005.2317].

[37] G. T. Horowitz and A. Strominger, "Black strings and P-branes," Nucl. Phys. B **360**, 197 (1991). 32

[38] S. A. Hartnoll, "Quantum critical dynamics from black holes," *Understanding Quantum Phase Transitions*, Taylor and Francis, Boca Raton, 2010 [arXiv:0909.3553v2]. 33

[39] V. Balasubramanian and P. Kraus "A stress tensor for anti-de Sitter gravity," Commun. Math. Phys. **208**, 413 (1999) [arXiv:hep-th/9902121] 34

[40] S. Kinoshita, S. Mukohyama, S. Nakamura and K. Oda, "A holographic dual of Bjorken flow," Prog. Theor. Phys. **121**, 121 (2009) [arXiv:0807.3797]. 34, 43, 75, 87

[41] S. de Haro, S. N. Solodukhin and K. Skenderis, "Holographic reconstruction of spacetime and renormalization in the AdS/CFT correspondence," Commun. Math. Phys. **217**, 595 (2001) [arXiv:hep-th/0002230]. 35, 45, 47, 53, 60, 61, 64, 65

K. Skenderis, "Lecture notes on holographic renormalization," Class. Quant. Grav. **19**, 5849 (2002) [arXiv:hep-th/0209067].

[42] R. C. Myers and S. E. Vazquez, "Quark soup al dente: applied superstring theory," Class. Quant. Grav. **25**, 114008 (2008) [arXiv:hep-th/0804.2423]. 37

[43] E. Witten "Anti-de Sitter space, thermal phase transition, and confinement in gauge theories," Adv. Theor. Math. Phys. **2**, 505 (1998) [arXiv:hep-th/9803131v2]. 36

[44] J. Erdmenger, N. Evans, I. Kirsch, and E. Threlfall "Mesons in gauge/gravity duals - A Review" [arXiv:hep-th/0711.4467v2]. 37

[45] T. Sakai and S. Sugimoto, "Low energy hadron physics in holographic QCD," *Prog. Theor. Phys.* **113** (2005) 843; [arXiv:hep-th/0412141]; 37

T. Sakai and S. Sugimoto, "More on a holographic dual of QCD," *Prog. Theor. Phys.* **114** (2006) 1083; [arXiv:hep-th/0507073].

[46] C. P. Herzog, A. Karch, P. Kovtun, C. Kozcaz, L. G. Yaffe, "Energy loss of a heavy quark moving through N=4 supersymmetric Yang-Mills plasma," JHEP **0607**, 013 (2006) [arXiv:hep-th/0605158]; 37

H. Liu, K. Rajagopal, Y. Shi, "Robustness and infrared sensitivity of various observables in the application of AdS/CFT to heavy ion collisions," JHEP **0808**, 048 (2008) [arXiv:0803.3214].

[47] J. D. Bekenstein, "Black holes and entropy," Phys. Rev. D **7**, 2333 (1973); 38

J. M. Bardeen, B. Carter and S. W. Hawking, "The Four laws of black hole mechanics," Commun. Math. Phys. **31**, 161 (1973);

S. W. Hawking, "Particle Creation By Black Holes," Commun. Math. Phys. **43**, 199 (1975);

T. Damour, "Surface effects in black hole physics," Proceedings of the "Second Marcel Grossmann Meeting on General Relativity," (1982);

T. Jacobson, "Thermodynamics of space-time: The Einstein equation of state," Phys. Rev. Lett. **75**, 1260 (1995).

[48] M. Natsuume "String theory and quark-gluon plasma," Presented at "Frontiers in the physics of quark-gluon plasma," Wako, Japan workshop, (2006) [arXiv:hep-ph/0701201]. 38

[49] A. Buchel, R. Myers, and A. Sinha, "Beyond $\eta/s = 1/4\pi$," JHEP **0903**, 084 (2009) [arXiv:0812.2521]; 40

G. Koutsoumbas, E. Papantonopoulos, and G. Siopsis, "Shear viscosity and Chern-Simons diffusion rate from hyperbolic horizons," Phys. Lett. B **677**, 74 (2009), [arXiv:0809.3388].

[50] M. Brigante, H. Liu, R. C. Myers, S. Shenker, and S. Yaida "Viscosity Bound and Causality Violation," Phys. Rev. Lett. **100**, 191601 (2008), [arXiv:0802.3318]; 40

A. Buchel and S. Cremonini, "Viscosity Bound and Causality in Superfluid Plasma," [arXiv:1007.2963].

[51] S. Lin and E. Shuryak "Toward the AdS/CFT gravity dual for high energy collisions: I.falling into the AdS.," Phys. Rev. D **77**, 085013 (2008) [arXiv:hep-ph/0610168]. 42

S. Lin and E. Shuryak "Toward the AdS/CFT gravity dual for high energy collisions: 2.The stress tensor on the boundary," Phys. Rev. D **77**, 085014 (2008) [arXiv:0711.0736].

S. Lin and E. Shuryak "Toward the AdS/CFT gravity dual for high energy collisions: 3.Gravitationally collapsing shell and quasiequilibrium," [arXiv:0808.0910].

[52] R. A. Janik, "Viscous plasma evolution from gravity using AdS/CFT," Phys. Rev. Lett. **98**, 022302 (2007) [arXiv:hep-th/0610144]. 43, 59, 71, 86, 87

[53] M. P. Heller and R. A. Janik, "Viscous hydrodynamics relaxation time from AdS/CFT," Phys. Rev. D **76**, 025027 (2007) [arXiv:hep-th/0703243]; 43, 87

P. Benincasa, A. Buchel, M. P. Heller, and R. A. Janik "On the supergravity description of boost invariant conformal plasma at strong coupling," Phys. Rev. D **77**, 046006 (2008) [arXiv:0712.2025];

A. Buchel and M. Paulos, "Second order hydrodynamics of a CFT plasma from boost invariant expansion," Nucl. Phys. B **810**, 40 (2009) [arXiv:0808.1601].

[54] A. Ashtekar and B. Krishnan, "Isolated and dynamical horizons and their applications," Living Rev. Rel. **7**, 10 (2004) [arXiv:gr-qc/0407042] 48

[55] D. T. Son and A. O. Starinets, "Hydrodynamics of R-charged black holes," JHEP **0603**, 052 (2006) [arXiv:hep-th/0601157]. 58

[56] S.-J. Sin, S. Nakamura and S. P. Kim, "Elliptic flow, Kasner universe and holographic dual of RHIC fireball," JHEP **0612**, 075 (2006) [arXiv:hep-th/0610113]. 59, 87

[57] K. Kajantie, J. Louko and T. Tahkokallio, "The gravity dual of 1+1 dimensional Bjorken expansion," Phys. Rev. D **76**, 106006 (2007) [arXiv:0705.1791]. 59, 60, 68, 69

[58] M. P. Heller, P. Surowka, R. Loganayagam, M. Spalinski and S. E. Vazquez, "On a consistent AdS/CFT description of boost-invariant plasma," Phys. Rev. Lett. **102** 041601 (2009) [arXiv:0805.3774]; 87

M. P. Heller, R. A. Janik and R. Peschanski, "Hydrodynamic flow of the quark-gluon plasma and gauge/gravity correspondence," Acta Phys. Polon. B **39**, 3183 (2008) [arXiv:0811.3113].

[59] J. J. Friess, S. S. Gubser, G. Michalogiorgakis and S. S. Pufu, "Expanding plasmas and quasinormal modes of Anti-de Sitter black holes," JHEP **04**, 080 (2007) [arXiv:hep-th/0611005]; 88, 91, 92, 96, 104, 107

[60] G. T. Horowitz and V. E. Hubeny "Quasinormal modes of AdS black holes and the approach to thermal equilibrium," Phys. Rev. D **62**, 024027 (2000) [arXiv:hep-th/9909056]; 88, 100

V. Cardoso and J. P. S. Lemos "Quasi-normal modes of Schwarzschild Anti-de Sitter black holes: electromagnetic and gravitational perturbations," Phys. Rev. D **64**, 084017 (2001) [arXiv:gr-qc/0105103];

G. Siopsis "Large mass expansion of quasi-normal modes in AdS_5," Phys. Lett. B **590**, 105 (2004) [arXiv:hep-th/0402083]

S. Musiri, S. Ness, G. Siopsis, "Perturbative calculation of quasi-normal modes of AdS Schwarzschild black holes," Phys. Rev. D **73**, 064001 (2006) [arXiv:hep-th/0511113]

[61] G. Siopsis, "Low frequency quasi-normal modes of AdS black holes," JHEP **0705**, 042 (2007) [arXiv:hep-th/0702079]. 88, 89, 93, 96, 97, 98, 99, 100, 104

[62] G. Michalogiorgakis and S. S. Pufu, "Low-lying gravitational modes in the scalar sector of the global AdS$_4$ black hole," JHEP **02**, 023 (2007) [arXiv:hep-th/0612065]. 88, 89, 98, 101, 102, 103, 104

[63] R. B. Mann, "Pair production of topological anti-de Sitter black holes," Class. Quant. Grav. **14**, L109 (1997) [arXiv:gr-qc/9607071]; 89

R. B. Mann, "Charged topological black hole pair creation," Nucl. Phys. B **516**, 357 (1998) [arXiv:hep-th/9705223].

[64] L. Vanzo, "Black holes with unusual topology," Phys. Rev. D **56**, 6475 (1997) [arXiv:gr-qc/9705004]. 89

[65] D. R. Brill, J. Louko and P. Peldan, "Thermodynamics of (3+1)-dimensional black holes with toroidal or higher genus horizons," Phys. Rev. D **56**, 3600 (1997) [arXiv:gr-qc/9705012]. 89

[66] D. Birmingham, "Topological black holes in anti-de Sitter space," Class. Quant. Grav. **16**, 1197 (1999) [arXiv:hep-th/9808032]. 89, 90

[67] R. Emparan, "AdS/CFT duals of topological black holes and the entropy of zero-energy states," JHEP **9906**, 036 (1999) [arXiv:hep-th/9906040]. 89

[68] J. Weeks, "SnapPea": A computer program for creating and studying hyperbolic 3-manifolds http://www.geometrygames.org/SnapPea/index.html 90, 92, 107

N. J.. Cornish and D. N. Spergel, "On the eigenmodes of compact hyperbolic 3-manifolds" [arXiv:math/9906017v1];

K. Inoue, "Numerical study of length spectra and low-lying eigenvalue spectra of compact hyperbolic 3-manifolds" YITP **00-59**, 19 (2000) [arXiv:math-ph/0011012v2];

118

K. Inoue, "Computation of eigenmodes on a compact hyperbolic 3-space" Class. Quant. Grav. **16**, 3071 (1999) [arXiv:astro-ph/9810034]. D. Muller, H. V. Fagundes, R. Opher, "Casimir energy in multiply connected static hyperbolic universes" Phys. Rev. D **66**, 083507 (2002) [arXiv:gr-qc/0209103];

N. L. Balazs and A. Voros, "Chaos on the pseudosphere," Phys. Reports **143(3)**, 109 (1986)

F. Sausset and G. Tarjus "Periodic boundary conditions on the pseudosphere," J. Phys. A **40**, 12873 (2007) [arXiv:cond-mat/0703326];

[69] D. Birmingham and S. Mokhtari, "Exact gravitational quasinormal frequencies of topological black holes," Phys. Rev. D **74**, 084026 (2006) [arXiv:hep-th/0609028v2]; 91

R. Aros, C. Martinez, R. Troncoso, and J. Zanelli "Quasinormal modes for massless topological black holes" Phys. Rev. D **67**, 044014 (2003) [arXiv:hep-th/0211024v2];

[70] A. Ishibashi and H. Kodama, "A master equation for gravitational perturbations of maximally symmetric black holes in higher dimensions," *Prog. Theor. Phys.* **110** (2003) 701 [arXiv:hep-th/0305147]. 92, 100, 104

[71] W. A. Horowitz and M. Gyulassy, "Heavy quark jet tomography of Pb + Pb at LHC: AdS/CFT drag or pQCD energy loss?," Phys. Lett. **B666**, 320 (2008). 107

Appendix

Appendix A

$\mathcal{N} = 4$ SYM Lagrangian

For a full review of the superconformal algebra see Ref. [35]. The Lagrangian for $\mathcal{N} = 4$ SYM theory with SU(N) gauge group was presented in Section 2.2.1 as

$$
\begin{aligned}
\mathcal{L} &= -\frac{1}{2g_{YM}^2} Tr \Big\{ \frac{1}{2} F^{\mu\nu} F_{\mu\nu} + D_\mu \phi^i D^\mu \phi^i + \frac{1}{2} [\phi^i, \phi^j][\phi^i, \phi^j] \\
&+ i(\bar{\lambda}_A \bar{\sigma}^\mu D_\mu \lambda^A + \lambda^A \sigma^\mu D_\mu \bar{\lambda}_A) + [\bar{\phi}_{AB}, \lambda^A]\lambda^B - [\phi^{AB}, \bar{\lambda}_A]\bar{\lambda}_B \Big\}.
\end{aligned}
$$

It is comprised of gauge fields (A_μ), scalars (ϕ^i) and Weyl spinors (λ^A), with $i = 1, \ldots, 6$ and $A, B = 1, \ldots, 4$. The fields ϕ^{AB} and $\bar{\phi}_{AB}$ follow from

$$
\phi^i = \frac{1}{2} \bar{\tau}^i_{AB} \phi^{AB} \ , \quad \phi^{AB} = -\phi^{BA} \ , \quad \bar{\phi}_{AB} = \frac{1}{2} \epsilon_{ABCD} \phi^{CD}, \tag{A.1}
$$

where $(\tau^i)^{AB}$ are the gamma matrices of SO(6). The fields are invariant under the supersymmetry transformations

$$
\begin{aligned}
\delta \phi^i &= (\bar{\tau}^i)_{AB} \lambda^{\alpha A} \eta_\alpha^{\ \beta} + (\tau^i)^{AB} \bar{\eta}_{\dot\alpha A} \bar{\lambda}^{\dot\alpha}_{\ B}, \\
\delta \lambda^A_\alpha &= -\frac{1}{2} F^-_\mu \nu (\sigma^{\mu\nu})_\alpha^{\ \beta} \eta_\beta^{\ B} + i\slashed{D}_{\alpha\dot\alpha} \phi^{AB} \bar{\eta}^{\dot\alpha}_{\ B} + \frac{1}{2} [\phi^i, \phi^j](\tau_{ij})^A_{\ B} \eta_\alpha^{\ B}, \\
\delta A_\mu &= -i\lambda^{\alpha A} (\sigma^\mu)_{\alpha\dot\alpha} \bar{\eta}^{\dot\alpha}_{\ A} - i\eta^{\alpha A} (\sigma^\mu)_{\alpha\dot\alpha} \bar{\lambda}^{\dot\alpha}_{\ A}. \tag{A.2}
\end{aligned}
$$

The generators of the algebra are the dilatation D, momenta P_μ, angular momenta $J_{\mu\nu}$, conformal momenta K_μ, Poincaré supercharges Q_A and $\bar{Q}^A$, superconformal charges S^A and $\bar{S}_A$ and R-symmetry charges T^A_B.

The bosonic sector is invariant under translations, Lorentz transformations, scale transformations and conformal boosts which are generated by

$$P_\mu = i\partial_\mu \ , \quad J_{\mu\nu} = i\left(x_\mu\partial_\nu - x_\nu\partial_\mu\right) \ , \quad D = ix^\mu\partial_\mu \ , \quad K_\mu = i\left(2x_\mu x^\nu\partial_\nu - x^2\partial_\mu\right), \quad \text{(A.3)}$$

and follow

$$
\begin{aligned}
\left[P_\mu, P_\nu\right] &= 0 \ , \quad \left[J_{\mu\nu}, P_\rho\right] = -i(\eta_{\mu\rho}P_\nu - \eta_{\nu\rho}P_\mu), \\
\left[J_{\mu\nu}, J_{\rho\sigma}\right] &= -i\left[\eta_{\mu\rho}J_{\nu\sigma} + \eta_{\nu\sigma}J_{\mu\rho} - \eta_{\nu\rho}J_{\mu\sigma} - \eta_{\mu\sigma}J_{\nu\rho}\right], \\
\left[K_\mu, K_\nu\right] &= 0 \ , \quad \left[J_{\mu\nu}, K_\rho\right] = -i(\eta_{\mu\rho}K_\nu - \eta_{\nu\rho}K_\mu) \ , \quad \left[P_\mu, K_\nu\right] = 2J_{\mu\nu} + 2\eta_{\mu\nu}D, \\
\left[D, D\right] &= 0 \ , \quad \left[D, J_{\mu\nu}\right] = 0 \ , \quad \left[D, P_\rho\right] = -iP_\rho \ , \quad \left[D, K_\rho\right] = iK_\rho. \quad \text{(A.4)}
\end{aligned}
$$

The fermionic generators satisfy

$$
\begin{aligned}
\{Q_A, \bar{Q}^B\} &= \delta_A^B \sigma^\mu P_\mu \ , \quad \{S^A, \bar{S}_B\} = \delta_B^A \sigma^\mu K_\mu \\
\{S^A, Q_B\} &= \delta_B^A \left(\frac{1}{2}\sigma^{\mu\nu}J_{\mu\nu} + D\right) + T^A_B, \\
\{Q_A, Q_B\} &= 0 \ , \quad \{S^A, S^B\} = 0 \ , \quad \{S^A, \bar{Q}^B\} = 0. \quad \text{(A.5)}
\end{aligned}
$$

The R-symmetry generators commute with all bosonic generators. However, the commutation relations fermionic generators is given by

$$\left[T^A_B, Q_C\right] = \delta_C^A Q_B - \frac{1}{4}\delta_B^A Q_C \ , \quad \left[T^A_B, S^C\right] = \delta_B^C S^A - \frac{1}{4}\delta_B^A S^C. \quad \text{(A.6)}$$

The final relations are composed of those between the bosonic and fermionic generators, which follow

$$
\begin{aligned}
\left[J_{\mu\nu}, Q_A\right] &= \frac{1}{2}\sigma_{\mu\nu}Q_A, \ \left[K_\mu, Q_A\right] = \sigma_\mu \bar{S}_A, \ \left[D, Q_A\right] = \frac{1}{2}Q_A, \ \left[P_\mu, Q_A\right] = 0 \\
\left[J_{\mu\nu}, S^A\right] &= \frac{1}{2}\sigma_{\mu\nu}S^A, \ \left[P_\mu, S^A\right] = \sigma_\mu \bar{Q}^A, \ \left[D, S^A\right] = -\frac{1}{2}S^A, \ \left[K_\mu, S^A\right] = 0 . \quad \text{(A.7)}
\end{aligned}
$$

The associated Noether currents comprise a traceless stress-energy tensor, fifteen R-symmetry currents, γ traceless current, three sets of scalars, two sets of spin $1/2$ fermions, and six antisymmetric tenors. Moreover, the theory exhibits a vanishing β function so that it lives on a superconformal fixed point.

Appendix B

Einstein Equations

The metric $(g_{\mu\nu})$ is the all-encompassing object of Einstein's Theory of General Relativity. It characterizes the geometric and causal structure of spacetime, allowing one to quantify the effects of gravity on distance, volume, and additional aspects. For the purpose of this text, we were concerned with solving the Einstein equations of asymptotically AdS space. In order to appreciate the nature of Eq. (2.62)

$$R_{\mu\nu} - \frac{1}{2}g_{\mu\nu}R + \Lambda g_{\mu\nu} = 0,$$

we must first discuss the concepts of curved spacetime.

In order to compare vectors in tangent spaces to points nearby on a curved manifold, we must introduce the connections. These come directly from the metric as

$$\Gamma^{\lambda}_{\mu\nu} = \frac{1}{2}g^{\lambda\sigma}\left(\partial_{\mu}g_{\nu\sigma} + \partial_{\nu}g_{\sigma\mu} - \partial_{\sigma}g_{\mu\nu}\right). \tag{B.1}$$

Named Christoffel symbols, this quantity, when combined with partial derivatives, form a well-defined tensor. Covariant derivatives take the place of derivatives when working in curved space. When acting on a vector or second rank tensor, we find

$$\nabla_{\mu}V^{\nu} = \partial_{\mu}V^{\nu} + \Gamma^{\nu}_{\mu\sigma}V^{\sigma} \ , \quad \nabla_{\sigma}T^{\mu\nu} = \partial_{\sigma}T^{\mu\nu} + \Gamma^{\mu}_{\lambda\sigma}T^{\lambda\nu} + \Gamma^{\nu}_{\lambda\sigma}T^{\lambda\mu}. \tag{B.2}$$

Furthermore, Christoffel symbols may be combined into a (1,3) tensor that characterizes the curvature of spacetime. This is known as the Riemann tensor and is cast in the form

$$R^{\rho}{}_{\sigma\mu\nu} = \partial_{\mu}\Gamma^{\rho}_{\nu\sigma} - \partial_{\nu}\Gamma^{\rho}_{\mu\sigma} + \Gamma^{\rho}_{\mu\lambda}\Gamma^{\lambda}_{\nu\sigma} - \Gamma^{\rho}_{\nu\lambda}\Gamma^{\lambda}_{\mu\sigma}. \tag{B.3}$$

The Einstein equations are formed with a contraction of the Riemann tensor, named the Ricci Tensor, and the trace of the Ricci Tensor. These quantities are found as

$$R_{\mu\nu} = R^{\lambda}{}_{\mu\lambda\nu} , \quad R = g^{\mu\nu}R_{\mu\nu} \tag{B.4}$$

and may now be used to place Eq. (2.62) in concrete form.

As an example, we would like to solve the Einstein equations for a five-dimensional anti-de Sitter large black hole. The first step is to choose a metric ansatz ($ds^2 = g_{\mu\nu}dx^{\mu}dx^{\nu}$)

$$ds^2 = \frac{1}{z^2}\left(-e^{a(z)}dt^2 + d\vec{x}^2 + e^{-a(z)}dz^2\right). \tag{B.5}$$

The non-zero Christoffel symbols are found as

$$\Gamma^z_{tt} = e^{2a}\left(\frac{a'}{2} - \frac{1}{z}\right) , \quad \Gamma^z_{xx} = \frac{e^a}{z} , \quad \Gamma^t_{tz} = \frac{a'}{2} - \frac{1}{z} ,$$

$$\Gamma^x_{xz} = -\frac{1}{z} , \quad \Gamma^z_{zz} = -\frac{1}{z} - \frac{a'}{2}. \tag{B.6}$$

We now may calculate the non-zero Riemann tensor components

$$R_{txtx} = -\frac{e^{2a}}{2z^4}(za' - 2) , \quad R_{tztz} = \frac{e^a}{2z^4}\left(2 - 2za' + z^2a'^2 + z^2a''\right) ,$$

$$R_{x^2x^1x^2x^1} = R_{x^3x^1x^3x^1} = R_{x^3x^2x^3x^2} = -\frac{e^a}{z^4} , \quad R_{zxzx} = \frac{za' - 2}{2z^4} , \tag{B.7}$$

and those of the Ricci tensor

$$R_{tt} = \frac{e^{2a}}{2z^2}\left(8 - 5za' + z^2a'^2 + z^2a''\right) , \quad R_{xx} = \frac{e^a}{z^2}\left(za' - 4\right) ,$$

$$R_{zz} = -\frac{1}{2z^2}\left(8 - 5za' + z^2a'^2 + z^2a''\right). \tag{B.8}$$

125

We are now at the point to calculate the Einstein equations for AdS$_5$. Upon using the AdS$_5$ cosmological constant $\Lambda_5 = -6$, the equations are reduced to the single one

$$-6 + 6e^a - \frac{3}{2}za'e^a = 0. \tag{B.9}$$

The solution is given as

$$a(z) = \ln\left(1 + 2\mu z^4\right), \tag{B.10}$$

where μ is an integration constant. This leads to the metric

$$ds^2 = \frac{1}{z^2}\left(-(1 - 2\mu z^4)dt^2 + d\vec{x}^2 + \frac{dz^2}{1 - 2\mu z^4}\right), \tag{B.11}$$

which can be seen to match Eqs. (4.2) - (4.4) and the generalized hyperbola of Eq. (2.38) for $\mu = 0$ and $z = \frac{L}{r}$.

Vita

James Ethan Alsup was born in Chattanooga, Tennessee on June 3, 1983 to Bob and Lota Alsup. After graduating from Red Bank High School he attended the University of Tennessee, Knoxville and remained in the program through Graduate School. In the Summer of 2010, he graduated with a Doctorate of Philosophy. He has accepted a position of Assistant Professor of Physics at Colorado State University–Pueblo.